Università degli Studi di Padova
Dipartimento di Ingegneria Industriale

Tesi di Laurea Magistrale in
Ingegneria Chimica e dei Processi Industriali

Sviluppo di un impianto pilota per la produzione di microalghe: misure di laboratorio e progetto di impianto

Development of a pilot plant for microalgae production: laboratory measurements and plant design

Relatore
Prof. Alberto Bertucco

Correlatrice
D.ssa Eleonora Sforza

Laureando
Mattia Enzo
Matricola: 622071-ICP

Anno Accademico 2011/2012

RIASSUNTO

In questa tesi si è affrontato il tema della produzione industriale di microalghe dapprima attraverso un approccio sperimentale e successivamente con la messa a punto di un modello di simulazione. In particolare, reattori in scala di laboratorio sono stati appositamente costruiti per la coltivazione di alghe e sono stati condotti test in condizioni di funzionamento sia batch che continue. I programmi di simulazione, scritti in Matlab®, hanno permesso di utilizzare un modello per simulare l'attenuazione della luce lungo la profondità della coltura microalgale e per correlare i parametri del modello (coefficiente di assorbimento, coefficiente di backscattering e costante di mantenimento) sui dati sperimentali ottenuti con il reattore continuo con riciclo. Le prestazioni del reattore in questione sono state valutate attraverso l'efficienza fotosintetica e il bilancio di energia. Inoltre, è stato condotto uno studio sulla massima produttività del sistema.
I parametri ottimizzati del modello hanno permesso di approfondire il comportamento di una coltura microalgale in un fotobioreattore pilota di 15 m^2 di superficie. Simulando sia la luce artificiale sia i cicli giorno/notte con luce solare, sono state valutate le prestazioni del reattore in termini di produttività ed efficienza fotosintetica. Infine, è stato valutato il bilancio energetico per stabilire la necessità di un sistema di termostatazione.

ABSTRACT

The industrial production of microalgae was investigated using both an experimental and a modelling approach. Lab-scale reactors were built for microalgae cultivation and batch and continuous tests were performed. Using Matlab® codes, the light attenuation along the culture depth and the experimental behaviour of the dynamic reactor with recycle were simulated by a model. The absorption coefficient, the backscattering coefficient and the maintenance constant of the microalga were so optimized on laboratory data. The reactor performances were evaluated in terms of photosynthetic efficiency and of the energy balance. Furthermore, a study on the maximum productivity of the system was performed.

The optimized model parameters were used to investigate the microalgal culture behaviour in a pilot-scale photobioreactor with an irradiated area of 15 m^2. Artificial radiation and day/night sunlight cycles permitted to determine the system performances in terms of productivity and photosynthetic efficiency. Finally, the energy balance was developed to understand whether a heating/cooling system is necessary to control properly the microalgae growth conditions.

RINGRAZIAMENTI

Desidero ringraziare innanzitutto il professor **Bertucco** che mi ha dato la possibilità di svolgere la tesi in questo gruppo di ricerca e che ha dimostrato un altissimo interesse in questo lavoro nelle varie fasi del suo sviluppo. Ringrazio la mia correlatrice **Eleonora** per l'impegno con cui mi ha sempre seguito e per essere stata un punto di riferimento durante questa esperienza. Infine, un grazie a **Barbara** con la quale è stata svolta gran parte dell'attività sperimentale riportata in questa tesi.

CONTENTS

1 INTRODUCTION

Many efforts have been made in these years to find an alternative to fossil fuels, which nowadays account for 88% of the primary energy consumption (Brennan and Owende 2010). In particular, they are responsible for greenhouse gas (GHG) emissions and their use is raising, mostly because of the development of new growing economies, such as China and India, leading to an ever more significant contribution to global warming. GHGs have other negative impacts on human life, e.g., the increase of CO_2 in the atmosphere will cause an higher concentration in oceans, turning the water pH gradually to more acidic and affecting negatively the marine ecosystem biodiversity (Mata, Martins, and Caetano 2010). In such a situation, together with the possible depletion of fossil sources, research in biofuels ranks as one of the most important challenge nowadays.

Biofuels can play a dominant role in transportation sector, replacing fossil fuels in the long term, contributing to mitigation of GHG emissions, offering diversification of income and fuel supply sources.

Biofuels scenario is mainly divided into three groups: first, second and third generation (Brennan and Owende 2010).

First generation biofuels are extracted from food and oil crops (rapeseed oil, sugarcane, sugar beet and maize) as well as vegetable oils and animal fats and present a relatively high economic level. Technologies for their production is by now well known, even if some problems remain: one among others is the competition for the use of arable land to produce food and fibre. In fact, a severe controversy on their use has been generated, especially with regards to the most vulnerable regions of the world economy, where first generation biofuels could lead to the rise of food prices, with potentially harmful social consequences. Other limitations are: regionally constrained market structures, lack of well managed agricultural practices in emerging economies, high water and fertiliser requirements, and a need for conservation of bio-diversity.

Second generation biofuels avoid the competition with food crops because they are obtained from agricultural and forest harvesting residues or wood processing wastes. On the other hand, the technology has not reached an industrial scale so far.

Finally, third generation biofuels are produced by microalgae. These photosynthetic microorganisms can be prokaryotic or eukaryotic and are able to grow with high rates under certain situations, such as light and CO_2 supply, in addition to other simple nutrients, exceeding the relatively low growth rate of plants and showing a more efficient cap-

ture of light. The peculiarity of microalgae is the ability to synthesize and accumulate lipids, proteins and carbohydrates that can be potentially converted into a variety of energy sources such as hydrogen, methane, ethanol and biodiesel.

The attention of this thesis work is focused on biodiesel, mostly because this compound is liquid at room temperature and can so play a fundamental role in the transportation sector. Biodiesel, which is a mixture of monoalkyl esters of long chain fatty acids, is obtained by transesterification process from lipids extracted from microalgae in the presence of a catalyst. Depending on species, microalgae can synthesize lipids from 20 to 80% of their dry weight, and this makes the application very attractive in terms of achievable productivities.

1.1 ADVANTAGES AND LIMITATIONS OF MICROALGAE FOR BIODIESEL PRODUCTION

Interest in the use of microalgae comes from a number of reasons:

- microalgae are able to grow and duplicate transforming light into chemical energy and under continuous supply of nutrients and they are able to adapt to different environments;
- growth rates are higher than those of agricultural plants, with the result of smaller areas required to produce a given amount of biofuel derived from any other crops;
- photosynthetic efficiency, which is the percentage of solar energy that can be stored as chemical energy thus producing biomass, is in the order of $3-8\%$, compared to 0.5% of terrestrial plants (Verma *et al.* 2010);
- CO_2 coming from power plants can be used as nutrients for microalgae; moreover, 1 kg of dry algal biomass uses about 1.83 kg of CO_2 (Chisti 2007), contributing to air quality maintenance and improvement.
- salty or brackish water can be fed to the microalgae culture and nutrients can be provided by waste water, leading to a partially treatment of effluents;
- as stated above, microalgae can accumulate not only lipids but also proteins and carbohydrate and other several interesting renewable energy sources such as hydrogen, methane and ethanol can be derived;

Table 1.1 clearly demonstrates the importance of microalgae for biodiesel production. The area needed in order to substitute 50% of total amount of fuels in the United States is considerably reduced even

with 30% oil microalgae. As shown, using an high efficiency and areal productivity oil like palm oil, a quarter of the entire US cropping area should be dedicated to biofuels production, which is clearly impractical.

Table 1.1: Comparison of some sources of biodiesel for meeting 50% of all transport fuel needs of the United States (ivi).

Crop	Oil yield [L/ha]	Land area needed [Mha]	US cropping area [%]
Corn	172	1540	846
Soybean	446	594	326
Canola	1190	223	122
Jatropha	1892	140	77
Coconut	2689	99	54
Palm oil	5950	45	24
Microalgae[a]	58700	4.5	2.5
Microalgae[b]	136900	2	1.1

[a] 30% oil content (dry weight)

[b] 70% oil content (dry weight)

In spite of number of advantages of this potential biofuel resource, the development of algal biofuel technology at a commercial scale is still limited because several issues have still to be properly addressed and solved, including:

- very low photosynthetic efficiencies for current technologies;
- negative value of the total energy balance, which takes into account water pumping, nutrients supply, separation and extraction of oil, leading to an unfeasible large scale industrial production;
- lack of a strong experience on this field, since few pilot units are in operation;
- lack of micfroalgae species able to balance production of biofuel and valuable co-products.

1.2 SCOPE OF THE THESIS

The goal of this thesis is the construction of a small photobioreactor (laboratory scale) to investigate a continuous microalgae production, with reference to the species *Scenedesmus obliquus* 276-7 (from SAG Goettingen), and to develop a model which simulates the behaviour of the microalgal culture in this system. The experimental data are

used to correlate the model parameters, and the model calibrated in this way is applied to the design of a pilot photobioreactor in order to investigate the performances in terms of productivity and photosynthetic efficiency that can be reached in an actual plant.

2 EXPERIMENTAL ACTIVITIES

After a first introduction on microalgae cultivation in laboratory, the arrangement of a continuous reactor with and without recycle will be presented and experimental data will be shown.

2.1 INTRODUCTION

When talking about the cultivation of a species of microalgae, the concept of axenic working conditions is that cultures must be pure and free of any other organisms, such as bacteria, fungi or other species of algae. This particular conditions cannot be reached if the culture medium is exposed directly to the atmosphere. Photobioreactors (PBR) are safe against competing microorganisms invasion, offering a closed environment where all conditions and parameters can be controlled.
One of the main goals of PBR is to allow light to pass through the reactor walls, so that it can be used by cultivated cells (Richmond 2004); for this reason, they are designed to present an high area to volume ratio. Micronutrients and CO_2 are fed by suitable delivery systems.

2.2 MATERIAL AND METHODS

2.2.1 *Microorganism*

The *Scenedesmus obliquus* 276-7 (from SAG Goettingen) microalga was used in all the experiments. In particular, this species lives in fresh water environments and has the important characteristic to show a constituent accumulation of lipids, i.e., this microorganism is able to produce lipids even in no-stress conditions.

2.2.2 *Experimental set up*

Several types of PBR have been proposed, but the one used for this experimental work is a flat plate vertical reactor (Figure 2.1). In particular, two transparent polycarbonate sheets are glued on both sides of a "U" support, and the size of this support affects the volume of the panel and the light path length. Mixing of the culture and CO_2-supply are assured by feeding CO_2-enriched air through a sparger (Posten 2009). The gas stream exits from the top of the system through a hole in the cap.

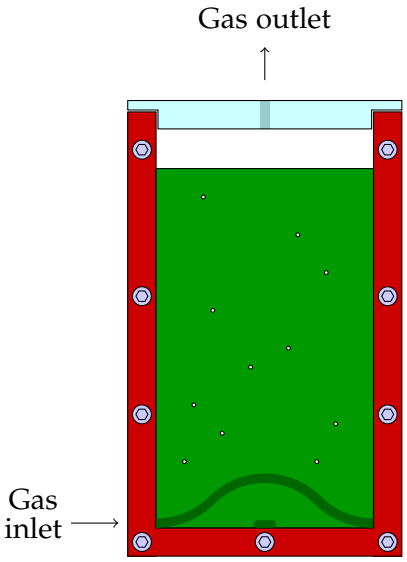

Figure 2.1: Scheme of batch system set up in laboratory.

The microalga was cultured in BG11 medium, which provides all the micronutrients required for *Scenedesmus obliquus* physiological and growth functions.

Initial tests were performed in batch conditions: medium containing micronutrients, and *Scenedesmus obliquus* were inoculated at the beginning in 150 mL volume reactors. Reactors were then placed in front of the light source (OSRAM white neon lamps) so that different light intensities, for different tests, reached the front side of the panel. The initial microalgal concentration ranged from 2.7 to 3.7 millions of cells per milliliter and tested irradiances reaching the panels were 10, 50, 150, 200, 350 and 1000 $\mu E/(m^2 s)$.

Table 2.1: System data related to batch tests.

Data	Symbol	U.m.	Value
Reactor volume	V_r	mL	150
Depth	h	cm	1.2
Irradiated area	A	m^2	$125 \cdot 10^{-4}$
CO_2-enriched air flow	$\dot{V}_{gas}$	L/h	1
CO_2 fraction in inlet flow	x_{CO_2}	%	5

The inlet gas was a mixture of air and CO_2 in a volumetric ratio 95/5, respectively, and the total flow rate was set to 1 L/h. This last value was obtained by mass transfer calculations between gas bubbles and liquid, while 5% CO_2 volume fraction permits high growth rate as reported by (Tang *et al.* 2011). Reactors were placed inside an incubator

(Frigomeccanica Andreaus) set at 23 °C, and all tests were carried out in duplicate, at least. Table 2.1 summarizes system characteristics for batch tests.

After batch tests, a continuous reactor test was performed. For this purpose, a flat plat reactor similar to the one used in the batch experiments (2 mm sheets thickness) with a volume of 250 mL and a depth of 1.2 cm was used (Figure 2.2). A hole on the reactor cap allowed to feed a solution containing micronutrients by Watson Marlow Sci-Q 400 peristaltic pump; the liquid level in the panel was controlled by an overflow pipe and the extracted biomass was collected in a bottle. The residence time (τ) in such a system is univocally affected by the peristaltic pump: slowing the speed of this device will cause an higher τ value. At the bottom of reactor a perforated rubber tube was used to feed CO_2-enriched air. The gas exited the system from the top after bubbling through the microalgal culture. As for batch tests, this assures a proper mass transfer between gas bubbles and liquid and concurs to mix the medium; however, an additional mixing system was applied, composed of magnetic bars in the liquid moved by a magnetic stirrer. White neon lamps were placed in front of the panel and were kept on for all the test time at an irradiance value of 150 $\mu E/(m^2 s)$, measured by a portable spectroradiometer (Delta OHM).

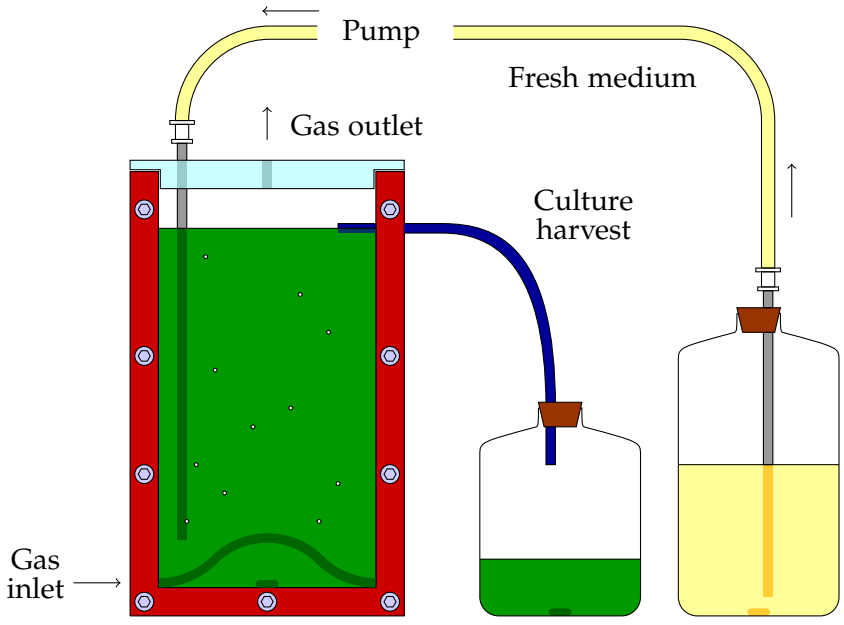

Figure 2.2: Scheme of lab-scale continuous reactor set up in laboratory.

Finally, a continuous reactor test with recycle was carried out and the same flat plate reactor as for the continuous test without recycle was used. The difference was the number and type of inlets: a first tube fed micronutrients and another one allowed the culture extracted from the reactor and collected in the product bottle to be fed

back to the reactor as the recycle (Figure 2.3). Since the pump was only one for both inlets deliveries, the recycle flow rate was half of the flow coming out of the reactor, so that the system could be operated at the same τ as for the continuous reactor without recycle was kept, so that comparisons between the two systems can be carried out.
This condition led to an accumulation of biomass solution in the collecting bottle, which was equipped with a magnetic bar moved by a stirrer, thus ensuring a perfect mixing.

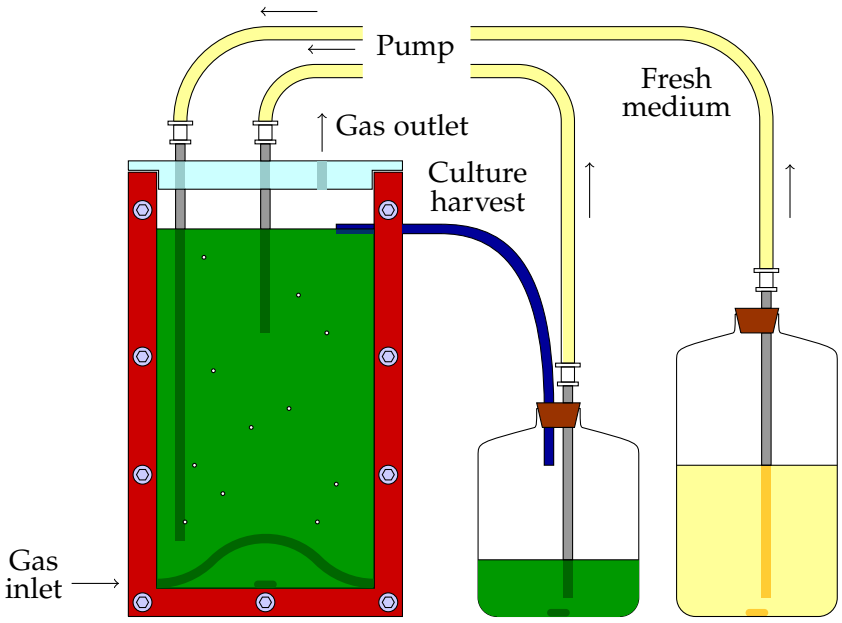

Figure 2.3: Scheme of lab-scale continuous reactor with recycle set up in laboratory.

System properties of the reactor used for both continuous experiment with and without recycle are summarized in Table 2.2.

Table 2.2: System data related to continuous tests.

Data	Symbol	U.m.	Value
Reactor volume	V_r	mL	250
Depth	h	cm	1.2
Polycarbonate thickness	s	mm	2
Polycarbonate light absorption	y_{PC}	%	11
Irradiated area	A	m^2	$209 \cdot 10^{-4}$
CO_2-enriched air flow	$\dot{V}_{gas}$	L/h	1
CO_2 amount on total flow	x_{CO_2}	%	5

2.2.3 *Analytical methods*

Microalgal concentrations was measured every day using a standard procedure:

1. a sample of microalgal solution was taken using BD Falcon™ Express™ Pipet-Aid®;
2. the absorbance of the sample, placed in a cuvette with path length $l = 1$ cm, was measured using Spectronic Unicam UV-500 UV-visible spectrometer at a wavelength of 750 nm. At this value chlorophyll does not absorb photons and light attenuation can be uniquely due to scattering phenomena, i.e., to cells concentration. As this device works in the absorbance range of $0.1 - 1$, the sample had to be diluted when the upper limit is exceeded;
3. the sample was diluted to achieve the necessary resolution of single cells in direct microscopic counting (Burker hemocytometer).

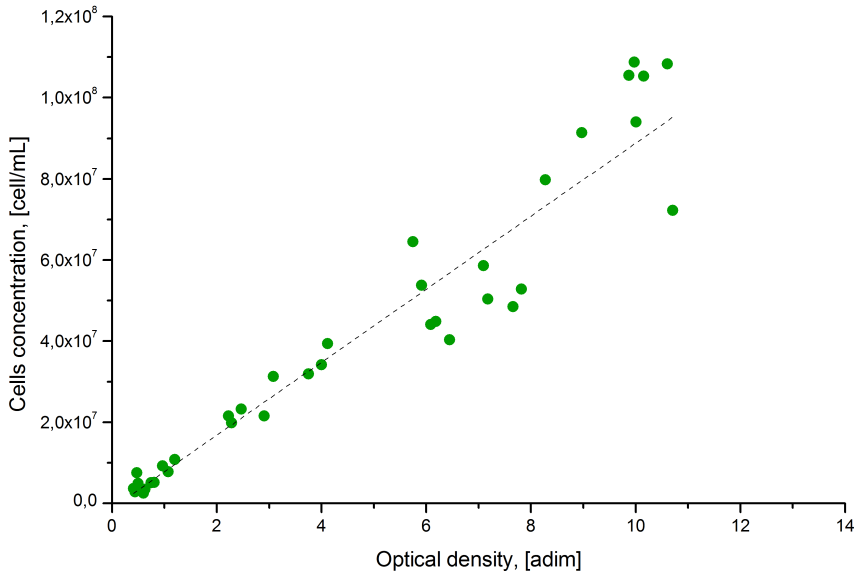

Figure 2.4: Cells concentration dependency on optical density. Regression line equation is $y = 9{\cdot}10^6x - 1{\cdot}10^6$, $R^2 = 0.9239$.

The absorbance, also called optical density (OD), obtained by spectrophotometer is directly linked to cells concentrations by Lambert-Beer law:

$$A_{750} = \varepsilon l c \tag{2.1}$$

where:

A_{750} sample absorbance at $\lambda = 750$ nm, [adim]
ε extinction coefficient, [cm^2/cell]
c cells concentration, [cell/mL]

The results of this procedure are plotted in Figure 2.4, where the relationship between microalgal concentration c, [cell/mL], and OD at $\lambda = 750$ nm is expressed by:

$$c = 9 \cdot 10^6 \, OD - 1 \cdot 10^6 \tag{2.2}$$

The figure clearly shows the linearity between x- and y-values mainly up to 50 millions of cell per milliliter; above that point the error is larger and direct microscopic counting is necessary.

The dry weight of microalgal biomass (DW) is a more realistic representation of the amount of microalgae per unit volume. For this reason, another procedure was used for continuous reactor with and without recycle, with the intention to link the optical density data to the quantity of biomass per unit volume. It is summarized by the following steps:

1. sampling and optical density measurement were the same as in the previous procedure;
2. a biomass filter was weighted, after few minutes in the oven to remove humidity, and placed in a suitable percolation device;
3. a known volume of microalgae sample was spilled on the filter: liquid flows through while biomass is retained;
4. the filter with the biomass was placed in the oven at 80 degree Celsius for 2 hours; this step permits to remove inter- and intra-cellular water so that the dry weight can be eventually measured;
5. the filter was weighted in an Atilon Acculab Sartorius Group microbalance (precision: $1{\cdot}10^{-4}$ g).

The evaluation of microalgae dry weight was done according to:

$$\text{Dry weight} = \frac{\text{(Filter+biomass) mass - Filter mass}}{\text{Sampled volume}} = \frac{g}{L} \tag{2.3}$$

These results are so plotted as function of optical density, as Figure 2.5 depicts. The regression line which relates cells concentration c, [g/L], and OD at $\lambda = 750$ nm is as follows:

$$c = 0.1958 \, OD - 0.1534 \tag{2.4}$$

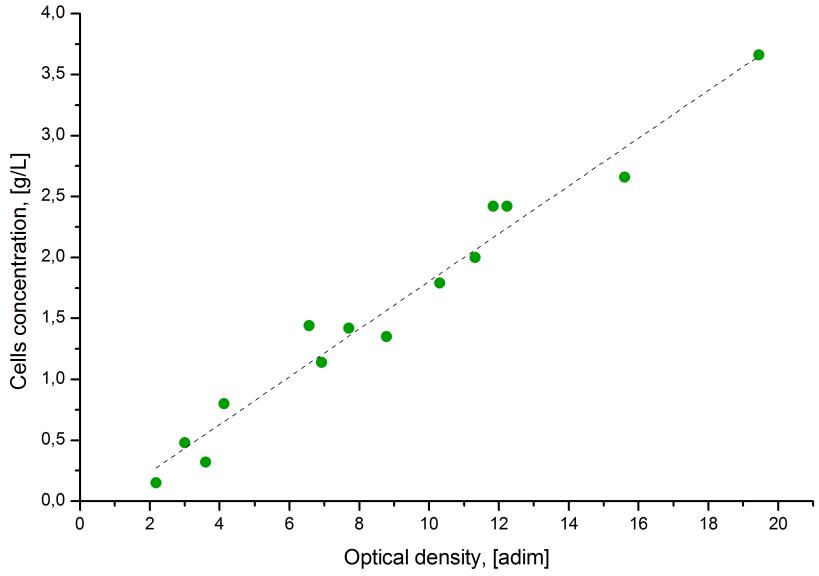

Figure 2.5: Dry weight dependency on optical density. Regression line equation is $y = 0.1958x - 0.1534$, $R^2 = 0.9684$.

The flux of photons reaching the first layer of the reactor is determined using a portable spectroradiometer for PAR wavelengths (Delta OHM). More measurements are done along the height of each reactor and averaged to provide the value of irradiance needed for the specific experiment. Table 2.3 summarizes these data and the averaged value of 165 $\mu E/(m^2 s)$ for continuous reactor test with recycle.

Table 2.3: Values of back irradiance at different measurement positions. Positions have to be intended as respective to the reactor.

Position	Back irradiance [$\mu E/(m^2 s)$]
Bottom left	147
Bottom right	139
Middle left	163
Middle right	159
Top left	192
Top right	188
Average	165

The same measurements are collected every day on the back of reactor used for continuous experiments (properties are summarized in Table 2.2), on the layer which is not exposed to direct illumination. These data, called back irradiances, provide a quantification of the

amount of light which is absorbed by the first polycarbonate sheet, the microalgae culture and the second polycarbonate sheet. It is clear that an higher concentration of biomass in the reactor is characterized by an higher turbidity effect so that irradiance measured behind the reactor will be lower. These experimental data are collected in Figure 2.6 and the relationship between cells concentration c, [g/L], and back irradiance I_{back}, [$\mu E/(m^2 s)$], is expressed as:

$$c = -0.753 \ln(I_{back}) + 3.2954 \tag{2.5}$$

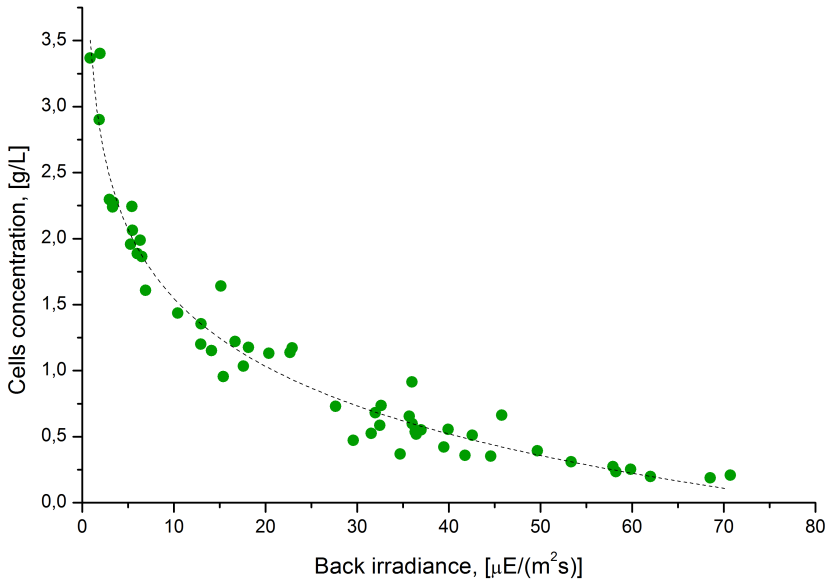

Figure 2.6: Back irradiance values measured at different cells concentrations. Dependency equation is y = -0.753ln(x)+3.2954, R^2 = 0.9610.

2.2.4 *Theoretical considerations*

As for any other microorganism, microalgae life passes through four fundamental phases in a batch reactor:

I. Lag phase:
   it represents the period of physiological adaptation to changes in the environment (nutritions or culture conditions); this could happen for instance when cells adapted to a certain light intensity are exposed to higher irradiance;

II. Exponential phase:
   when cells get used to the new environmental condition, they start to multiply at the highest rate and, as long as micronutrients and light are not limiting, microalgae divide and grow as an exponential function of time;

III. Steady phase:
at a certain point of growth, light or micronutrients will become limiting and this phenomenon characterizes a period of linear growth;

IV. Death phase:
after a certain time, some micronutrients are totally consumed and this lack leads to cells death, so that their concentration lowers.

In batch mode, the system is described by a simple mass balance:

$$\frac{dc_x}{dt} = r_x \tag{2.6}$$

where:

c_x biomass concentration, [g/L]
r_x biomass production rate, [g/(L·d)]

The expansion of r_x term is not simple if Equation 2.6 has to model the all growth curve. However, from an engineering point of view the interest is to obtain biomass in the highest production rate, i.e., at the exponential growth rate; this is possible when nutrients are non-limiting. In this particular condition r_x can be written as:

$$r_x = Kc_x \tag{2.7}$$

where K, $[d^{-1}]$, is the specific growth rate. By solving Equation 2.6, this constant can be written in the form:

$$K = \frac{\ln(c_x^{(2)}) - \ln(c_x^{(1)})}{t_2 - t_1} \tag{2.8}$$

where:

$c_x^{(2)}$ biomass concentration at time t_2, [g/L]
$c_x^{(1)}$ biomass concentration at time t_1, [g/L]

and K can be graphically determined for the exponential phase.
Determination of these values are fundamental when a continuous reactor has to be set up. In fact, at the beginning of each continuous experiment, the system is run in a batch mode. Since a continuous photobioreactor has to work at the maximum cells growth rate to enhance biomass productivity, microalgae have to grow and duplicate before the continuous mode is started. The batch period permits reaching high cells concentration and growth rate from an initial diluted culture. Thus, growth curves obtained by batch tests are useful to determine the continuous mode starting point; the latter has to be characterized by the maximum biomass production rate, that is the highest value of r_x.

2.3 RESULTS AND DISCUSSION

2.3.1 *Batch tests*

Several tests were carried out and Figure 2.7 shows growth curves for each value of irradiance hitting the reactor.

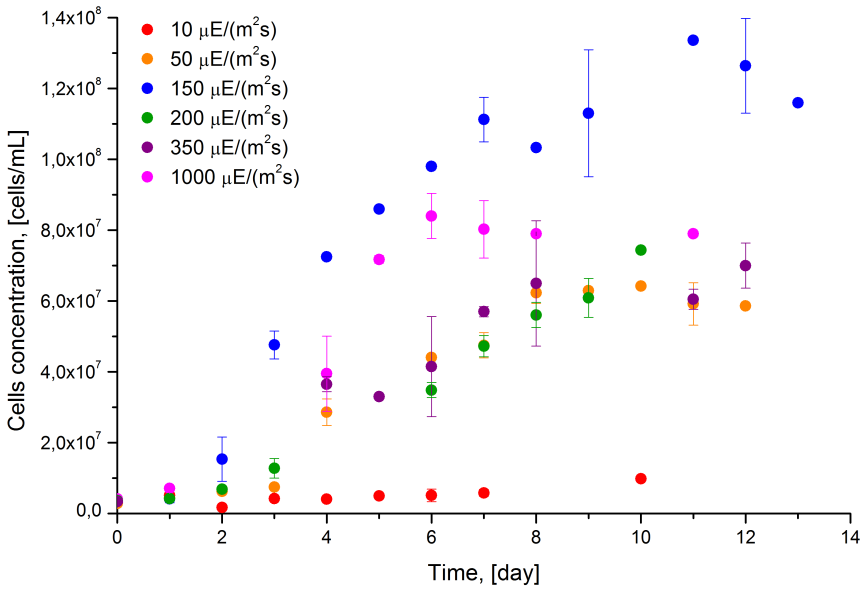

Figure 2.7: Growth curves at different irradiances. Each curve was obtained by an average of several measurements of batch cultures exposed at the same irradiance.

As clearly visible, a cells concentration of ca. 120 millions of cells per milliliter were reached for tests at $I = 150\ \mu E/(m^2 s)$, and this represents the highest concentration observed among all batch tests.
Evaluation of specific growth rate K follows Equation 2.8: a table containing cells concentration at each cultivation day and the respective logarithm is performed; the latter was plotted as a function of time. Table 2.4 shows data for test at $I = 150\ \mu E/(m^2 s)$, whereas Figure 2.8 depicts how the specific growth rate was graphically determined for all tests.
From this figure the exponential phase can be easily deduced: starting from day 0, logarithm of concentration has a linear increase until a certain day which separates exponential and stationary phases, the latter being characterized by a plateau. K-values are so calculated as the slope of points representing the exponential phase, and Table 2.5 summarizes these data for all performed tests.
Using data collected in Equation 2.8, specific growth rate values were plotted with respect to irradiance, Figure 2.9.

Table 2.4: Microalgal growth data for test at I = 150 μE/(m^{2}s). Data refer to an average of several measurements of batch cultures exposed at I = 150 μE/(m^{2}s).

Time [d]	Cells concentration [cell/mL]	ln(c) [ln(cell/mL)]
0	$3.3 \cdot 10^6$	15.0
1	$4.2 \cdot 10^6$	15.2
2	$15.4 \cdot 10^6$	16.5
3	$47.6 \cdot 10^6$	17.7
4	$72.5 \cdot 10^6$	18.1
5	$86.0 \cdot 10^6$	18.3
6	$98.0 \cdot 10^6$	18.4
7	$111.2 \cdot 10^6$	18.5
8	$103.3 \cdot 10^6$	18.5
9	$113.0 \cdot 10^6$	18.5
11	$133.6 \cdot 10^6$	18.7
12	$126.5 \cdot 10^6$	18.7
13	$116.0 \cdot 10^6$	18.6

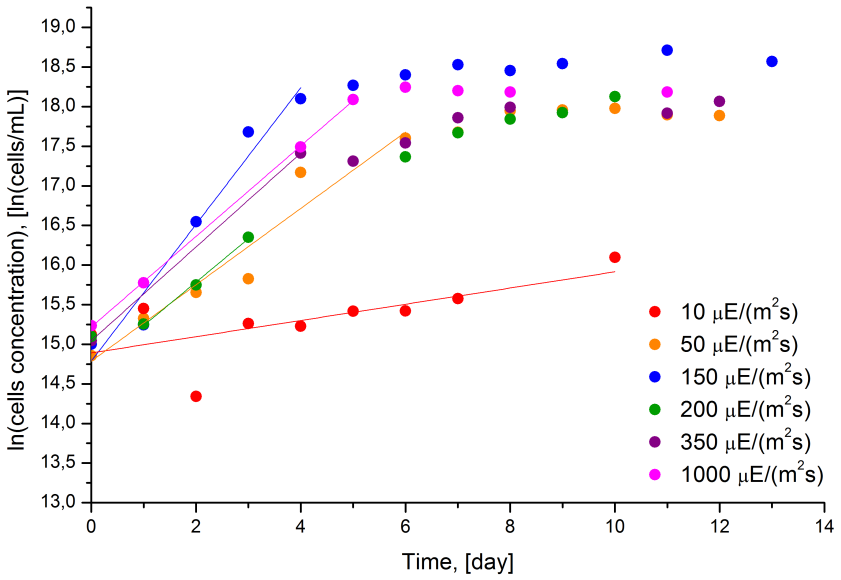

Figure 2.8: Logarithmic growth curves at different irradiances. Each curve was obtained by an average of several measurements of batch cultures exposed at the same irradiance.

Table 2.5: Specific growth rates for tests carried out at different irradiances. Each K-values was obtained by an average of several measurements of batch cultures exposed at the same irradiance.

Irradiance	Specific growth rate [d^{-1}]
10	0.102
50	0.482
150	0.863
200	0.548
350	0.493
1000	0.571

There are visibly two zones where the growth constant has a different dependency on irradiance: until a certain value called light saturation irradiance, the rate of microalgae growth and duplication increases with the number of photons reaching the culture; this phase is called photosaturation. Above this point, a plateau is commonly observed, where physiological reactions become rate limiting, whereas higher irradiance values produce the decline of the curve, and the system enters the photoinibition phase.

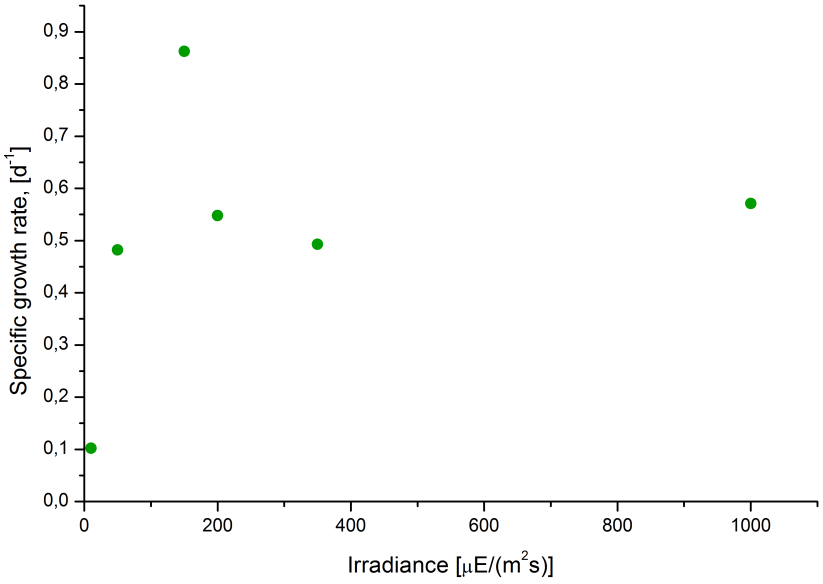

Figure 2.9: Specific growth rate dependency on irradiance. Growth rate constants are averaged on the entire exponential phase for each test performed at the respective irradiance value.

2.3.2 *Continuous test without recycle*

As already stated in Section 2.2.4, any continuous reactor has to operate in batch mode firstly: this allows microalgae to reach high concentration and specific growth rate, so that the biomass productivity of continuous reactor is the maximum; furthermore, Table 2.5 suggested to use an irradiance of 150 $\mu E/(m^2 s)$ in order to take advantage of the highest specific growth rate.
For this system, an initial cells concentration of 3.8 millions of cells per milliliter was inoculated in the reactor at day 0. As the culture started to grow and duplicate, cells counting was performed every day. Table 2.6 resumes the data collected.

Table 2.6: Microalgal growth data referring to the initial batch mode for continuous test at $I = 150\ \mu E/(m^2 s)$.

Time [d]	Cells concentration [cell/mL]	ln(c) [ln(cell/mL)]
0	$3.8 \cdot 10^6$	15.2
1	$3.7 \cdot 10^6$	15.1
2	$15.2 \cdot 10^6$	16.5
3	$24.1 \cdot 10^6$	17.0
6	$29.5 \cdot 10^6$	17.2
7	$53.9 \cdot 10^6$	17.8

In order to determine the optimum day for the switch from batch to continuous mode, the logarithm of cells concentration was plotted as a function of time and the the value of K was determined as the slope of the entire exponential phase as Figure 2.10 shows.
At day 7, microalgae concentration is 53.9 millions of cells per milliliter and the specific growth rate is 0.603 d^{-1}: in this condition, biomass production rate is $r_x = 32.5$ millions of cells per milliliter per day. So, at day 8, the system was switched to continuous mode.

One thing to be avoided when running a biological process in a photobioreactor is wash-out, i.e., the withdrawal of all the biomass from the system; this phenomenon happens when one of these two conditions occurs:

1. the outlet flow rate is higher than the inlet one;
2. the biomass extraction rate is higher than the biomass production rate in the photobioreactor.

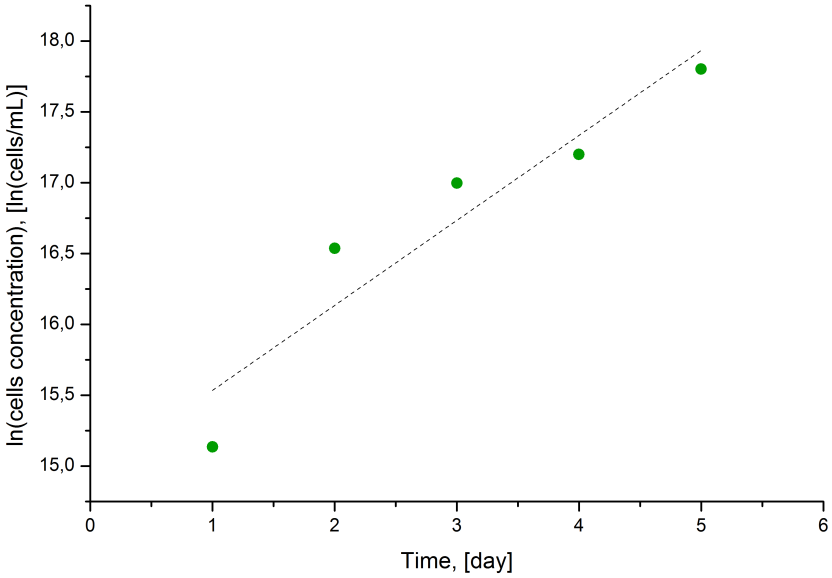

Figure 2.10: Logarithmic growth curves referring to the initial batch mode for continuous test at $I = 150\ \mu E/(m^2 s)$. Regression line equation is $y = 0.603x + 13.582$.

The first condition is avoided when using an overflow system. For the second condition, more discussion is needed. If the system can be approximated to a CSTR, for the particular mixing conditions, the mass balance is expressed by:

$$V_r \frac{dc_{out}}{dt} = \dot{V}_{in} c_{in} - \dot{V}_{out} c_{out} + V_r r_{x,out} \tag{2.9}$$

where:

V_r	reactor volume, [L]
$\dot{V}_{in}$	volumetric inlet flow, [L/d]
$\dot{V}_{out}$	volumetric outlet flow ($= \dot{V}_{in} = \dot{V}$), [L/d]
c_{in}	biomass concentration of inlet flow, [g/L]
c_{out}	biomass concentration of outlet flow, [g/L]
$r_{x,out}$	biomass production rate, [g/(L·d)], expressed as Kc_{out}

At steady state condition there is no change of cells concentration in time, so that there is a balance between the rate of biomass produced in the reactor and the rate of biomass extracted; so, Equation 2.9 is reduced to:

$$\begin{aligned} 0 &= \cancel{\dot{V} c_{in}} - \dot{V} c_{out} + V_r K c_{out} \\ &= -\dot{V} \cancel{c_{out}} + V_r K \cancel{c_{out}} \\ \tau &= \frac{1}{K} \end{aligned} \tag{2.10}$$

where τ is the residence time, defined as:

$$\tau = \frac{\text{Reactor volume}}{\text{Volumetric outlet flow}} = \frac{V_r}{\dot{V}} \tag{2.11}$$

Using $K = 0.603\ d^{-1}$:

$$\tau = \frac{1}{0.603} = 1.66\,d \tag{2.12}$$

and

$$\tau = \frac{V_r}{\dot{V}} \Longrightarrow \dot{V} = \frac{V_r}{\tau} = \frac{250}{1.66} = 151\ mL/d \tag{2.13}$$

This result states that for the system under investigation, characterized by specific growth rate of $0.603\ d^{-1}$, a continuous volumetric inflow (and outflow) of 151 mL/d satisfies the stationary mass balance of a CSTR: in other words, if 151 mL/d of micronutrients are fed continuously into the reactor starting from day 8, then the system should keep a condition of steady state corresponding to the initial concentration when switching to the continuous mode; system should maintain a concentration of ca. 50 millions of cells per milliliter after the eighth day, as visible from Figure 2.11.

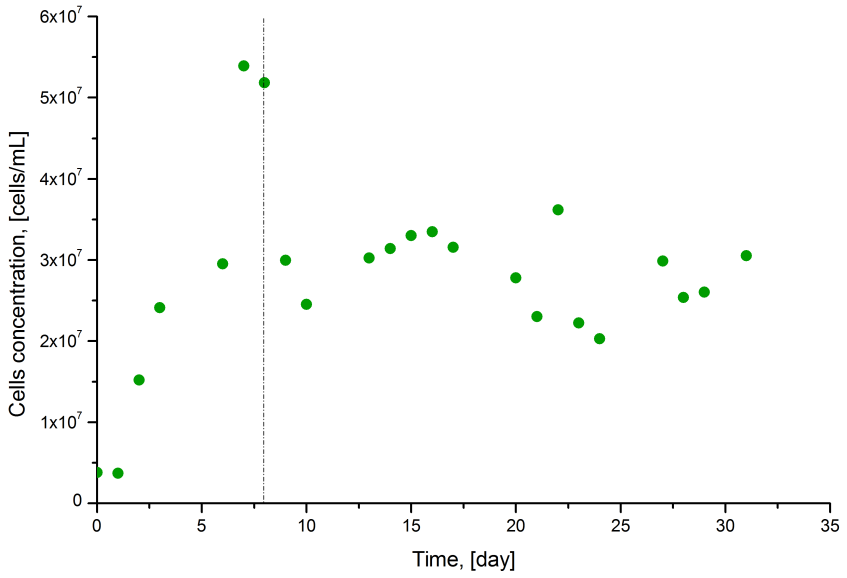

Figure 2.11: Collected data for continuous reactor experiment. Points before the vertical bar characterizes the batch period before the switch to continuous mode.

On the contrary, the system tends to a different stationary concentration, which can be approximated to 30 millions of cell per milliliter. This deviation can be explained considering that continuous mode starts at day 8, when cells are in the late exponential phase. At this

point, micronutrients start to be limiting and the specific growth rate lowers. When the pump is switched on and fresh medium is fed into the reactor at 151 mL/d, the microalgae culture extraction is started, but because of its low growth rate constant the ratio between produced biomass and extracted biomass is lower than 1, and the overall concentration decreases; in fact, it is necessary about one day and a half to provide the volume of fresh medium, such that cells can reinstate the K-value to 0.603, satisfying Equation 2.10. Steady state is so kept at 30 millions of cells per milliliter, which correspond to 0.52 g/L using Equation 2.2 and Equation 2.4.

Table 2.7: System data related to continuous reactor test.

Data	Symbol	U.m.	Value
Micronutrients inlet flow	$\dot{V}_{in}$	mL/d	151
Culture outlet flow	$\dot{V}_{out}$	mL/d	151
Specific growth rate	K	d^{-1}	0.603
Residence time	τ	d	1.66
Stationary cells concentration	c_{out}	g/L	0.52
Areal biomass productivity	P_a	$g/(m^2 d)$	3.75
Volumetric biomass productivity	P_v	$kg/(m^3 d)$	0.314

It is noteworthy that $\tau = 1.66$ d represents a lower limit for this system: in fact, using a residence time lower than this value leads to wash-out condition.
For a continuous reactor at stationary condition, the biomass productivity per unit exposed area is defined as:

$$P_a = \frac{V_r r_x}{A} = \frac{\dot{V} c_{out}}{A} \tag{2.14}$$

whereas the biomass productivity per unit volume is:

$$P_v = \frac{V_r r_x}{V_r} = \frac{\dot{V} c_{out}}{V_r} \tag{2.15}$$

For the performed continuous test, $P_a = 3.75$ g/(m^2d) and $P_v = 0.314$ kg/(m^3d). Table 2.7 resumes system properties after the switch to continuous mode.

2.3.3 *Continuous test with recycle*

A second continuous reactor test was performed with the goal to obtain a stationary production of biomass and then to switch the system from simply continuous to continuous with recycle.
Instead of starting with a low concentration of cells, passing through

the batch phase and then switching the system to continuous mode, a concentrated microalgae solution was directly inoculated into the reactor which was operated in continuous mode. This initial concentration was 104.8 millions of cells per milliliter, or 2.15 g/L. The irradiance reaching the panel was 165 $\mu E/(m^2 s)$ and the residence time was maintained at the same value as for the previous test (Section 2.3.2). Figure 2.12 depicts the trend of cells concentration as a function of time of this experiment before switching on the recycle of biomass.

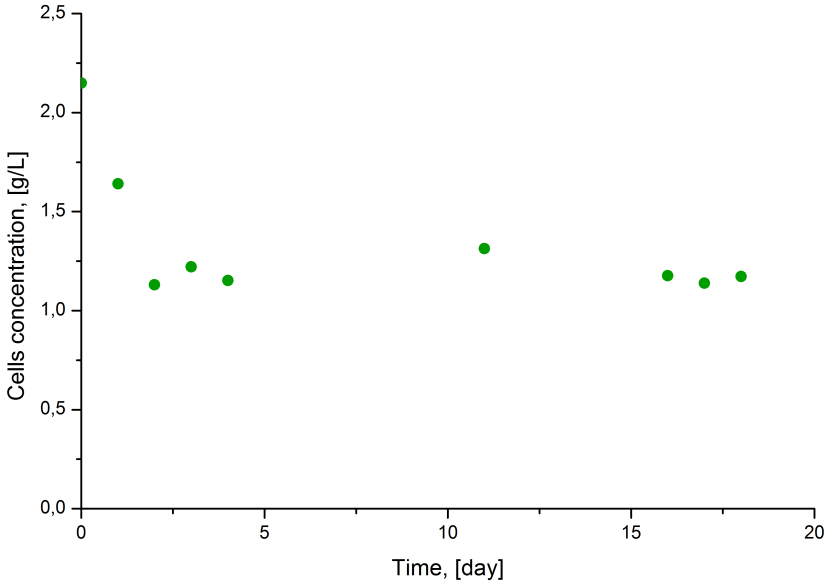

Figure 2.12: Collected data referring to the initial continuous mode without recycle for continuous test with recycle.

As visible, the cells concentration reached a stationary value of 1.2 g/L. Specific growth rate at steady state condition was still 0.603 d^{-1} because τ was kept at 1.66 d, fulfilling Equation 2.10, thus leading to a biomass productivity $P_a = 8.66$ $g/(m^2 d)$. Table 2.8 shows system in this condition.

At day 25 the recycle was started, by feeding back the biomass from the collecting bottle. As Section 2.2.3 underlines, only one pump was used for both micronutrients feed and recycle, so that the recycle flow rate could only be one half of the flow coming out the reactor: this allowed to keep $\tau = 1.66$ so comparisons between continuous reactor test with and without recycle could be carried out. Both micronutrients inlet flow (which was more concentrated to provide the necessary amount of vital conpounds) and recycle flow were 75 mL/d, so the reactor outflow was kept at 151 mL/d. For the particular system properties, the collecting bottle accumulated 75 mL/d of biomass solution. Figure 2.13 shows collected data during the entire test.
Cells concentration achieved an higher steady state value, that is 2.2 g/L.

Table 2.8: System data referring to the initial continuous mode without recycle for continuous test with recycle.

Data	Symbol	U.m.	Value
Micronutrients inlet flow	$\dot{V}_{in}$	mL/d	151
Culture outlet flow	$\dot{V}_{out}$	mL/d	151
Specific growth rate	K	d^{-1}	0.603
Residence time	τ	d	1.66
Stationary cells concentration	c_{out}	g/L	1.2
Areal biomass productivity	P_a	$g/(m^2 d)$	8.66
Volumetric biomass productivity	P_v	$kg/(m^3 d)$	0.725

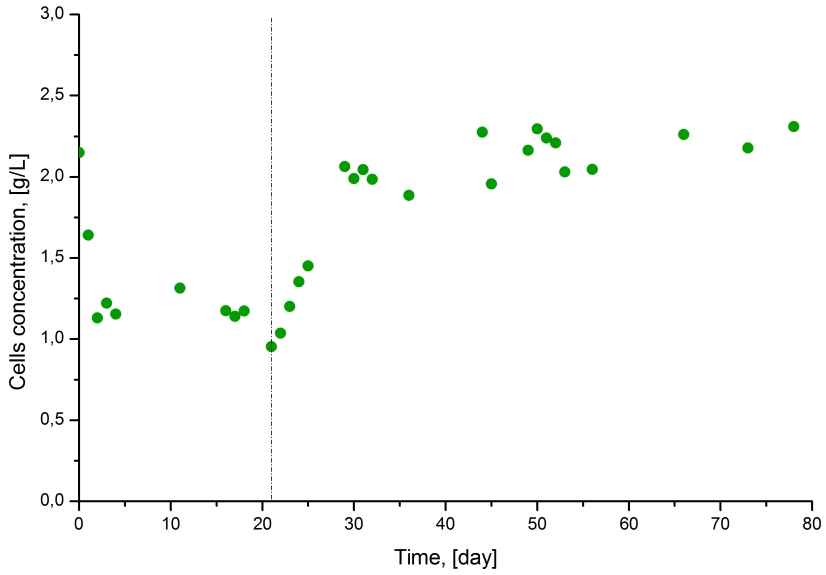

Figure 2.13: Collected data for continuous reactor test with recycle. Before recycle starts (day 25), the continuous reactor is at a steady state condition, as points before day 25 demonstrate.

The system with recycle can be represented by the scheme drawn in Figure 2.14.

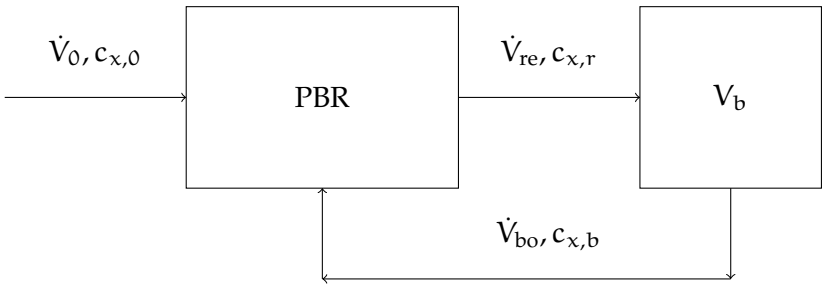

Figure 2.14: Scheme of the lab-scale reactor with recycle.

The equations describing the system are:

$$\begin{aligned} \dot{V}_0 + \dot{V}_{bo} &= \dot{V}_{re} \\ \dot{V}_{bo} &= R\dot{V}_0 \\ \dot{V}_{re} &= \frac{dV_b}{dt} + \dot{V}_{bo} \end{aligned} \tag{2.16}$$

and:

$$\begin{aligned} V_r \frac{dc_{x,r}}{dt} &= \dot{V}_{bo} c_{x,b} - \dot{V}_{re} c_{x,r} + V_r r_x \\ V_b \frac{dc_{x,b}}{dt} &= \dot{V}_{re} c_{x,r} - \dot{V}_{bo} c_{x,b} - c_{x,b} \frac{dV_b}{dt} \end{aligned} \tag{2.17}$$

where:

$\dot{V}_0$	micronutrients inflow at reactor, [L/d]
$\dot{V}_{bo}$	recycle inflow at reactor, [L/d]
$\dot{V}_{re}$	reactor outflow, [L/d]
R	recycle ratio, [adim]
V_r	reactor volume, [L]
V_b	collecting bottle volume, [L]
$c_{x,r}$	biomass concentration in reactor, [g/L]
$c_{x,b}$	biomass concentration in collecting bottle, [g/L]

At steady state condition, biomass concentration sent back to the reactor can be approximated to biomass concentration in the reactor. So, considering the photobioreactor alone:

$$\begin{aligned} 0 &= \dot{V}_{bo} \cancel{c_{x,b}} - \dot{V}_{re} \cancel{c_{x,r}} + V_r K \cancel{c_{x,r}} \\ &= \dot{V}_{bo} - \dot{V}_{re} + V_r K \\ K &= \frac{\dot{V}_{re} - \dot{V}_{bo}}{V_r} = 0.302\ d^{-1} \end{aligned} \tag{2.18}$$

Finally, productivity for a continuous reactor with recycle can be calculated as:

$$P_a = \frac{V_r r_x}{A} = \frac{\dot{V}_{bo} c_{x,b} - \dot{V}_{re} c_{x,r}}{A} \tag{2.19}$$

or:

$$P_v = \frac{V_r r_x}{V_r} = \frac{\dot{V}_{bo} c_{x,b} - \dot{V}_{re} c_{x,r}}{V_r} \tag{2.20}$$

The result are $P_a = 7.89$ g/(m^{2}d) and $P_v = 0.660$ kg/(m^{3}d).

Table 2.9 summarizes system properties for continuous test with recycle.

Table 2.9: System data related to continuous reactor test with recycle.

Data	Symbol	U.m.	Value
Micronutrients inlet flow	$\dot{V}_0$	mL/d	75
Culture outlet flow	$\dot{V}_{re}$	mL/d	151
Recycle inlet flow	$\dot{V}_{bo}$	mL/d	75
Recycle ratio	R	adim	1
Specific growth rate	K	d^{-1}	0.302
Residence time	τ	d	1.66
Stationary cells concentration	$c_{x,r}$	g/L	2.2
Areal biomass productivity	P_a	g/(m^{2}d)	7.89
Volumetric biomass productivity	P_v	kg/(m^{3}d)	0.660

For this test, a comparison between the continuous reactor before and after the recycle can be carried out. In fact, before day 25, 151 mL/d of biomass was continuously extracted from the system at 1.2 g/L and the productivity was 8.66 g/(m^{2}d) or 0.725 kg/(m^{3}d); when the recycle is on, 75 mL/d of biomass at 2.2 g/L can be extracted from the system at the steady state and this leads to a lower productivity of 7.89 g/(m^{2}d) or 0.660 kg/(m^{3}d).
As for any other biological reactor, a partial recycle of biomass is necessary to avoid wash-out problems and furthermore it raises the cells concentration inside the reactor. Nevertheless, the arrangement of this test did not show an improvement of reactor performances when the recycle started, as values of biomass productivity clearly demonstrate.

2.4 CONCLUSIONS

Several experimental tests were performed. Part of them was focused on the determination of *Scenedesmus obliquus* growth curves to obtain specific growth rates at different irradiances and another part was focused on the continuous production of biomass. From batch tests, the microalgae cultures irradiated at 150 $\mu E/(m^2 s)$ demonstrated the best results in terms of maximum cells concentration at stationary phase and specific growth rate. A first continuous reactor test was carried out after an initial batch mode necessary to reach an high microalgae concentration and specific growth rate inside the reactor; the stationary cells concentration was expected higher than the obtained one, 0.52 g/L. For this test a biomass productivity of 3.75 $g/(m^2 d)$ or 0.314 $kg/(m^3 d)$ was calculated. A second continuous reactor test at 165 $\mu E/(m^2 s)$ was set up, starting with a concentrated cells solution: the steady state was found to be at 1.2 g/L, with a biomass productivity of 8.66 $g/(m^2 d)$ or 0.725 $kg/(m^3 d)$. After 25 days the recycle was started and the residence time, defined as the ratio between the reactor volume and the volumetric outflow, was kept at the same value as previous continuous tests, 1.66 d. Cells concentration laid at 2.2 g/L and biomass productivity was 7.89 $g/(m^2 d)$ or 0.660 $kg/(m^3 d)$.

3

PHOTOBIOREACTOR MODELLING

The experimental section is useful to provide data which are the basis for the development of a model able to represent them. The first part of this chapter will focus on the description of Cornet model (Cornet, Dussap, and Gros 1995), generalized by Pruvost (Pruvost *et al.* 2011); the subject will be expanded on solar radiation which will be a topic of Chapter 5.
Three phenomena have to be modelled for simulating a photobioreactor:

1. the value of photosynthetic active radiation (PAR) hitting the surface of the reactor;
2. the determination of irradiance profile along the reactor depth;
3. the growth rate as a function of light along the reactor depth.

In particular, biomass growth is a complex process, affected by multiple effects such as photosynthesis, fluid-dynamics and light attenuation. In case of non-limiting nutrients conditions, light is the most relevant factor for photosynthetic growth: microalgae culture are normally limited by radiant energy availability, which decreases along the reactor depth because of both absorption and scattering phenomena, leading to the presence of highly irradiated and dark zones, respectively. For this reason, a mixing system may help cells movement among zones of different light intensities and improve performance of the system: this so called flashing light effect enhances the photobioreactor productivity, as many authors reported (Grobbelaar, Nedbal, and Tichy 1996; Tichy *et al.* 1995).
In the following, two important items for the definition of photobioreactor performance are presented: the biomass productivity and the photosynthetic efficiency.

3.1 CORNET MODEL

As already stated, light availability is the most important variable for biomass growth. In order to simulate the behaviour of a photobioreactor, a mathematical model has to be developed to represent the correct profile of irradiance inside the reactor. An efficient mixing does not assure homogeneity of this distribution: light radiation is function of total radiation hitting the culture surface, optical properties of biomass and distance from the surface.
The Cornet approach to these problems is divided into four subsequent operations:

- irradiance values at each point z of the reactor is determined through an exponential law;
- growth rate at each point is linked to the corresponding irradiance value at the same point;
- values of the reaction rate constant are averaged along the reactor depth to provide a unique growth rate;
- the latter is used in mass balances.

3.1.1 *Light distribution*

It is far beyond this thesis scope to illustrate and explain all the mathematical concepts necessary for the formulation of the light distribution law; details are presented by Sciortino 2010. Among them, it can be recall that the Cornet model refers to an isotropic radiative field and the scattered part of light is considered to be parallel to the main radiation direction. Furthermore, the method refers to artificial light but can be expanded to consider the dynamic nature of solar radiation, expressed by incident angle variations and ratio between direct and diffuse light changing during the day.
Accordingly, the extinction profile of direct and diffused radiation along z-dimension (depth) of the photobioreactor can be expressed by:

$$\frac{I_{dir}(z)}{I_{dir}(0)} = \frac{2}{\cos\theta}\frac{(1+\alpha)\exp[-\delta_{dir}(z-h)] - (1-\alpha)\exp[\delta_{dir}(z-h)]}{(1+\alpha)^2\exp[\delta_{dir}h] - (1-\alpha)^2\exp[-\delta_{dir}h]} \tag{3.1}$$

$$\frac{I_{dif}(z)}{I_{dif}(0)} = 4\frac{(1+\alpha)\exp[-\delta_{dif}(z-h)] - (1-\alpha)\exp[\delta_{dif}(z-h)]}{(1+\alpha)^2\exp[\delta_{dif}h] - (1-\alpha)^2\exp[-\delta_{dif}h]} \tag{3.2}$$

$$\delta_{dir} = \frac{\alpha c_x}{\cos\theta}(Ea + 2bEs) \tag{3.3}$$

$$\delta_{dif} = 2\alpha c_x(Ea + 2bEs) \tag{3.4}$$

$$\alpha = \sqrt{\frac{Ea}{(Ea + 2bEs)}} \tag{3.5}$$

where:

$I_{dir}(z)$ direct PAR at depth z, $[\mu E/(m^2 s)]$
$I_{dir}(0)$ direct PAR at depth 0, $[\mu E/(m^2 s)]$
$I_{dif}(z)$ diffuse PAR at depth z, $[\mu E/(m^2 s)]$
$I_{dif}(0)$ diffuse PAR at depth 0, $[\mu E/(m^2 s)]$

θ incident radiation angle with respect to normal direction of reactor surface, [rad]

h depth of PBR, [m]

z reactor dimension along the depth, [m]

E_a absorption mass coefficient, [m^2/kg]

E_s scattering mass coefficient, [m^2/kg]

b backscattering fraction, [adim]

Knowing the irradiance reaching the surface ($I_{dir}(0)$, $I_{dif}(0)$ and θ) and the optical properties of the microalgae species (E_a, E_s and b), the irradiance values at each point along the reactor depth can be calculated:

$$I(z) = I_{dir}(z) + I_{dif}(z) \tag{3.6}$$

3.1.2 *Kinetic growth: photosynthesis and maintenance*

As Luo and Al-Dahhan 2003 suggested, two kinds of model exist describing the photosynthesis rate as a function of irradiance: the static types and dynamic ones. Static models are the simplest and the most used for photobioreactor performance determination and reactor design; they are based on empirical or semi-empirical data but they lack generality, ignoring the dynamic nature of represented phenomena. Dynamic models are able of representing physiology phenomena, such as photoinibition and photolimitation; the relation between growth rate and irradiance is in this case based on cell physiology and not on experimental data, but on the other hand these models are more complex than static ones.
Cornet model belongs to the first category but it is considered as one of the most accurate to represent the system of interest (Palma 2011).

When a mass balance on a continuous photobioreactor has to be solved (Equation 2.17), this implies determining the biomass growth rate r_x, which is actually a mean value. This average is caused by the heterogeneous light distribution inside the culture volume, given by absorption and scattering phenomena (Pruvost *et al.* 2011). In particular, for the described laboratory system, where light undergoes a one-dimensional attenuation, the mean growth rate consists in a simple integration along the reactor depth:

$$r_x = \frac{1}{h}\int_0^h r_{x,t} \cdot dz \tag{3.7}$$

Biomass is produced at each point of the reactor according to this global reaction rate $r_{x,t}$; however, this value is considered as a difference of two contributions: a biomass duplication rate and a maintenance respiration term, which also considers the death kinetic, thanks

to this definition. The concept is expressed by the following equation:

$$r_{x,t} = r_{x,p} - r_{x,m} \tag{3.8}$$

where $r_{x,p}$ represents the growth due to photosynthesis and $r_{x,m}$ the maintenance process.
The Cornet model provides a formulation for photosynthetic growth as a function of irradiance at each point of the reactor depth:

$$r_{x,p}(z) = \rho_m \frac{K}{K + I(z)} \phi E a I(z) c_x \tag{3.9}$$

where:

- $r_{x,p}(z)$ biomass growth rate at z-depth, [kg/(m^{3}s)]
- ρ_m maximum energetic yield for photon conversion, [adim]
- K half saturation constant for photosynthesis, [μE/(m^{2}s)]
- ϕ mass quantum yield for Z-scheme of photosynthesis, [kg/μE]

The maintenance contribution has to be taken into account when quantifying a kinetic growth, because it limits somehow the duplication rate ($r_{x,p}$) diverting part of light energy from production of new cell material to cell physiological functions. These include (Bodegom 2007):

- shifts in metabolic pathways;
- cell motility;
- changes in stored polymeric carbon;
- osmoregulation;
- proofreading, synthesis and turnover of enzymes and other macromolecular compounds;
- defence against O_2 stress.

These limitations are represented by a negative contribution to Equation 3.8, which can be expressed as:

$$r_{x,m} = \mu_e c_x \tag{3.10}$$

where μ_e is the maintenance constant, [time^{-1}].
Thus, Equation 3.8 can be written as:

$$r_{x,t} = \mu_{eff} c_x = \rho_m \frac{K}{K + I(z)} \phi E a I(z) c_x - \mu_e c_x \tag{3.11}$$

$$= \mu c_x - \mu_e c_x \tag{3.12}$$

and

$$\mu_{eff} = \mu - \mu_e \tag{3.13}$$

where:

μ_{eff} specific growth rate measured experimentally, $[d^{-1}]$
μ specific duplication rate (Cornet model), $[d^{-1}]$

Determination of μ_e can be carried out experimentally, by extrapolating the relation between μ_{eff} and irradiance at $I = 0$, with the assumption that this relation is linear at low irradiance, that is:

$$\mu_{eff} = \alpha_i I - \mu_e \tag{3.14}$$

where α_i is the initial slope, $[m^2 s/(\mu E \cdot d)]$.

3.2 MAXIMUM BIOMASS PRODUCTIVITY

Understanding the upper limit in production of biomass is a fundamental step to address correctly the performance of any photobioreactor system. The maximum productivity is calculated as maximum biomass production per year per unit area by considering that each photon reaching the system is converted into chemical energy and this energy is totally used for production of new material rather than partially diverted into maintenance processes.

As for any other physical process, the first law of thermodynamics limits the microalgae production:

$$\dot{E}_{in,area} \geqslant \dot{E}_{stored,area} \tag{3.15}$$

where:

$\dot{E}_{in,area}$ power of solar radiation per unit area, $[W/m^2]$
$\dot{E}_{stored,area}$ energy flux per unit area stored as biomass, $[W/m^2]$

so the energy stored as biomass cannot exceed the amount of the incident sun energy. In particular, photosynthesis is responsible for this conversion, and it can be approximated by the following reaction:

$$CO_2 + H_2O + 8\,\text{photons} \longrightarrow CH_2O + O_2 \tag{3.16}$$

where CH_2O is considered as $1/6$ of glucose.
Maximum biomass production can be so calculated as:

$$P_{max} = \frac{N_{CO_2,red} E_{carb}}{E_{bio}} \tag{3.17}$$

where:

$N_{CO_2,red}$	yearly CO_2 moles reduced to carbohydrate per unit area, [mol/(m^{2}y)]
E_{carb}	carbohydrate heat of combustion, [J/mol]
E_{bio}	biomass heat of combustion, [J/g]

Moreover, the term $N_{CO_2,red}$ can be calculated as follows:

$$N_{CO_2,red} = \frac{E_{sun}(\%PAR/100)}{E_{pho}QR} \tag{3.18}$$

where:

E_{sun}	yearly total solar energy reaching the system per unit area, [J/(m^{2}y)]
%PAR	PAR percentage of total solar energy, [%]
E_{pho}	average energy per mole of photons, [J/mol]
QR	quantum requirement, [moles of photons/moles of reduced CO_2]

3.2.1 *Total solar energy*

The term E_{sun} is provided by the online Photovoltaic Geographical Information System (*PVGIS Solar Irradiation Data, 2007*). For the location of Padua this value is calculated as 4541 MJ/(m^{2}y).

3.2.2 *Photosynthetic Active Radiation percentage*

Microalgae can absorb only a portion of the total radiation coming from the sun, and this part corresponds to wavelengths that can be used for photosynthesis. It is represented by the solar spectrum limited by wavelength between 400 and 700 nm:

$$\begin{aligned} \%PAR &= \frac{\text{PAR energy}}{\text{Full-spectrum energy}} \times 100 \\ &= \frac{\int_{\lambda = 400\text{ nm}}^{700\text{ nm}} E_{sun}(\lambda)d\lambda}{\int_{\lambda = 0\text{ nm}}^{4000\text{ nm}} E_{sun}(\lambda)d\lambda} \end{aligned} \tag{3.19}$$

For this calculation, the reference solar spectral irradiance at air mass 1.5 is used (*Reference Solar Spectral Irradiance: Air Mass 1.5*): values of solar power per unit area are provided for all wavelengths and the stated integrals can be carried out. %PAR is so determined to be 42.98%. Although the value is in agreement with published literature, it is fundamental to remind that pigments absorbs best at the edges of the range called photosynthetically active (blue and red light) rather than in the middle (green), so that %PAR could overestimate the real amount of available radiation for microalgae (Weyer *et al.* 2010).

3.2.3 *Photon energy*

Planck law allows to determine the energy of any photon knowing the respective wavelength:

$$E_{pho} = c_l \frac{h_p}{\lambda} \tag{3.20}$$

where:

h_p Planck constant $= 6.63 \cdot 10^{-34}$ [Js]
c_l speed of light $= 2.998 \cdot 10^{8}$ [m/s]
λ wavelength, [m]

At the edge $\lambda = 400$ nm the photon energy is around 299 kJ/mol and at $\lambda = 700$ nm the value is ca. 171 kJ/mol. Considering a mean wavelength of $\lambda = 531$ nm, $E_{pho} = 225.3$ kJ/mol can be obtained.

3.2.4 *Carbohydrate energy content*

This term derives from the simplification of Equation 3.16, where solar energy is stored as simple CH_2O. An average value is reported to be 482.5 kJ/mol (ivi).

3.2.5 *Quantum requirement*

The quantum requirement term represents the moles of photons to reduce a mole CO_2 to CH_2O; with the assumption of perfect efficiency, QR should be 3, because 3 of the least energetic photons (700 nm) have an energy slightly higher than the required 482.5 kJ/mol. A more realistic number is still subject of debate even if a quantum requirement value of 8 seems to obtain more consents (Hartmut 2012).

3.2.6 *Biomass energy content*

E_{bio} represents the biomass heat of combustion. Literature values for E_{bio} ranges from 20 to 23.75 kJ/g, depending on the percentage of lipids (and on the type) that microalgae accumulate.

3.3 REAL BIOMASS PRODUCTIVITY

Equation 3.17 presents two unrealistic assumptions, i.e., all photons are captured by cells and they are diverted to new material production. For this reason the equation has to be modified by adding some efficiencies which take into account the non-ideality of the system:

$$P_r = \frac{N_{CO_2,red} E_{carb}}{E_{bio}} \eta_{ft} \eta_{fu} \eta_{ba} \tag{3.21}$$

where:

- η_{ft} photons transmission efficiency, [moles of transmitted photons/moles of hitting photons]
- η_{fu} photons utilization efficiency, [moles of used photons/moles of transmitted photons]
- η_{ba} biomass accumulation efficiency, [adim]

3.3.1 *Photons transmission efficiency*

This efficiency accounts for losses of incident light due to the geometry of the system, such as reflection or absorption by the external surfaces of the reactor, or to microalgae scattering phenomena; even if a value of 100% is unreal, a good setting of the entire system could rise this efficiency to 90%.

3.3.2 *Photons utilization efficiency*

Microalgae living under optimal environmental conditions could absorb and use almost all the energy reaching the culture; but non-optimal conditions (high-light levels, temperature too far from normal growth value) force cells to re-emit part of the income photons as heat or chlorophyll fluorescence (Baker 2008).

3.3.3 *Biomass accumulation efficiency*

This term represents the portion of energy that is diverted to cellular functions rather than stored as biomass; it measures cell maintenance and for this reason its estimation depends on the species and environmental aspects. Literature values ranges from 10-90% (Weyer *et al.* 2010) but generally this efficiency is included in the photobioreactor kinetic model with the maintenance constant.

3.4 PHOTOSYNTHETIC EFFICIENCY

The photosynthetic efficiency for a microalgae system is a kind of "real gauge" of the photobioreactor performance; in fact, it represents the part $\dot{E}_{stored}$ of the total energy (light) income per unit time $\dot{E}_{in}$ used for production of biomass:

$$\psi = \frac{\dot{E}_{stored}}{\dot{E}_{in}} \tag{3.22}$$

Determination of the energy stored as biomass per unit time refers to a steady state condition, when the microalgae concentration extracted from the photobioreactor does not change with time, and it can be car-

ried out using either the enthalpy of formation of microalgae (ΔH_f^0) or using the lower heating value (LHV).

3.4.1 *Enthalpy of formation of microalgae*

This method can be applied for any reactive system and it presumes that the specific enthalpies of compounds of the reaction are known. The enthalpy rate of change due to the reaction $\Delta\dot{H}$, [J/s], is calculated by:

$$\Delta\dot{H} = \dot{E}_{stored} = \sum \dot{m}_{out} H_{out} - \sum \dot{m}_{in} H_{in} \tag{3.23}$$

where:

$\dot{m}_{out}$	mass flow of each product, [kg/s]
$\dot{m}_{in}$	mass flow of each reactant, [kg/s]
H_{out}	specific enthalpy of each product, [J/kg]
H_{in}	specific enthalpy of each reactant, [J/kg]

Values of specific enthalpies are expressed by the following formula:

$$H = \Delta H_f^0 + \int_{T_{ref}}^{T} c_p \, dT \tag{3.24}$$

where:

ΔH_f^0	standard enthalpy of formation, [J/kg]]
c_p	specific heat, [J/(kg·K)]
T_{ref}	reference temperature, [K]

The reference temperature is usually set to 25 °C. Since the growth temperature of microalgae is usually close to this value, the integral term can be neglected.
For microalgae production, the reaction of biomass formation can be approximated by:

$$CO_2 + H_2O \longrightarrow \text{microalgae} + O_2 \tag{3.25}$$

In this case, microalgae are considered to be an output of the simplified reaction, thus ΔH_f^0 of microalgae has to be determined. O_2 has zero enthalpy of formation since it is considered an elementary compound, so it will be neglected in the following steps.
Equation 3.23 requires the knowledge of the amount of reactants needed for microalgae formation; this link is provided by the elemental analysis of biomass:

$$\dot{m}_{CO_2} = w_C P \frac{MM_{CO_2}}{MM_C}$$

$$\dot{m}_{H_2O} = w_O P \frac{MM_{H_2O}}{MM_O}$$

where:

w_C	mass fraction of carbon in microalgae, [adim]
w_O	mass fraction of oxygen in microalgae, [adim]
P	biomass production at steady state, [g/s]
MM_{CO_2}	molar mass of carbon dioxide, [g/mol]
MM_{H_2O}	molar mass of water, [g/mol]
MM_C	molar mass of carbon, [g/mol]
MM_O	molar mass of oxygen, [g/mol]

The final equation to be solved is:

$$\dot{E}_{stored} = P \cdot H_{algae} = P\Delta H^0_{f,algae} - \dot{m}_{CO_2}\Delta H^0_{f,CO_2} - \dot{m}_{H_2O}\Delta H^0_{f,H_2O} \quad (3.26)$$

The work of Palma 2011 reported that $\Delta H^0_{f,algae}$ can be calculated directly from the lower heating value E_{bio}. In particular, a specific Aspen Plus™ flowsheet for a combustion feasibility study provided the standard enthalpy of formation of microalgae once E_{bio} was defined. The process was run at 25 °C and 1 atm, and all the following calculations refer to 1 kg of microalgae.
A flow of biomass elemental compounds, which corresponds to the microalgae elemental analysis reported in Table 4.1, is initially sent to a combustion reactor and the heating value $\Delta H_{comb,elem}$, [J/kg], is evaluated:

$$\begin{aligned} C + N + O + H &\longrightarrow CO_2 + N_2 + H_2O \\ \Delta H_{comb,elem} &= \Delta H^0_{f,prod} - \Delta H^0_{f,elem} \end{aligned} \quad (3.27)$$

where:

$\Delta H^0_{f,prod}$	standard enthalpy of formation of combustion products, [J/kg]
$\Delta H^0_{f,elem}$	standard enthalpy of formation of elemental compounds, [J/kg]

In the same way, it is possible to determine the microalgae heating value $\Delta H_{comb,algae}$, [J/kg]:

$$\begin{aligned} \text{microalgae} &\longrightarrow CO_2 + N_2 + H_2O \\ \Delta H_{comb,algae} &= \Delta H^0_{f,prod} - \Delta H^0_{f,algae} \end{aligned} \quad (3.28)$$

In this process, the author stated a negative value for $\Delta H_{comb,algae}$, so that it corresponds to $-E_{bio}$.
Subtracting Equation 3.27 and Equation 3.28 the standard enthalpy of formation of microalgae can be calculated:

$$\Delta H^0_{f,algae} = \Delta H^0_{f,prod} - \Delta H_{comb,algae} \quad (3.29)$$

where $\Delta H^0_{f,elem} = 0$ because it refers to elemental compounds. Moreover, Equation 3.26 can be expressed as:

$$\begin{aligned}\dot{E}_{stored} &= P\Delta H^0_{f,algae} - \dot{m}_{prod}\Delta H^0_{f,prod} \\ &= \cancel{\dot{m}_{prod}\Delta H^0_{f,prod}} - P\Delta H_{comb,algae} - \cancel{\dot{m}_{prod}\Delta H^0_{f,prod}} \\ &= -P\Delta H_{comb,algae} \\ &= P \cdot E_{bio} \end{aligned} \tag{3.30}$$

So the energy stored as biomass E_{stored} can be determined by the standard enthalpy of formation of microalgae or directly by the biomass heat of combustion E_{bio}.

3.4.2 *Lower heating value*

The following method can be used for the determination of photosynthetic efficiency, because most of the time ΔH^0_f of microalgae is not available. The energy stored as biomass is expressed as:

$$\dot{E}_{stored} = P(w_{oil}LHV_{oil} + w_{residue}LHV_{residue}) = P \cdot E_{bio} \tag{3.31}$$

where:

w_{oil}	mass fraction of oil in microalgae, [adim]
$w_{residue}$	mass fraction of residue (non-oil) in microalgae, [adim]
LHV_{oil}	lower heating value of oil, [J/g]
$LHV_{residue}$	lower heating value of residue, [J/g]

So, the biomass energy E_{bio} is dependent on the heat of combustion of both the oil contained in it and the cell residue, which have to be known for the correct estimation of $\dot{E}_{stored}$.

3.5 MAXIMUM PHOTOSYNTHETIC EFFICIENCY

Photosynthetic efficiency presents an upper limit which cannot be exceeded for thermodynamic reasons; this edge is expressed as:

$$\psi_{max} = \frac{E_{carb}}{E_{pho}QR}\frac{\%PAR}{100} \tag{3.32}$$

Using the same values for terms described in Section 3.2, a maximum photosynthetic efficiency of 30.68% of PAR can be calculated. This means that only 30.68% of solar photosynthetic active energy is available for conversion to biomass, or 13.19% of total solar energy.

4

MODELLING RESULTS

This chapter presents simulation results of the lab-scale reactor with recycle using the modelling procedure described in Chapter 3. In particular, the model parameters, i.e., optical properties of *Scenedesmus obliquus* (absorption coefficient E_a and backscattering coefficient b_{Es}) and maintenance term μ_e are determined based on measurements of the dynamics of the system and on the irradiance attenuation inside the reactor, using Matlab® codes developed in this thesis. The photosynthetic efficiency s calculated and the energy balance is discussed for this system. Finally, the maximum biomass production rate is investigated and a comparison between CSTR or PFR approximation for the reactor is made in order to identify the best performances.

4.1 MODEL PARAMETERS

In Section 2.3.3 the system is modelled by two groups of equations (Equation 2.16, Equation 2.17), under the assumption that both the reactor and the collecting bottle can be approximated to CSTRs. It is clear that the correct interpretation of experimental data shown in Figure 2.13 implies a good modelling of the variable r_x, which is the only unknown term. As already explained, the Cornet model, as generalized by Pruvost, needs the knowledge of some parameters specific for each microalga, which will be determined in the following.

4.1.1 *Absorption, scattering and backscattering coefficient*

In order to describe accurately the light transfer inside the reactor, optical properties of the specific microalga have to be known. In fact, any microalgae culture can be considered as a dispersion of particles where the light entering the liquid is partially absorbed and partially scattered. The former phenomenon is caused by microalgae pigments, such as chlorophyll and carotenoids, and the latter one by the fact that cells have a countable volume.
A predictive determination of these coefficients is reported by Pottier *et al.* 2005, according whom optical properties of any microalgae culture can be determined once the following terms are known:

- type and amount of each pigment contained in the solution;
- microalgae dimensions distribution;
- microalgae shape.

Furthermore, in vivo spectra of all pigments have to be available. Once these data are available, the Lorenz-Mie theory can be used, which is based on the complex refractive index of the particle m:

$$m = n \pm ik_\lambda \tag{4.1}$$

where:

- n real part responsible for scattering, [adim]
- k_λ imaginary part responsible for absortion, [adim]

Determination of n can be done by simple transmittance measurements of the culture at an irradiance wavelength where microalgae do not absorb, so that only scattering phenomenon occurs. The imaginary part k_λ is expressed by:

$$k_\lambda = \frac{\lambda}{4\pi}\rho_{dm}\frac{1-x_w}{x_w}\sum_{i=1}^{N} Ea_{pig.i}(\lambda)w_{pig.i} \tag{4.2}$$

where:

- $Ea_{pig.i}$ in vivo spectral mass absorption coefficient of pigment i, [m^2/kg]
- $w_{pig.i}$ mass fraction of pigment i, [kg/kg of biomass]
- ρ_{dm} density of biomass dry material, [kg/m^3]
- x_w in vivo volume fraction of water in the cell, [adim]

The latter is determined by equation:

$$x_w = 1 - \frac{c_x}{N_p}\frac{1}{V_{32}}\frac{1}{\rho_{dm}} \tag{4.3}$$

where:

- N_p cell number density, [$1/m^3$]
- V_{32} mean (Sauter) particle volume, [m^3], taking into account the given size distribution

Starting from these relations, the calculation of the optical properties of the microalga can be performed using Lorenz-Mie theory and assuming spherical particles. In particular, absorption and scattering cross-sections C_{ABS} and C_{SCA}, [m^2], are firstly quantified, and then used as follows:

$$Ea_\lambda = \frac{C_{ABS,\lambda}}{V_{32}\rho_{dm}(1-x_w)} \tag{4.4}$$

$$Es_\lambda = \frac{C_{SCA,\lambda}}{V_{32}\rho_{dm}(1-x_w)} \tag{4.5}$$

Authors advise not to simply average values referred to single wavelengths, but to adopt a more precise method which will not be described here.

These parameters play a fundamental role for the correct simulation of a real photobioreactor, but a databank of the entire pigments range and their properties related to the known microalgae is still missing and literature is lacking of data. For these reasons, the predictive method described above was not used and absorption $E\alpha$ and backscattering bEs coefficients for *Scenedesmus obliquus* were directly evaluated from laboratory experimental results.
It is noteworthy that the calculated optical properties offer the highest precision in the particular system conditions where they have been obtained from; in fact, the most the operative conditions change, the less accurate optical properties will be in the prediction of the system behaviour.

4.1.2 *Maximum energetic yield for photon conversion*

Following the statement reported in (Pruvost *et al.* 2011), the maximum energy yield for photon dissipation in antennae can be considered as a moderately species-independent value, so that $\rho_m = 0.8$.

4.1.3 *Half saturation constant for photosynthesis*

This term can be determined by Figure 2.9 and it represents the value of irradiance at which half of the maximum exponential growth rate is reached: K was set to 75 $\mu E/(m^2 s)$ accordingly.

4.1.4 *Mass quantum yield for Z-scheme of photosynthesis*

This parameter represents the amount of biomass produced per mole of photons captured by the cells.

Table 4.1: Elemental analysis of *Scenedesmus obliquus* with 25% oil.

Element	Mass fraction [%]
C	52.1
H	8.04
N	8.05
O	28
P	0.35

Elemental analysis of *Scenedesmus obliquus* reported in Table 4.1 permits to write the overall stoichiometry of the microalga:

$$CH_{1.852}N_{0.132}O_{0.403}P_{\sim 0} \tag{4.6}$$

Biomass weight per mole of carbon has a value of $x_{alga} = 22.15$ g/mol_C. Equation 3.16 shows that 8 moles of photons, n_{pho}, are required for the formation of a mole of 1/6 of glucose, that is a mole of carbon, n_C, so:

$$\phi = \frac{x_{alga} n_C}{n_{pho}} \tag{4.7}$$

The result is $\phi = 2.77 \cdot 10^{-9}$ kg/µE.

4.1.5 *Maintenance term*

As Equation 3.11 underlines, μ_e represents a limitation to cell duplication and it can be obtained by extrapolation at $I = 0$ of the relation between specific growth rate measured experimentally and irradiance; Herman and Luuc 1980 reported a value of $8 \cdot 10^{-3}$ h^{-1} for *Scenedesmus obliquus*.

4.2 OPTICAL PROPERTIES DETERMINATION

Knowledge of absorption coefficient $E\alpha$, scattering coefficient Es and backscattering fraction b are of primary importance when trying to simulate the behaviour of a microalgae culture in a photobioreactor. In order to represent correctly such a system, not only the dynamics of the reactor has to be predicted, but also the distribution of light along the rector depth. This is due to the connection between irradiance and growth rate expressed by Cornet model (Equation 3.9), typical of a light-limited system. Due to the particular setting of the reactor with recycle it is not possible to experimentally measure the values of irradiance at each point of the reactor depth; a good compromise is to use back irradiances which represent irradiance values after the back sheet of the reactor and can be linked to the internal cells concentrations (Figure 2.6).
It is noteworthy that Cornet model always considers the term bEs, i.e. the product between backscattering fraction and scattering coefficient, that is the only part of light back scattered to the direction of the irradiance source. This comes from the assumption that the scattered part of light is parallel to the main radiation direction.
At this point, irradiance reaching the front side of the reactor is known and an exponential attenuation law given by Cornet model can simulate the distribution of light along the reactor depth. In particular, back irradiances can be calculated and compared to the experimental values. A Matlab® code called *optim1.m* optimizes values of $E\alpha$ and

bEs (the latter considered as a unique parameter to be determined) to minimize the error between calculated back irradiances and experimental ones.
Inputs for this code are:

- irradiance reaching the reactor $I = 165\ \mu E/(m^2 s)$;
- depth of the reactor $h = 0.012$ m;
- values of experimental back irradiances and corresponding cells concentrations;
- initial estimation of the two parameters Ea and bEs.

These terms are considered the arguments of *fminsearch* function which is divided into the following steps:

1. a *for* loop determines the light attenuation along the reactor depth using the provided inputs, that is, for the initial estimation of Ea and bEs, an evaluation of back irradiances at different cells concentrations is performed using the Cornet model (Equation 3.1);
2. the obtained vector containing the calculated back irradiances at the corresponding cells concentrations $I_{back,calc}$, $[\mu E/(m^2 s)]$, is compared to the vector containing the experimental values $I_{back,exp}$, $[\mu E/(m^2 s)]$, as shown in Figure 2.6; the error is define as:

$$\varepsilon_I = \text{norm}\left(\frac{I_{back,calc} - I_{back,exp}}{I_{back,exp}}\right) \tag{4.8}$$

3. if norm $\varepsilon_I < 1{\cdot}10^{-4}$, then the function prints the optimized parameters; if this condition is not fulfilled, Ea and bEs are automatically changed until the error value is lower than the tolerance.

Table 4.2: Optical properties of two microalgae

Microalga	Ea $[m^2/kg]$	Es $[m^2/kg]$	b [adim]	bEs $[m^2/kg]$
Arthrospira platensis [a]	162	636	0.03	19.08
Neochloris oleoabundans [b]	360	2380	0.003	7.14

[a] (Pruvost *et al.* 2010)
[b] (Pruvost *et al.* 2011)

The initial estimation of the two parameters can be decided considering optical properties of other microalgae, as reported in Table 4.2. The regression code provides the following results:

$$Ea = 14\,m^2/kg \tag{4.9}$$

$$bEs = 342\,m^2/kg \tag{4.10}$$

and the correlation is shown in Figure 4.1.

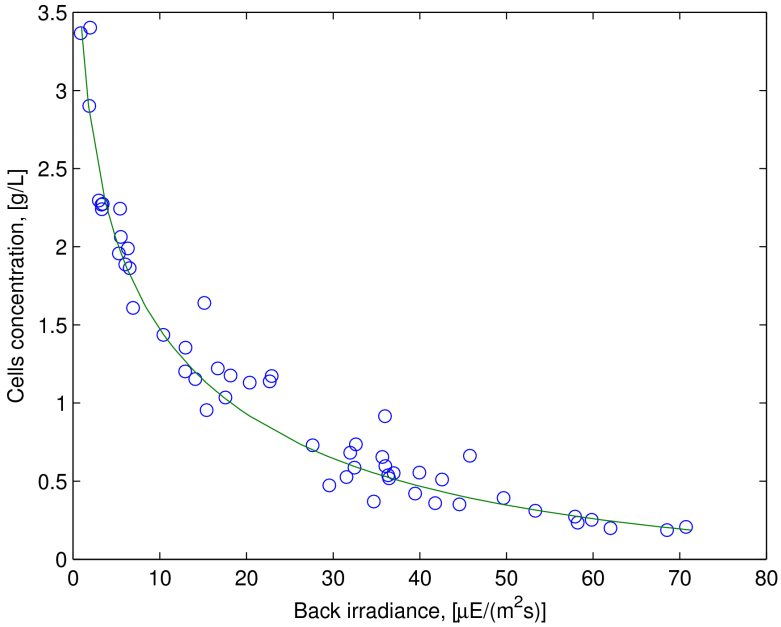

Figure 4.1: Back irradiance values at different cells concentrations using $Ea = 14\ m^2/kg$ and $bEs = 342\ m^2/kg$. Blue circles represent back irradiances measured experimentally and the green line represents the model correlation of back irradiances.

In order to validate these results, another code is performed, *massbalance.m*, where the lab-scale reactor system with recycle is simulated. For this purpose, code inputs are represented by:

- irradiance reaching the reactor $I = 165\ \mu E/(m^2 s)$;
- reactor volume $V_r = 0.25$ L;
- depth of the reactor $h = 0.012$ m;
- accumulation of volume in the collecting bottle $\frac{dV_b}{dt} = 0.075$ L/d;
- micronutrients inflow at the reactor $\dot{V}_0 = 0.075$ L/d;
- recycle inflow at the reactor $\dot{V}_{bo} = 0.075$ L/d;
- reactor outflow $\dot{V}_{re} = 0.151$ L/d;

- at $t = 0$ (switch on of the recycle): values of cells concentration in the reactor $c_{x,r} = 0.95$ g/L and in the collecting bottle $c_{x,b} = 0.95$ g/L, and collecting bottle volume $V_b = 1 \cdot 10^{-6}$ L. Values for cells concentrations are provided by Figure 2.13, whereas V_b is set to a non-zero low value to avoid numerical problems;
- values of ρ_m, K, ϕ, μ_e as reported in the previous section, and values of Ea and bEs determined by *optim1.m*.

The code *massbalance.m* solves the ordinary differential equations described in Section 2.3.3 from day 0, when the recycle starts, until day 60. In particular, the term r_x is implemented following Equation 3.7. Figure 4.2 shows this simulation.

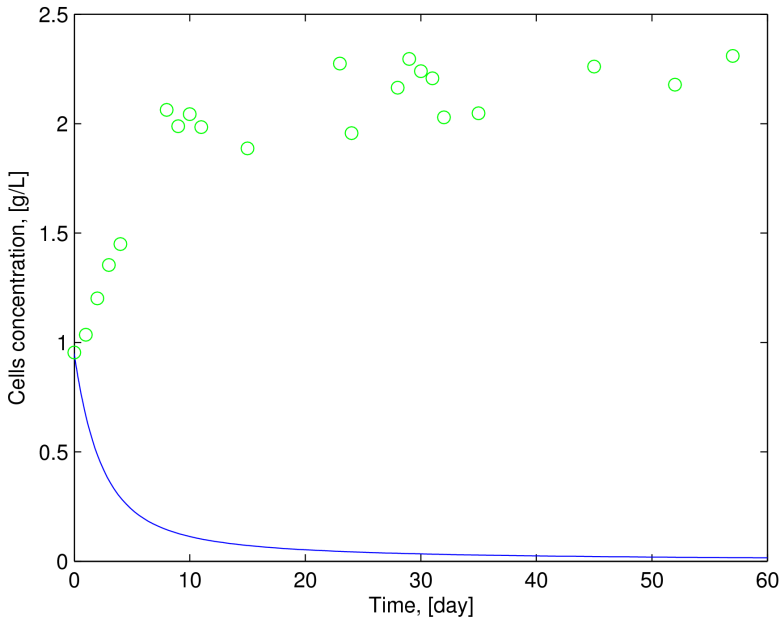

Figure 4.2: Dynamics of the reactor test with recycle using Ea = 14 m^2/kg and bEs = 342 m^2/kg. Green circles represent experimental data and the blue line represents the model correlation.

It is clear that the optical properties determined by *optim1.m* can not describe correctly the dynamics of the system: cells concentration goes rapidly to zero whereas it should reach 2.2 g/L at the steady state condition. Furthermore, the comparison between calculated Ea and bEs for *Scenedesmus obliquus* and values reported in Table 4.2 for the other two microorganisms indicates the huge difference between values of absorption and backscattering coefficients for other microalgae.
Therefore, the reactor dynamics is used, in order to determine the optical properties suitable for a correct simulation of the system. In fact, from Equation 3.11 the growth rate presents a dependency on the irradiance at each reactor point and on the absorption coefficient; the

latter has a relevant effect on $r_{x,t}$ and more generally on the correct representation of the reactor behaviour by mass balances described in Section 2.3.3. Another Matlab® code, *overall.m*, was so developed to this scope. It is divided into three steps:

1. value of bEs is estimated and absorption coefficient is changed by a first *fminsearch* function which simulates dynamics of the reactor with recycle; in particular, ε_c is minimized:

$$\varepsilon_c = \text{norm}\left(\frac{c_{x,calc} - c_{x,exp}}{c_{x,exp}}\right) \tag{4.11}$$

   where:

   $c_{x,calc}$ vector of calculated cells concentrations from the beginning of the reactor experiment with recycle (day 0) and the achievement of the steady state condition, [g/L]

   $c_{x,exp}$ vector of experimental cells concentrations from the beginning of the reactor experiment with recycle (day 0) and the achievement of the steady state condition, [g/L], as shown in Figure 2.13

2. this so determined Ea is fixed and a second *fminsearch* function minimizes ε_I changing bEs;

3. the absolute difference between bEs obtained by point 2., bEs_{hypo}, and bEs assumed in point 1., bEs_{calc}, is calculated:

$$\varepsilon_{fin} = |bEs_{hypo} - bEs_{calc}| \tag{4.12}$$

These three points are repeated changing at every loop the initial estimation of bEs, for an established number of times. bEs_{hypo} is so changed from 1 m^2/kg to 50 m^2/kg and Table 4.3 reports results of the simulation for *Scenedesmus obliquus*.
It is clear that $bEs = 40$ provides the lowest difference between the assumed and calculated term: using this value as a first estimation at point 1., a certain absorption coefficient is determined after minimization of ε_c; the value of Ea is then fixed and bEs is calculated in order to minimize ε_I; the obtained bEs_{calc} is so 0.56 m^2/kg higher or lower than bEs_{hypo}, that is a neglectable difference.
The code *overall.m* provides the following final results:

$$Ea = 114\,m^2/kg \tag{4.13}$$

$$bEs = 40\,m^2/kg \tag{4.14}$$

Figure 4.3 and Figure 4.4 graphically demonstrate model correlation of experimental data.
Values of absorption and backscattering coefficients provided by *overall.m* are considered the correct parameters for the system simulation.

Table 4.3: Values of bEs_{hypo} and respective ε_{fin} for *Scenedesmus obliquus* obtained by *overall.m* code.

bEs_{hypo}, $[m^2/kg]$	ε_{fin}, $[m^2/kg]$
1	71.42
10	54.67
20	36.66
30	18.15
36	6.96
37	5.09
38	3.21
39	1.33
40	0.56
41	2.44
42	4.34
43	6.23
44	8.12
50	19.75

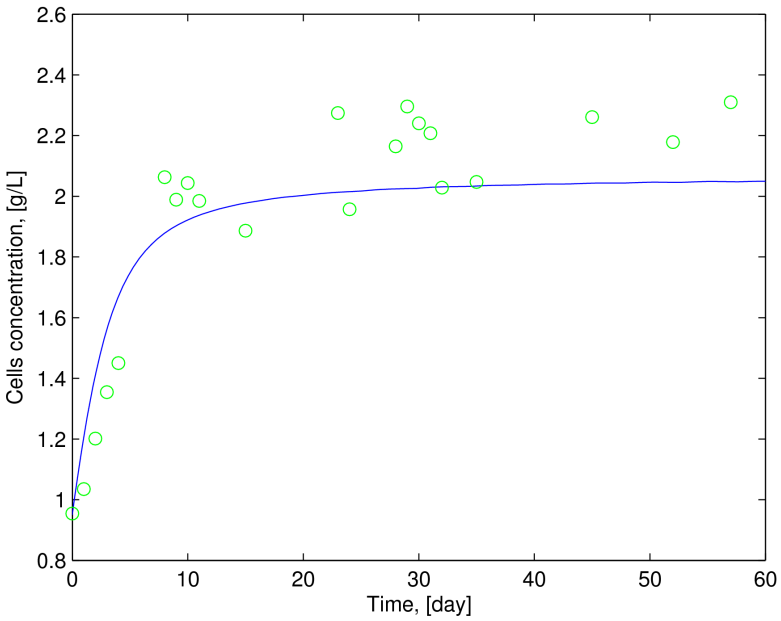

Figure 4.3: Dynamics of reactor test with recycle using $Ea = 114\ m^2/kg$ and $bEs = 40\ m^2/kg$. Green circles represent cells concentrations in the reactor measured experimentally and the blue line represents the model correlation of cells concentrations.

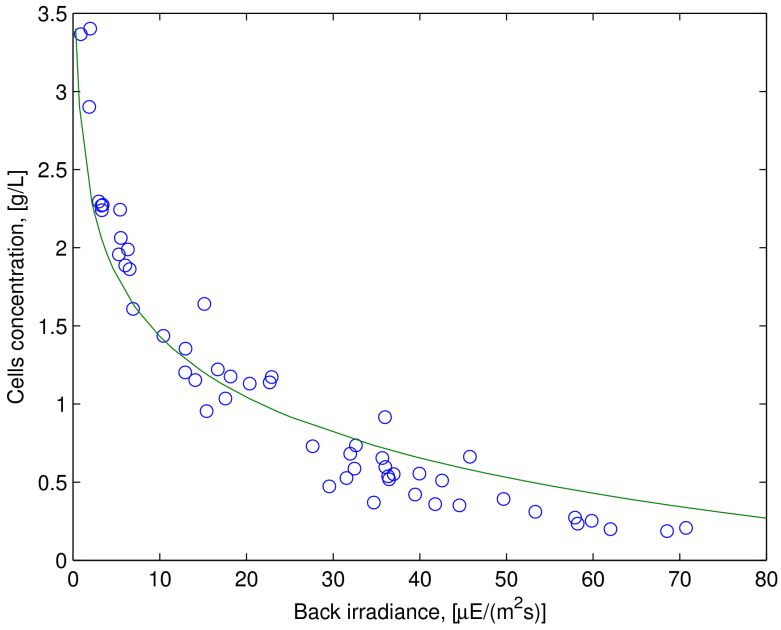

Figure 4.4: Back irradiances at different cells concentrations using $Ea = 114$ m^2/kg and $bEs = 40$ m^2/kg. Blue circles represent experimental data and the green line represents the model correlation.

The comparison between Figure 4.1 and Figure 4.4 underlines the lower correlation accuracy obtained by this code in the interpretation of back irradiances; nevertheless, the correlation of the reactor dynamics is surely improved and the model predicts a concentration of ca. 2.05 g/L at the steady state condition.

4.2.1 *Maintenance term validation*

The value of the maintenance constant affects appreciably the growth rate of any microalgal culture, limiting the duplication process. In the described simulation of the reactor with recycle described above it has a value of $\mu_e = 8{\cdot}10^{-3}$ h^{-1}, as reported in Section 4.1.5.
A test to validate this value can be performed: in fact the system is characterized by a cells concentration of 2.2 g/L at the steady state condition; if the recycle is instantaneously set to zero and the volumetric flow rate values are according to Table 2.7, the system has to reach a lower stationary cells concentration. In particular, this concentration should be the one of the continuous experiment without recycle, as represented in Figure 2.13 (steady cells concentration of 1.2 g/L before the switch to recycle mode). For this reason, the code *massbalance.m* was modified in order to simulate the instantaneous change from continuous mode with recycle to continuous mode without recycle; inputs for this code are the following:

- irradiance reaching the reactor $I = 165\ \mu E/(m^2 s)$;
- reactor volume $V_r = 0.25$ L;
- depth of the reactor $h = 0.012$ m;
- micronutrients inflow at the reactor $\dot{V}_0 = 0.151$ L/d;
- reactor outflow $\dot{V}_{re} = 0.151$ L/d;
- at $t = 0$: values of cells concentration in the reactor $c_{x,r} = 2.2$ g/L and in the collecting bottle $c_{x,b} = 2.2$ g/L, and collecting bottle volume $V_b = 1{\cdot}10^{-6}$ L;
- values of ρ_m, K, ϕ, μ_e as reported in the previous section, and values of Ea and bEs determined by *overall.m*, Equation 4.13 and Equation 4.14.

Figure 4.5 displays the results: at day 0, the recycle ratio is set to zero, 151 mL/d of micronutrients are fed to the reactor and 151 mL/d of biomass solution are extracted from it; steady state cells concentration calculated by the model is ca. 0.95 g/L whereas its experimental value is 1.2 g/L.

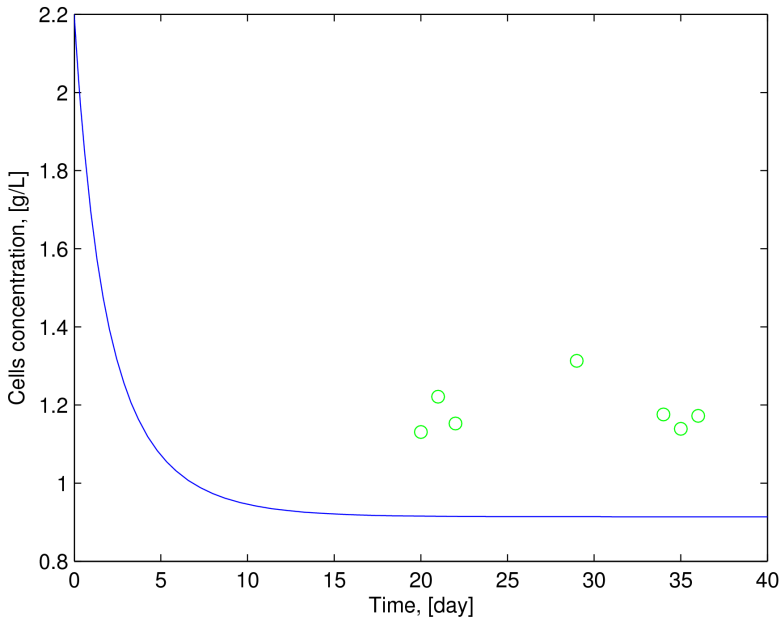

Figure 4.5: Dynamics of lab-scale reactor with recycle when the recycle is set to zero (day 0) using $Ea = 114\ m^2/kg$ and $bEs = 40\ m^2/kg$. Green circles represent the experimental stationary cells concentrations and the blue line represents the model correlation.

Both the simulations of the reactor with recycle and reactor without recycle underestimate the experimental values of cells concentrations at the steady state condition: for the first case, the model predicts a

value of 2.05 g/L against 2.2 g/L; for the second case, a value of 0.9 g/L is calculated instead of 1.2 g/L. As the absorption and backscattering coefficients are already optimized to represent also back irradiances, the term μ_e can be slightly changed to enhance the model accuracy. Table 4.4 resumes the calculated cells concentrations at the steady state condition for the continuous reactor with recycle and without recycle.

Table 4.4: Calculated cells concentrations at stationary condition using different maintenance constant. c_I and c_{II} represent the calculated concentration for the reactor with recycle and without recycle, respectively.

μ_e, $[h^{-1}]$	c_I, [g/L]	c_{II}, [g/L]
$8{\cdot}10^{-3}$	2.05	0.91
$7.5{\cdot}10^{-3}$	2.11	0.95
$7{\cdot}10^{-3}$	2.18	0.99
$6.5{\cdot}10^{-3}$	2.24	1.03
$6{\cdot}10^{-3}$	2.31	1.06

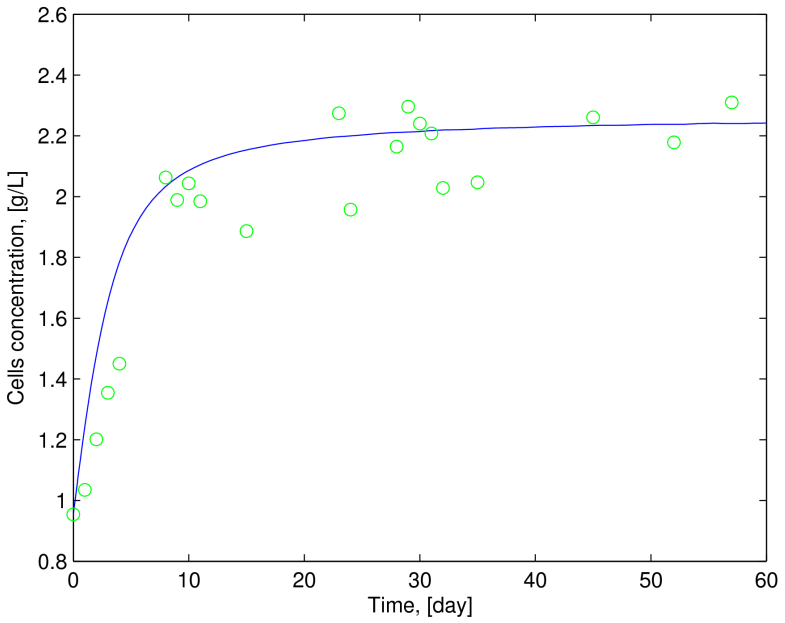

Figure 4.6: Dynamics of reactor test with recycle using $Ea = 114$ m^2/kg, $bEs = 40$ m^2/kg and $\mu_e = 6.5{\cdot}10^{-3}$ h^{-1}. Green circles represent cells concentrations in the reactor measured experimentally and blue line represents model correlation of cells concentrations.

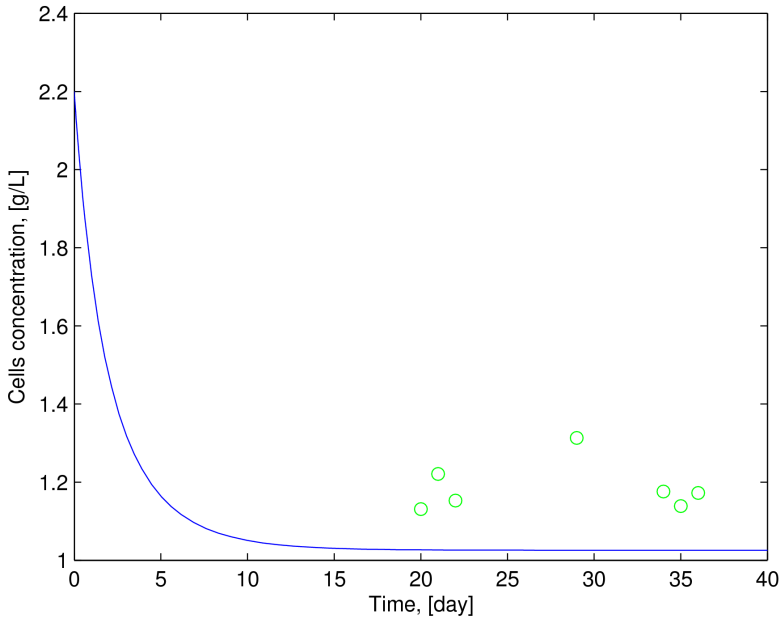

Figure 4.7: Dynamics of lab-scale reactor with recycle when the recycle is set to zero (day 0) using $Ea = 114\ m^2/kg$, $bEs = 40\ m^2/kg$ and $\mu_e = 6.5{\cdot}10^{-3}\ h^{-1}$. Green circles represent the experimental stationary cells concentrations and blue line represents the model correlation.

A decrease of the maintenance term means that the part of income light energy converted to new biomass increases and this is demonstrated by the increase of the calculated cells concentration at steady state.
A value of $\mu_e = 6.5{\cdot}10^{-3}\ h^{-1}$ allows a good representation of both systems (with and without recycle), as Figure 4.6 and Figure 4.7 show. Table 4.5 summarizes the values of parameters used in the Cornet model for the simulations of the lab-scale reactor tests.

Table 4.5: Values of parameter used in the Cornet model.

Parameter	U.m.	Value
ρ_m	adim	0.8
K	$\mu E/(m^2 s)$	75
ϕ	$kg/\mu E$	$2.77{\cdot}10^{-9}$
Ea	m^2/kg	114
bEs	m^2/kg	40
μ_e	h^{-1}	$6.5{\cdot}10^{-3}$

4.3 PHOTOSYNTHETIC EFFICIENCY

The performance of the reactor test with recycle can be expressed in terms of photosynthetic efficiency, that is the amount of inlet energy which is stored as biomass. As clarified in Section 3.5, this term cannot be higher than 30.68% of PAR, because of thermodynamic limits. Photosynthetic efficiency is calculated at the steady state condition, i.e., assuming a production of biomass P given by:

$$P = V_r r_x = \dot{V}_{re} c_{x,r} - \dot{V}_{bo} c_{x,b} \tag{4.15}$$

At steady state condition, $c_{x,b} = c_{x,r} = 2.2$ g/L, $\dot{V}_{re} = 151$ mL/d and $\dot{V}_{bo} = 75$ mL/d, so $P = 0.16$ g/d. In order to solve Equation 3.26, enthalpy of formation of *Scenedesmus obliquus* has to be known. As reported in Section 3.4.1, a predictive determination of this term can be done once the elemental analysis and the fraction of oil are known; for a 25% oil content, $\Delta H^0_{f,algae} =$ -10712.89 kJ/kg. Accordingly, $\dot{E}_{stored}$ can be calculated: $\dot{E}_{stored} = 3.3{\cdot}10^{-2}$ W.

Fluorescent lamps are characterized by a visible emission spectrum and for this reason the assumption of $E_{pho} = 225.3$ kJ/mol, which corresponds to $\lambda = 531$ nm, can be used. This assumption is the base for the calculation of power of radiation hitting the reactor, $\dot{E}_{in}$, which can be expressed as:

$$\dot{E}_{in} = I_{layer} E_{pho} A \tag{4.16}$$

where:

I_{layer} PAR reaching the first layer of microalgae, that is after the first sheet of polycarbonate, = $I(1 - y_{PC})$, [$\mu E/(m^2 s)$]. Value of y_{PC} is reported in Table 2.2.

It results $\dot{E}_{in} = 69.1{\cdot}10^{-2}$ W.
Solving Equation 3.22, photosynthetic efficiency for the lab-scale test has a value of 4.78% of PAR, which corresponds to 2.05% of total incident solar energy.

4.4 ENERGY BALANCE

The dynamic energy balance for a photobioreactor approximated to a CSTR is expressed by the following equation:

$$\frac{dE_{tot}}{dt} = \dot{E}_{in,tot} - \dot{E}_{out,tot} \tag{4.17}$$

where:

$\dot{E}_{in,tot}$ energy entering the reactor, [W]
$\dot{E}_{out,tot}$ energy exiting the reactor, [W]

In particular:

$$\dot{E}_{in,tot} = \dot{E}_{in} + \dot{H}_{nut,in} + \dot{H}_{nut,re} + \dot{H}_{rec,in} \tag{4.18}$$

$$\dot{E}_{out,tot} = \dot{E}_{out} + \dot{H}_{bio,out} + \dot{E}_{main} + \dot{H}_{nut,out} + \dot{E}_c + \dot{E}_k \tag{4.19}$$

where:

- $\dot{E}_{in}$ power of incident radiation, [W]
- $\dot{H}_{nut,in}$ enthalpy of micronutrients entering the reactor, [W]
- $\dot{H}_{nut,re}$ enthalpy of micronutrients entering the reactor through the recycle, [W]
- $\dot{H}_{rec,in}$ enthalpy of biomass entering the reactor through the recycle, [W]
- $\dot{E}_{out}$ power of radiation lost to the environment, [W]
- $\dot{H}_{bio,out}$ enthalpy of biomass exiting the reactor, [W]
- $\dot{E}_{main}$ energy required for maintenance process, [W]
- $\dot{H}_{nut,out}$ enthalpy of micronutrients exiting the reactor, [W]
- $\dot{E}_c$ convective heat transfer between the system and the external environment, [W]
- $\dot{E}_k$ conductive heat transfer between the system and the external environment, [W]

Expanding Equation 4.17, in a stationary condition the system is modelled as follows:

$$\dot{E}_{in} + \dot{H}_{nut,in} + \dot{H}_{rec,in} + \dot{H}_{rec,in} = \dot{E}_{main} + \dot{E}_{out} + \dot{H}_{bio,out} + \dot{H}_{nut,out} + \cancel{\dot{E}_c} + \dot{E}_k \tag{4.20}$$

where $\dot{E}_c$ is neglected. In fact, it can be neglected because there is not an appreciable movement of the liquid inside the reactor with respect to the internal polycarbonate layer. Energy losses are so represented by conductive heat transfer contribution only.
The previous expression can be further expanded:

$$\dot{E}_{in} + \cancel{\dot{m}_{nut,in} H_{nut}} + \dot{m}_{rec,in} H_{algae} + \cancel{\dot{m}_{nut,re} H_{nut}} = \dot{E}_{main} + \dot{E}_{out} + \dot{m}_{bio,out} H_{algae} + \cancel{\dot{m}_{nut,out} H_{nut}} + \dot{E}_k \tag{4.21}$$

where:

- $\dot{m}_{nut,in}$ micronutrients mass inflow entering the reactor, [g/s]
- $\dot{m}_{nut,re}$ micronutrients mass inflow entering through the recycle, [g/s]
- $\dot{m}_{nut,out}$ micronutrients mass outflow exiting the reactor, [g/s]
- H_{nut} micronutrients inlet enthalpy, [J/g]
- $\dot{m}_{rec,in}$ biomass inflow through the recycle, [g/s]
- H_{algae} recycle inlet enthalpy, [J/g]
- $\dot{m}_{bio,out}$ biomass outflow, [g/s]

The vital compounds are provided in excess to the culture and the difference between the enthalpy of micronutrients entering the reactor and exiting it is neglected with respect to the other terms.
It can be noted that:

$$\dot{m}_{bio,out} H_{algae} - \dot{m}_{rec,in} H_{algae} = P \cdot H_{algae} = \dot{E}_{stored} \tag{4.22}$$

and the last identity derives from Equation 3.26.
Finally:

$$\dot{E}_{in} = \dot{E}_{stored} + \dot{E}_{main} + \dot{E}_{out} + \dot{E}_{k} \tag{4.23}$$

Value of $\dot{E}_{stored}$ at steady state condition is provided in the previous section, the other terms will be quantified in the following.

4.4.1 *Radiation hitting the reactor*

The term $\dot{E}_{in}$ is calculated in Section 4.3 where it is defined as the radiation reaching the first layer of microalgae, that is after the first sheet of polycarbonate. Here, energy balance boundaries are set outside the sheets of polycarbonate and the equation which defines $\dot{E}_{in}$ becomes:

$$\dot{E}_{in} = I E_{pho} A \tag{4.24}$$

so the polycarbonate light absorption is not considered. The result is $\dot{E}_{in} = 77.7 \cdot 10^{-2}$ W.

4.4.2 *Maintenance energy*

Quantification of this term is not simple, mostly because of the variety of processes that have to be taken into account. A more general consideration on this kind of energy per unit time can be performed using Equation 3.8. In fact, the duplication process $r_{x,p}$ is limited by $r_{x,m}$ which represents the amount of biomass per unit time that maintenance diverts from production; this mass per unit time is a loss of energy, which is used for various cellular functions. For this reason, maintenance energy is quantified as a potential E_{stored} which would be entirely used for new cells formation if no maintenance processes were required.
At stationary condition, cells concentration in the reactor is 2.2 g/L and $r_{x,m} = 0.343$ g/(L·d), which corresponds to 0.09 g/d of biomass diverted from duplication, for a 250 mL volume reactor. Comparison between this value and 0.16 g/d representing the stationary production of biomass obtained in Section 4.3 denotes the relevance of $r_{x,m}$ on the overall growth process.
The energy per unit time related to 0.09 g/d of biomass is calculated according to Equation 3.26 (with $\Delta H^0_{f,alga}$) and it represents the energy absorbed by cells in the reactor but is not used for duplication, i.e., $\dot{E}_{main}$. A value of $\dot{E}_{main} = 1.8 \cdot 10^{-2}$ W is obtained.

4.4.3 *Radiation exiting the reactor*

This term can be easily determined using Equation 2.5: at 2.2 g/L the irradiance measured on the back of the reactor is 4.89 μE/(m^2s). This value is inserted in Equation 4.24, obtaining $\dot{E}_{out} = 2.3{\cdot}10^{-2}$ W.

4.4.4 *Energy losses*

This term is represented by the conductive heat transfer $\dot{E}_k$ only. In fact, at the stationary condition, the temperature inside the photobioreactor is higher than the external one, leading to a heat loss quantified as:

$$\dot{E}_k = U_t A_t (T_{in} - T_{out}) \tag{4.25}$$

$$\frac{1}{U_t} = \frac{1}{U_{air}} + \frac{1}{U_{PC}} + \frac{1}{U_{med}} \tag{4.26}$$

where:

- U_t overall heat transfer coefficient of the system, [W/(m^2°C)]
- A_t reactor surface in contact with the external environment, [m^2]
- T_{in} temperature of the medium, [°C]
- T_{out} temperature of the external environment, [°C]
- U_{air} air free convection, [W/(m^2°C)]
- U_{PC} conductance of the polycarbonate, [W/(m^2°C)]
- U_{med} medium free convection, [W/(m^2°C)]

A value of $U_{air} = 15$ W/(m^2°C) is assumed for the air free convection outside the reactor, whereas $U_{med} \simeq \infty$ because of the low thermal resistivity of water compared to air and polycarbonate. Conductance for a 2 mm polycarbonate sheet is given by PALSUN® datasheet $U_{med} = 5.6$ W/(m^2°C). Thermal energy exits the system mainly through two surfaces: the one facing the light source and the one facing the opposite direction; each surface has an area of $209{\cdot}10^{-4}$ m^2, so $A_t = 418{\cdot}10^{-4}$ m^2. Temperature measurements were performed using Tc Direct K R5 thermocouple and $T_{in} = 29$ °C, $T_{out} = 25.5$ °C were determined.
The energy losses contribution to the overall balance is so calculated $\dot{E}_k = 59.7{\cdot}10^{-2}$ W.
Table 4.6 reports the obtained values of energy terms.
It is noteworthy that the energy balance is validated, since the sum of the terms on the right side of Equation 4.23 is consistent with the term on the left side. In particular:

- most of the inlet energy is converted into heat, represented by a ΔT between inside and outside the reactor;

- the energy required for maintenance process has a relevant value with respect to the energy stored as biomass; this states that the energy absorbed by the microalga is the sum of these two energies, but only a part is diverted to the formation of new cells.

However, this result is affected by a certain number of approximations:

- U_{air} is considered 15 W/(m^2°C) which represents a mean value of the air free convection range 5-25 W/(m^2°C);
- this so calculated $\dot{E}_k$ takes into account the two main reactor surfaces; energy is also lost through the side reactor areas, and through contact surface between medium and air on the top of the reactor;
- temperature measurements have an high accuracy error and it lacks of reliability.

Table 4.6: Energy contributions for the reactor test with recycle at the steady state condition.

Term	Value, [W]
$\dot{E}_{in}$	$77.7 \cdot 10^{-2}$
$\dot{E}_{stored}$	$3.3 \cdot 10^{-2}$
$\dot{E}_{main}$	$1.8 \cdot 10^{-2}$
$\dot{E}_{out}$	$2.3 \cdot 10^{-2}$
$\dot{E}_k$	$59.7 \cdot 10^{-2}$

4.5 MAXIMUM BIOMASS PRODUCTION RATE

The continuous tests were operated using $\tau = 1.66$ d; this value was estimated by a tentative value of the specific growth rate $K = 0.603$ d^{-1} which is linked to the residence time by Equation 2.10 at steady state condition. The scope now is to determine the τ-value which ensures the maximum biomass production rate for the continuous reactor with recycle. At the beginning, the continuous reactor without recycle (CSTR and PFR) is considered, then the system is simulated as a PFR to understand the influence of the recycle on the maximum biomass production rate.

The maximum biomass production rate can be investigated considering the biomass production rate r_x as a function of cells concentra-

tion c_{out}; the highest value of r_x and the corresponding c_{out} are used in the equation of a CSTR at the steady state condition:

$$\begin{aligned} 0 &= \cancel{\dot{V}c_{in}} - \dot{V}c_{out} + V_r r_x \\ &= -\dot{V}c_{out} + V_r r_x \\ \tau &= \frac{c_{out}}{r_x} \end{aligned} \tag{4.27}$$

The residence time ensuring the maximum biomass production rate can so be calculated. The lab-scale continuous reactor reached a stationary cells concentration of 1.2 g/L and a biomass productivity of 8.66 g/(m^{2}d) with a residence time of 1.66 d.
A Matlab® code developed for this scope, called *rx_conc.m*, provides the value of r_x at different c_{out}. Inputs for this code are:

- irradiance reaching the reactor $I = 165$ µE/(m^{2}s);
- depth of the reactor $h = 0.012$ m;
- values of ρ_m, K, ϕ, Ea, bEs and μ_e as reported in Table 4.5.

In particular, the biomass production rate is determined using Equation 3.7 for a cells concentration ranging from 0.01 g/L to 3 g/L. Figure 4.8 shows results for this simulation.

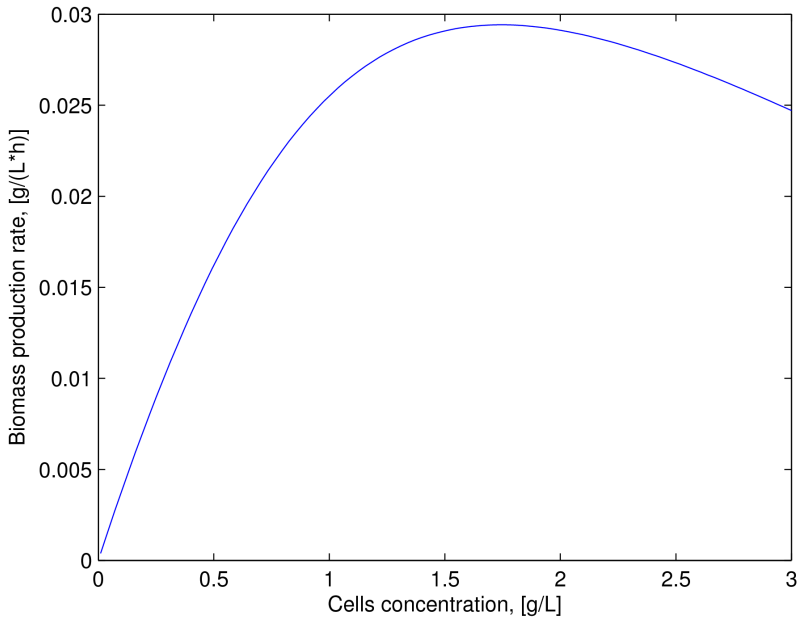

Figure 4.8: Biomass production rate as a function of cells concentration.

The code provides a biomass production rate of 0.0275 g/(L·h) for a stationary cells concentration of 1.2 g/L. As a consequence, the predicted biomass productivity is 7.89 g/(m^{2}d) instead of 8.66 g/(m^{2}d). This difference is consistent with the reactor modelling reported in

Section 4.2.1 which calculates a stationary cells concentration of 1.03 g/L instead of 1.2 g/L.
According to Figure 4.8, the maximum value for r_x is 0.0294 g/(L·h) and the corresponding c_{out} is 1.75 g/L. If these results are used in Equation 4.27 $\tau = 2.48$ d is obtained. In particular, for a 250 mL volume reactor:

$$\tau = \frac{V_r}{\dot{V}} \Longrightarrow \dot{V} = \frac{V_r}{\tau} = \frac{250}{2.48} = 101\ \text{mL/d} \tag{4.28}$$

So, running the photobioreactor with a micronutrients inflow of 101 mL/d and a microalgae solution outflow of 101 mL/d, would ensure the maximum biomass production rate for the lab-scale continuous reactor test. A corresponding maximum biomass productivity of 8.44 g/(m^2d) is calculated. Table 4.7 resumes the obtained data.

Table 4.7: Simulated continuous reactor test performance. Biomass production rate and biomass productivity labels refer to the predicted stationary cells concentration of 1.03 g/L.

Data	U.m.	Value
Biomass production rate	$g/(L \cdot h)$	0.0275
Biomass productivity	$g/(m^2 d)$	7.89
Maximum biomass production rate	$g/(L \cdot h)$	0.0294
Maximum biomass productivity	$g/(m^2 d)$	8.44

4.5.1 *Light attenuation*

It is interesting to investigate the light distribution along the reactor depth for the case of maximum biomass production rate.
In fact, this condition is characterized by the maximum duplication rate, a term which is directly affected by the light availability at each reactor point.
For this purpose, the code *rx_conc.m* was modified in order to print the light distribution inside the reactor for a given value of cells concentration. The trend of light intensity along the reactor depth is always calculated for the determination of r_x. Figure 4.9 represents the light attenuation along the reactor depth at $c_{out} = 1.75$ g/L (solid line), that is at the cells concentration corresponding to the maximum biomass production rate, at $c_{out} = 1.61$ g/L (dashed line) and $c_{out} = 1.88$ g/L (dotted line). When c_{out} is lower than 1.75 g/L, the availability of light in the reactor is higher but a lower cells concentration negatively affects the achievable r_x; on the other hand, an higher cells concentration could increase r_x but the light availability decreases as effect of more considerable scattering phenomena.

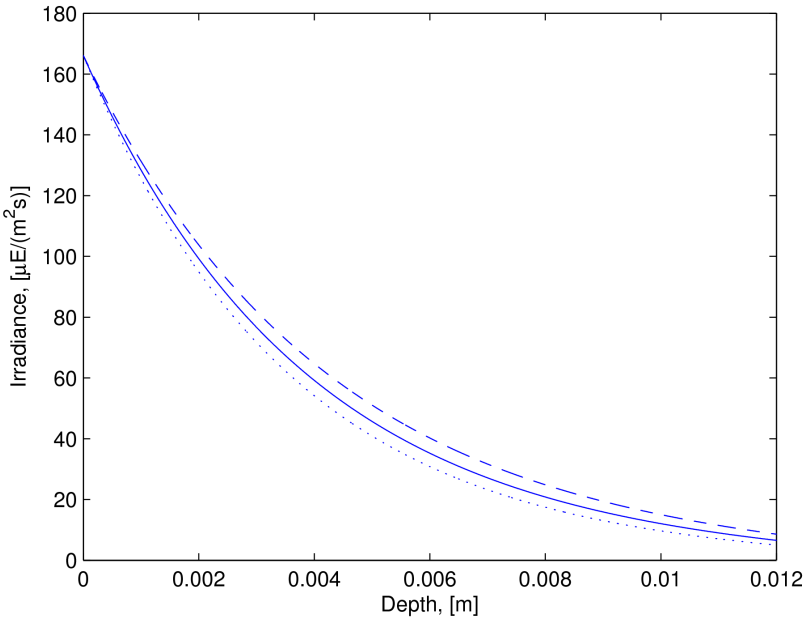

Figure 4.9: Light attenuation along the reactor depth. Solid line refers to $c_{out} = 1.75$ g/L, dashed line refers to $c_{out} = 1.61$ g/L and dotted line refers to $c_{out} = 1.88$ g/L.

4.5.2 *CSTR vs. PFR*

In the previous section, the lab-scale continuous reactor has been considered a CSTR because of its particular mixing condition, and using this approximation, the maximum biomass production rate has been evaluated. The reactor is now approximated to a PFR and the micronutrients inlet flow is set to 101 mL/d, so that different recycle ratios can be tested. This condition fixes the residence time of the overall system to 2.48 d, but the τ-value of the photobioreactor, τ_r, changes with the recycle ratio. In fact, now the system is modelled by the following equations (referring to Figure 2.14):

$$\begin{aligned}
&\dot{V}_0 + \dot{V}_{bo} = \dot{V}_{re} \\
&\dot{V}_{bo} = R\dot{V}_0 \\
&\dot{V}_{re} = \frac{dV_b}{dt} + \dot{V}_{bo} \\
&\frac{dc_x}{dt} = -\frac{\dot{V}_0 + \dot{V}_{bo}}{A_r}\frac{dc_x}{dz} + r_x \\
&V_b\frac{dc_{x,b}}{dt} = \dot{V}_{re}c_{x,r} - \dot{V}_{bo}c_{x,b} - c_{x,b}\frac{dV_b}{dt}
\end{aligned} \tag{4.29}$$

where:

A_r cross-section area, [m^2]

and τ_r is expressed as:

$$\tau_r = \frac{V_r}{\dot{V}_0(1+R)} \tag{4.30}$$

The hypothetical flow $\dot{V}_{in} = \dot{V}_0 + \dot{V}_{bo}$ enters the reactor from the bottom and exits from the top; the cross section area for this reactor is $A_r = m^2$.
The equations describing the system can be solved at different recycle ratio and corresponding stationary cells concentration can be evaluated. These calculations have been carried out by the modified code *massbalance.m* where the equation describing the CSTR is substituted by the one describing the PFR. Table 4.8 reports results of calculation.

Table 4.8: Stationary cells concentrations and reactor residence time at different recycle ratios for the case $\tau = 2.48$ d.

Recycle ratio [adim]	Cells concentration [g/L]	τ_r [d]
0.1	0	2.25
0.2	0.51	2.06
0.3	0.99	1.90
0.5	1.35	1.65
1	1.60	1.24
2	1.71	0.83
3	1.73	0.62

A plug flow reactor tends to a CSTR when the recycle ratio increases: at the borderline case, a PFR with an infinite R corresponds to a CSTR. The results demonstrate that the system presents the best performance if the reactor is considered a CSTR. In fact, a decrease of the recycle ratio leads to a decrease of the stationary cells concentration which is a measure of the biomass production rate, as the outlet flow rate is kept constant in all simulations. The wash-out problem occurs at $R \leqslant 0.1$, when the biomass production rate gets lower than the biomass extraction rate, and the biomass in the photobioreactor is totally withdrawn.
It is also noteworthy that a recycle ratio of 3 is enough to approximate the CSTR conditions.

4.6 WATER ABSORPTION

In Section 4.4 the energy balance for the lab-scale reactor with recycle is discussed. In particular, Table 4.6 underlines that most of the energy entering the reactor is converted into heat and this phenomenon

is represented by a ΔT between inside and outside the reactor. In order to understand the reason of the rise in the culture temperature, it is useful to evaluate the absorption of water in the light visible spectrum, that is the emission spectrum of the fluorescent lamp. Figure 4.10 shows the spectral power distribution of a Philips fluorescent lamp, characterized by the same irradiance properties of the OSRAM lamps used in laboratory.

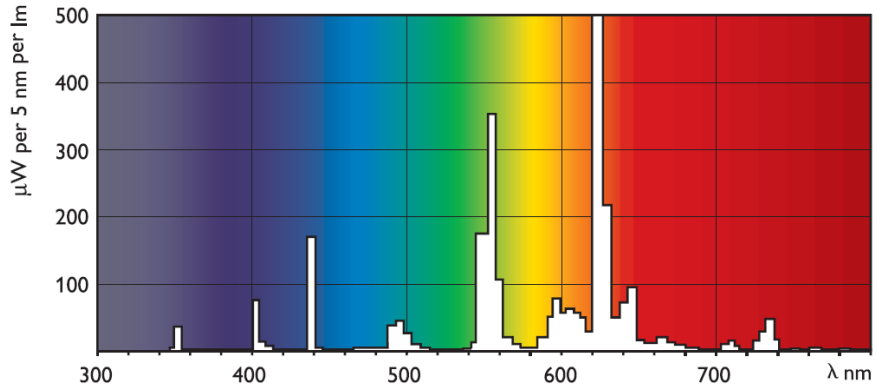

Figure 4.10: Spectral power distribution of a Philips fluorescent lamp, characterized by a luminous flux $L_m = 1350$ lm.

At each wavelength, the emitted power can be calculated, knowing that the luminous flux is $L_m = 1350$ lm for this lamp; the sum of all contributions is the lamp total power: $W_e = 18.5$ W.
A power corresponding to $W_e \cdot y_{PC}$ is absorbed by the polycarbonate, so the power reaching the first layer of microalgae is $W_e \cdot (1 - y_{PC}) = W_0 = 16.5$ W. This calculation is done at each wavelength. At this point, the ratio between the transmitted light and the incident light is given by the following expression:

$$\frac{W}{W_0} = e^{-\mu_a(\lambda)l} \tag{4.31}$$

where:

W	transmitted light, [W]
W_0	incident light, [W]
$\mu_a(\lambda)$	absorption coefficient, [m^{-1}]
l	reactor path length, [m]

So, the absorption coefficient for water at each wavelength has to be known. Pope and Fry 1997 reported these values for pure water.
The transmitted light after a path length $l = 0.012$ m can be computed at each λ and the sum of all contributions provides the total transmitted light intensity. The result is $W = 15.7$ W.
It is clear that the water can be considered transparent in the light visible spectrum, so the increase in internal temperature has to be a

consequence of the part of light absorbed by the polycarbonate. In fact, 2 mm thick polycarbonate sheet absorbs $y_{PC} = 11\%$ of the incident light in the visible spectrum and this leads to an heating effect of this material which can transfer thermal energy to the culture, thus raising its temperature.

Different results are obtained when the energy source is the sunlight. In fact, as Figure 4.11 underlines, the spectrum of the solar radiation is represented by visible and infrared light, the latter ranging from $\lambda = 700$ nm to $\lambda = 1$ mm.

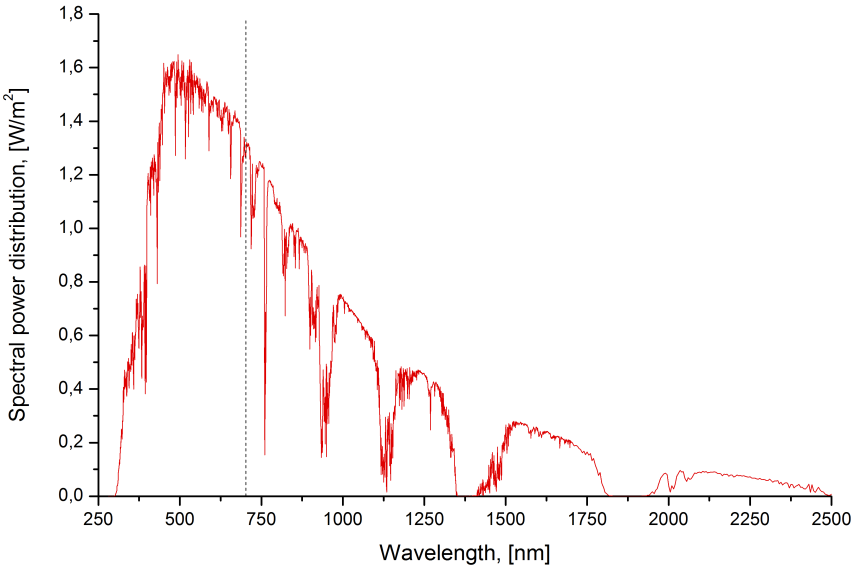

Figure 4.11: Spectral power distribution of the reference solar radiation at air mass 1.5 (*PVGIS Solar Irradiation Data, 2007*).

The reference solar spectral irradiance at air mass 1.5 (*PVGIS Solar Irradiation Data, 2007*) is so used to determine the percentage of infrared radiation on the overall energy and the result is $\%IR = 48.01\%$. Figure 4.12 shows $\mu_a(\lambda)$, [cm], for water at wavelength ranging from less than 100 nm to almost 1 mm. It is appreciable that the water has an absorption coefficient of 0.01 cm^{-1} at the end of the visible portion of spectrum, whereas it assumes values about 10000 times higher at $\lambda = 2500$ nm. This high absorption of the infrared portion of sunlight causes a heating effect of the water and its temperature could reach values unsustainable for the microalgae growth.

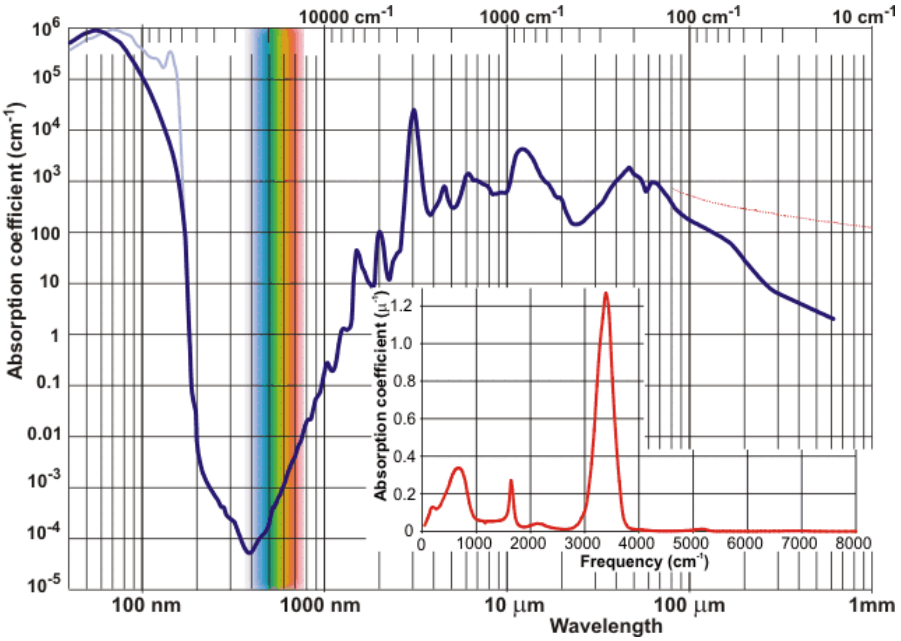

Figure 4.12: Absorption spectrum of liquid water (*Water structure and science*).

5

PILOT PLANT

This chapter will focus on the simulation and design of a pilot plant for microalgae production using the modelling criteria described in Chapter 3 with the parameters values obtained in Chapter 4. A possible plant arrangement is firstly examined. An investigation on the maximum biomass production rate is carried out for the case of continuous artificial radiation; the photosynthetic efficiency is calculated and the energy balance is discussed in order to verify whether the presence of a temperature control is necessary. The performance of the photobioreactor is then simulated modelling day/night sunlight cycles for the location of Padua. The photosynthetic efficiency and the energy balance are determined, accordingly.

5.1 PILOT PLANT ARRANGEMENT

The photobioreactor proposed for the pilot plant installation is a horizontal flat-plate type with an exposed area of 15 m^2. The microalgae culture depth is a design parameter and it is investigated in Section 5.3. The channel width and length are 0.75 m and 20 m, respectively, and it is characterized by a "U" curve after 10 m, so that inflow and outflow are placed on the same reactor side, as Figure 5.1 shows.

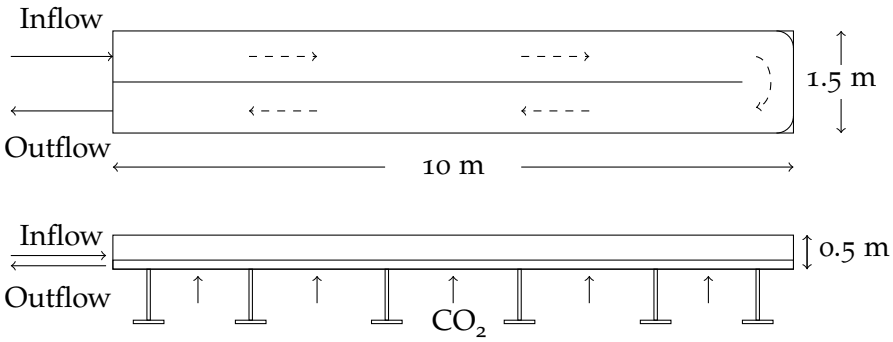

Figure 5.1: Photobioreactor layout. Dashed arrows indicate the flow direction along the channel.

The bottom of the reactor and the channel partition wall are made of stainless steel, whereas the material of the other reactor walls (1 cm thick) is polycarbonate.
The gas, that is CO_2-enriched air, is ensured by three parallel sparger lines placed on the bottom of the reactor and it exits through a chimney close to the microalgae outflow. These spargers provide also an

appropriate culture mixing and prevents microalgae from settling. The most critical points for a good mixing are the two reactor angles at the "U" curve: for this reason, two bent stainless steel foils are placed on these points.
Three coils are placed over the three parallel spargers: heating or cooling water can be pumped inside them to control the culture temperature.
A height of 50 cm separates the bottom and the top of the reactor; the latter is made of polycarbonate panels (1 cm thick) hinged on the central partition wall. In this way, the internal part of these panels, which is exposed to the microalgae culture, can be periodically cleaned.
Temperature and pH affect considerably the microalgal growth conditions and a control of these variables is necessary: two temperature sensors and pH sensors are placed at the microalgae inflow and outflow, and another temperature sensor is located at the "U" curve. The level control is provided by a pump and an overflow system.

The photobioreactor is inserted in a process scheme as shown in Figure 5.2: in particular, part of the extracted biomass is recycled back to the reactor ($\dot{V}_R$) together with the fresh medium ($\dot{V}_0$), and the other part exits the system ($\dot{V}_p$).

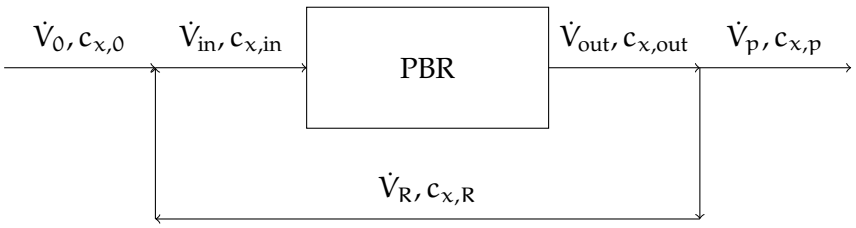

Figure 5.2: Scheme of the pilot plant. A recycle stream sends part of the extracted microalgae culture back to the reactor.

Clearly:

$$c_{x,out} = c_{x,R} = c_{x,p} \tag{5.1}$$

Furthermore, the volumetric flows in and out of the reactor can be considered the same:

$$\dot{V}_{in} = \dot{V}_{out} \tag{5.2}$$

The equations describing the system depend on the reactor behaviour. In fact, a perfect mixing implies that the reactor behaves as a CSTR:

$$\begin{aligned}
&\dot{V}_0 + \dot{V}_R = \dot{V}_{in} \\
&\dot{V}_{out} = \dot{V}_p + \dot{V}_R \\
&\dot{V}_0 c_{x,0} + \dot{V}_R c_{x,R} = \dot{V}_{in} c_{x,in} \\
&\dot{V}_{out} c_{x,out} = \dot{V}_p c_{x,p} + \dot{V}_R c_{x,R} \\
&V_r \frac{dc_{x,out}}{dt} = \dot{V}_{in} c_{x,in} - \dot{V}_{out} c_{x,out} + V_r r_x
\end{aligned} \tag{5.3}$$

The culture mixing system can alternatively be designed to provide a good mixing along the flow cross-section only, so that the photobioreactor is approximated to a PFR:

$$\begin{aligned}
&\dot{V}_0 + \dot{V}_R = \dot{V}_{in} \\
&\dot{V}_{out} = \dot{V}_p + \dot{V}_R \\
&\dot{V}_0 c_{x,0} + \dot{V}_R c_{x,R} = \dot{V}_{in} c_{x,in} \\
&\dot{V}_{out} c_{x,out} = \dot{V}_p c_{x,p} + \dot{V}_R c_{x,R} \\
&\frac{dc_x}{dt} = -\frac{\dot{V}_{in}}{A_r}\frac{dc_x}{dz} + r_x
\end{aligned} \tag{5.4}$$

The make-up flow $\dot{V}_0$ is the feed of the fresh medium, so $c_{x,0} = 0$. Owing to the low concentration of microalgae, the output volumetric flow can be assumed equal to the input one, so $\dot{V}_p = \dot{V}_0$. The make-up flow and the recycle flow are linked by the recycle ratio R:

$$\dot{V}_R = R\dot{V}_0 \tag{5.5}$$

Moreover, mass balance equation for CSTR needs an initial condition at $t = 0$, for instance:

$$c_{x,out}\big|_{t=0} = 1\,g/L \tag{5.6}$$

In the same way, the PFR approximation needs both an initial and a boundary condition, such as:

$$c_x\big|_{t=0} = 1\,g/L \tag{5.7}$$

$$c_x\big|_{z=0} = c_{x,in} \tag{5.8}$$

The reactor is operated in batch mode until cells concentration reaches a value of 1 g/L: at this point, the CSTR or PFR approximation is decided and simulations of continuous photobioreactor can be obtained.

5.2 IRRADIANCE CONDITIONS

5.2.1 *Continuous artificial radiation*

As done for the experimental tests, fluorescent lamps are equally distributed over the photobioreactor: in this way, the photosynthetic active radiation reaching the first microalgae layer, I_0, has a unique value which does not change with time. As a basis for the calculation of this value, the total solar energy reaching Padua in one year, E_{sun}, reported in Section 3.2.1, is used:

$$I_0 = \frac{E_{sun}\%PAR}{E_{pho}} = \frac{4541 \cdot 10^6 \cdot 42.98\%}{225300 \cdot 365 \cdot 24 \cdot 60 \cdot 60} = 272\,\mu E/(m^2 s) \tag{5.9}$$

This value ensures that the energy reaching the photobioreactor in one year does not exceed the thermodynamic limit of E_{sun} for Padua, that is 4541 MJ/(m^2y).

5.2.2 *Day/night sunlight cycles*

Padua is located at a latitude of 45°24′N and at a longitude of 11°52′E. *PVGIS Solar Irradiation Data, 2007* provides the monthly direct and diffuse solar radiation for this location reaching a horizontal surface; Table 5.1 resumes these data.

Table 5.1: Solar radiation data for the location of Padua (ivi).

Month	Total radiation [MJ/(m^{2}d)]	Direct radiation [MJ/(m^{2}d)]	Diffuse radiation [MJ/(m^{2}d)]
January	4.63	1.81	2.82
February	6.82	2.80	4.02
March	11.11	4.89	6.22
April	15.04	7.22	7.82
May	18.31	8.60	9.70
June	21.38	10.90	10.47
July	21.82	12.00	9.82
August	18.40	9.94	8.46
September	13.96	7.54	6.42
October	8.51	4.00	4.51
November	5.25	2.10	3.15
December	3.70	1.26	2.44

The reported data represent the entire sun energy, whereas the interest of the present work is focused on the photosynthetic active part. For this reason, Equation 5.9 is used to determine the photosynthetic active radiation from solar total radiation values. Figure 5.3 shows the average daily trend of PAR for four months corresponding to the four seasons of the year. It is appreciable the gap between the insolation level of the different months: a peak of more than 1200 μE/(m^{2}s) reaches the photobioreactor during summer, whereas 400 μE/(m^{2}s) does during winter at most. These leads to a high variation in biomass productivity of the photobioreactor during the year.
The ratio between diffuse and direct radiation changes during the year: in December it has a value of 0.66, in July a value of 0.45. Figure 5.4 underlines how the total photosynthetic active radiation is divided into diffuse and direct parts during the day (July).

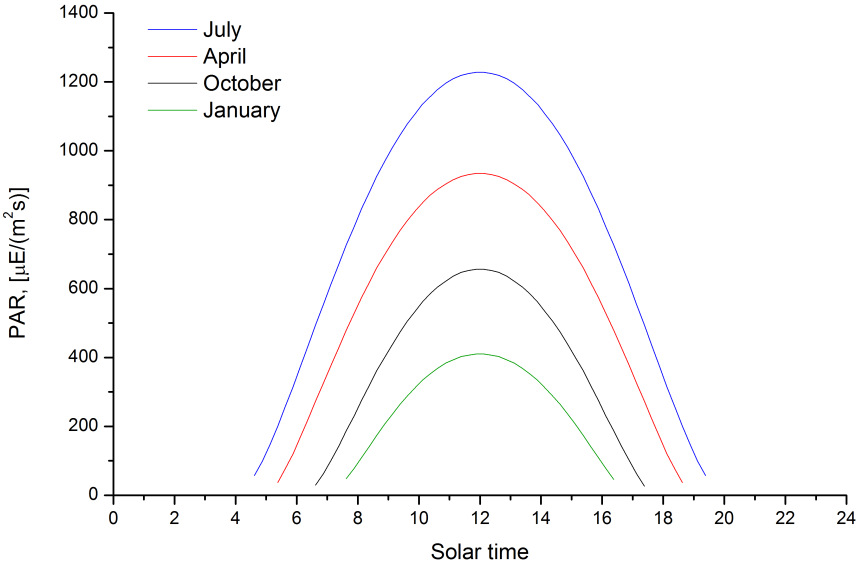

Figure 5.3: Average daily trend of the total photosynthetic active radiation reaching the photobioreactor for four characteristic months.

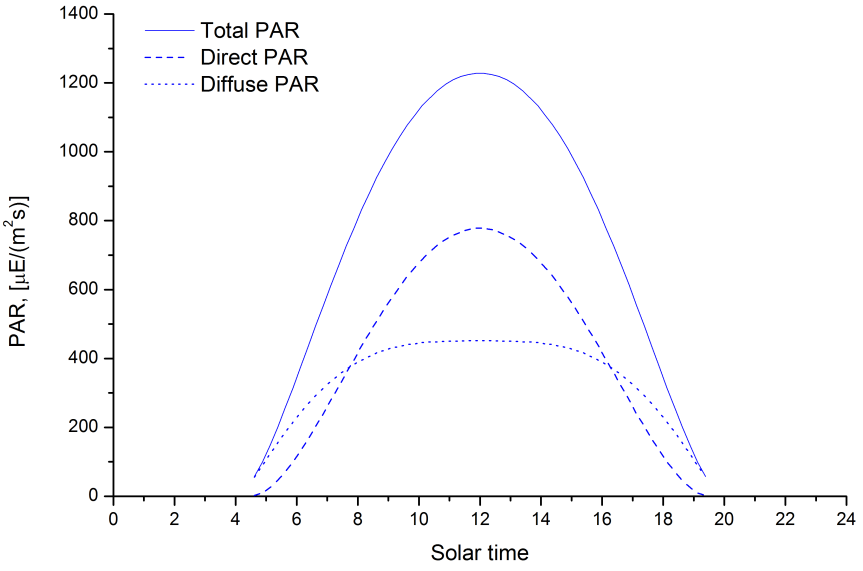

Figure 5.4: Average daily trend of the total, direct and diffuse photosynthetic active radiations reaching the photobioreactor for the month of July.

The values for the average daily trend of PAR in each month are reported by the on-line database every 15 minutes; as the ordinary differential equation solver built in Matlab® has a shorter integration time, the PAR hitting the microalgae culture has to be estimated with a higher frequency than once in a quarter of a hour: so, a polynomial regression was used to relate the direct and diffuse PAR (y) to the solar time (x) from the sunrise to the sunset. For the month of July, direct and diffuse PAR reaching the photobioreactor during a typical day are given by the following equations, respectively:

$$y = 0.2181x^4 - 10.467x^3 + 162.16x^2 - 877.51x + 1522.6 \quad (5.10)$$

$$y = -0.0789x^4 + 3.7888x^3 - 71.518x^2 + 625.26x - 1657.1 \quad (5.11)$$

and for the month of January:

$$y = 0.2982x^4 - 14.324x^3 + 242.43x^2 - 1691.9x + 4146.9 \quad (5.12)$$

$$y = -9.1458x^2 + 219.5x - 1089.9 \quad (5.13)$$

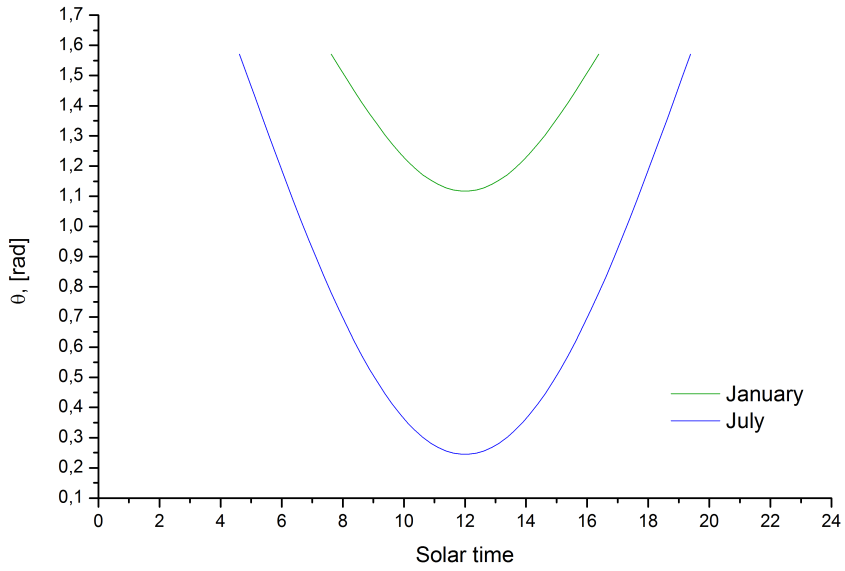

Figure 5.5: Incident radiation angle with respect to normal direction of terrestrial surface during a typical day of July and January.

The database provides also θ_t, [rad], which is the incident radiation angle with respect to normal direction of terrestrial surface at the maximum insolation time, that is at 12:00. This value is needed at any solar time to simulate the different positions of the sun in the sky during the day, and can be calculated as a function of the solar time and of θ_t:

$$\theta = \frac{\pi}{2} - \left(\frac{\pi}{2} - \theta_t\right) \sin\left(\frac{(t - t_{in})}{(t_{out} - t_{in})}\pi\right) \quad (5.14)$$

where:

t	solar time
t_{in}	time of sunrise
t_{out}	time of sunset

Figure 5.5 shows value of θ during a typical day of July and January. In Matlab® code, θ (y) is calculated at any solar time (x) using the following polynomial regressions for the month of July:

$$y = -0.0001x^4 + 0.0048x^3 - 0.0574x^2 - 0.0179x + 2.4453 \quad (5.15)$$

and January:

$$y = 0.0241x^2 - 0.5794x + 4.6034 \quad (5.16)$$

5.3 PLANT SIMULATIONS WITH ARTIFICIAL RADIATION

In Section 5.1, the geometrical properties of the photobioreactor are reported, except for the microalgae culture depth h. In fact, the biomass production rate r_x quantifies the performance of the system and the irradiance attenuation along the reactor depth strongly affects this term; at a given value of cells concentration and irradiance reaching the reactor, an increase of h leads to an increase of the dark volume, thus raising the influence of the maintenance process on the overall r_x value (Equation 3.8). For this reason, three values of depth have been considered in the photobioreactor simulation: 1.2 cm, 5 cm and 13.3 cm. Values of reactor volume are so fixed to 180 L, 750 L and 2000 L, respectively.

Operating a plant at the maximum performance is of primary importance and the system has to be designed for this scope. Initially, the photobioreactor is considered as a CSTR, so the recycle ratio is set to zero and the following identities are valid:

$$\dot{V}_0 = \dot{V}_{in} = \dot{V}_{out} = \dot{V}_p \quad (5.17)$$

The highest performance is reached when the biomass production rate r_x is maximized: the same procedure developed in Section 4.5 was applied. In particular, the Matlab® code *rx_conc.m* is used with the following inputs:

- irradiance reaching the reactor $I_0 = 272$ $\mu E/(m^2 s)$;
- depth of the reactor: $h = 0.012$ m, $h = 0.05$ m, $h = 0.133$ m;
- values of ρ_m, K, ϕ, Ea, bEs and μ_e as reported in Table 4.5.

Figure 5.6 shows results of this simulation for the three different values of depth.

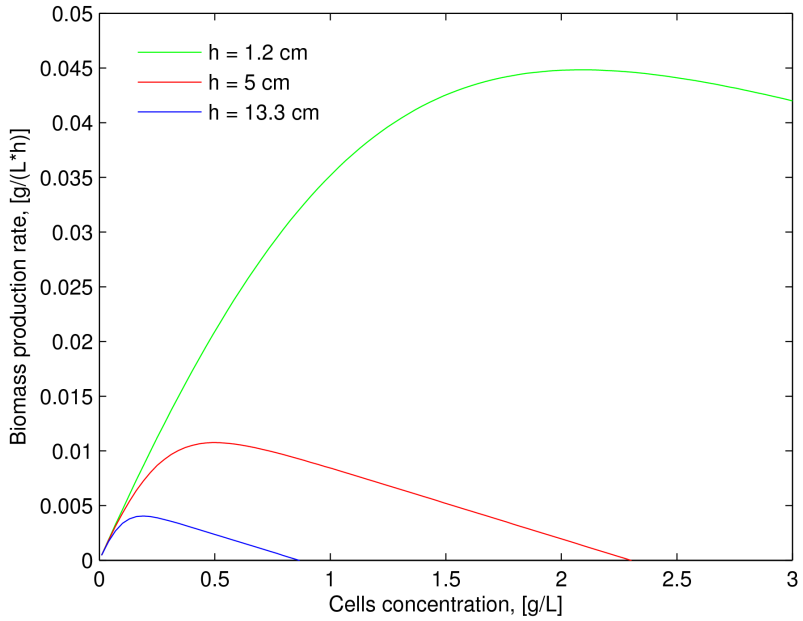

Figure 5.6: Biomass production rate as a function of cells concentration for the three considered values of depth.

Table 5.2: System properties at the maximum biomass production rate for the three considered values of depth.

Depth [m]	$r_{x,max}$ [g/(L · h)]	$c_{x,out}$ [g/L]	τ [h]	$\dot{V}_0$ [L/h]	P_r [tons/(ha · y)]
0.012	0.0448	2.09	46.65	3.86	47.11
0.05	0.0108	0.49	45.37	16.53	47.30
0.133	0.0040	0.19	47.50	42.11	46.73

The obtained data are summarized in Table 5.2. Values of τ and $\dot{V}_0$ are determined by Equation 4.27 and Equation 4.28, respectively. The value of the culture depth clearly affects the biomass production rate and in particular $r_{x,max}$, which is one order of magnitude lower at $h = 13.3$ cm with respect to $h = 1.2$ cm. On the other hand, the volumetric flow rate increases with the depth.
The residence time at maximum production does not change appreciably, and for the three cases, the expected areal productivity is about 47 tons of microalgae per hectare per year. The volumetric productivity depends on the reactor volume and for the three cases it is 393 kg/(m^3y), 94 kg/(m^3y) and 35 kg/(m^3y), respectively.

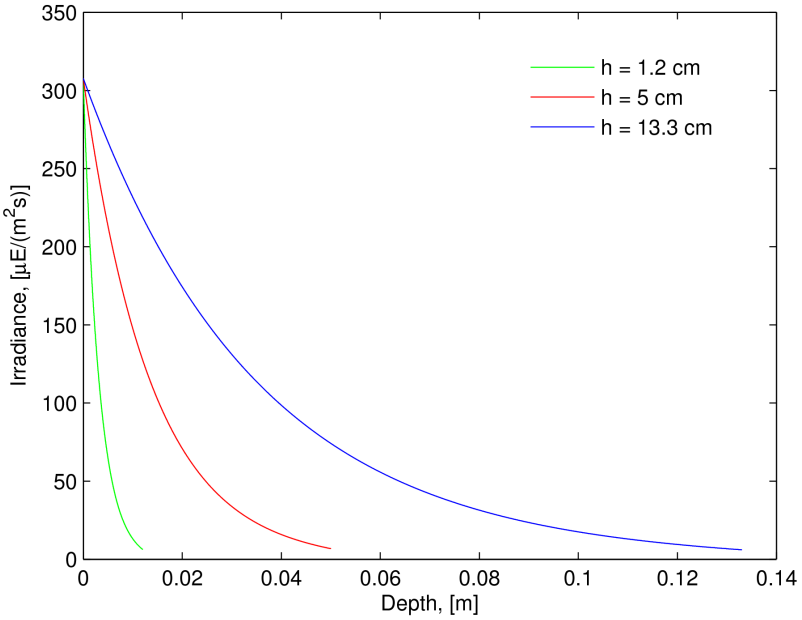

Figure 5.7: Irradiance trend along the culture depth at cells concentration corresponding to the highest biomass production rate for the three considered values of depth.

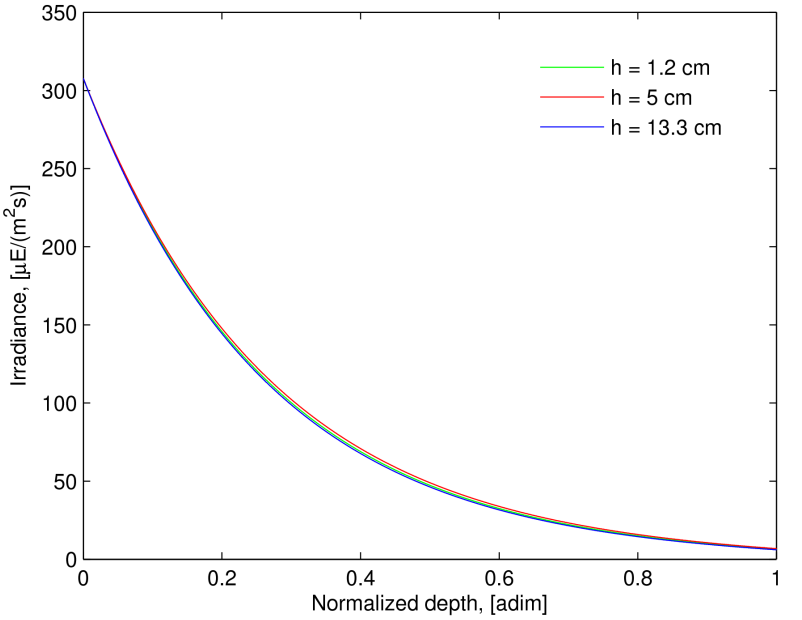

Figure 5.8: Irradiance trend normalized on the culture depth at cells concentration corresponding to the highest biomass production rate for the three considered values of depth.

Once the cells concentration and I_0 are fixed, h has a negative effect on the biomass production rate, as expressed at the beginning of this section. Nevertheless, if the aim is to reach the highest performance, an increase of the culture depth forces the system to operate at a lower stationary cells concentration, so that the irradiance can be utilized along all the depth; in this way, the best compromise between the duplication and the maintenance processes is reached. Figure 5.7 shows the light attenuation along the culture depth for the three considered cases. It is noteworthy that if a normalized value of depth is used (Figure 5.8), the irradiance trend is the same, and it ensures the highest performance of the system.

5.3.1 *Considerations on recycle*

In the following part, the photobioreactor is modelled as a PFR and different recycle ratios are simulated: in fact, the design of any biological process should take into account a recycle flow which sends back part of the extracted biomass, in order to avoid wash-out problems.
The procedure described in Section 4.5.2 is used to evaluate the performance of the system with recycle for the three values of culture depth. In particular, for each case, the residence time τ and $\dot{V}_0$ have the same value as reported in Table 5.2, whereas τ_r and $\dot{V}_{in}$ change depending on the recycle ratio R.
Values of the cross-section area A_r at $h = 1.2$ cm, $h = 5$ cm and $h = 13.3$ cm are $9{\cdot}10^{-3}$ m^2, $37.5{\cdot}10^{-3}$ m^2 and $100{\cdot}10^{-3}$ m^2, respectively.
At this point, the code *massbalance.m* can solve the equations for a PFR, reported in Section 5.1, at different recycle ratios, once the culture depth is set. Stationary cells concentrations and reactor residence time τ_r are collected in Table 5.3.
As for the lab-scale reactor case, with the residence time of the system determined so that the maximum biomass production rate is reached, the simulation of the photobioreactor as a PFR yields a negative effect on the performance. As expected, the performances of the plug flow reactors always tend to those of the CSTRs when the recycle ratio increases. This suggests that the photobioreactor can be designed as a CSTR in order to reach the highest biomass productivity. In practice, it is difficult to achieve a perfect mixing; instead, with a scheme like the one in Figure 5.1, the reactor is likely to behave closer to a PFR. So, the safety issues linked to the wash-out problem of a PFR force to design the reactor as a PFR with a high value of the recycle ratio, in this case $R = 3$.
Finally, a culture depth of 13.3 cm and thereby a culture volume of 2000 L are chosen for the design of the photobioreactor, as lower values are considered impractical for a pilot-scale plant.
Figure 5.9 shows the neglectable difference in terms of performance using the CSTR and the PFR.

Table 5.3: Stationary cells concentrations and reactor residence time at different recycle ratios for the three considered values of depth. Values of system residence time are $\tau = 46.65$ h, $\tau = 45.37$ h and $\tau = 47.50$ h, respectively.

Depth [m]	Recycle ratio [adim]	Cells concentration [g/L]	τ_r [h]
0.012	0.1	0	42.39
	0.2	0.33	38.86
	0.5	1.58	31.09
	0.7	1.77	27.43
	1	1.9	23.32
	2	2.03	15.54
	3	2.06	11.66
0.05	0.1	0	41.25
	0.2	0.04	37.81
	0.5	0.35	30.25
	0.7	0.4	26.69
	1	0.44	22.69
	2	0.47	15.12
	3	0.48	11.34
0.133	0.1	0	43.18
	0.2	0.04	39.58
	0.5	0.15	31.66
	0.7	0.16	27.94
	1	0.18	23.75
	2	0.19	15.83
	3	0.19	11.87

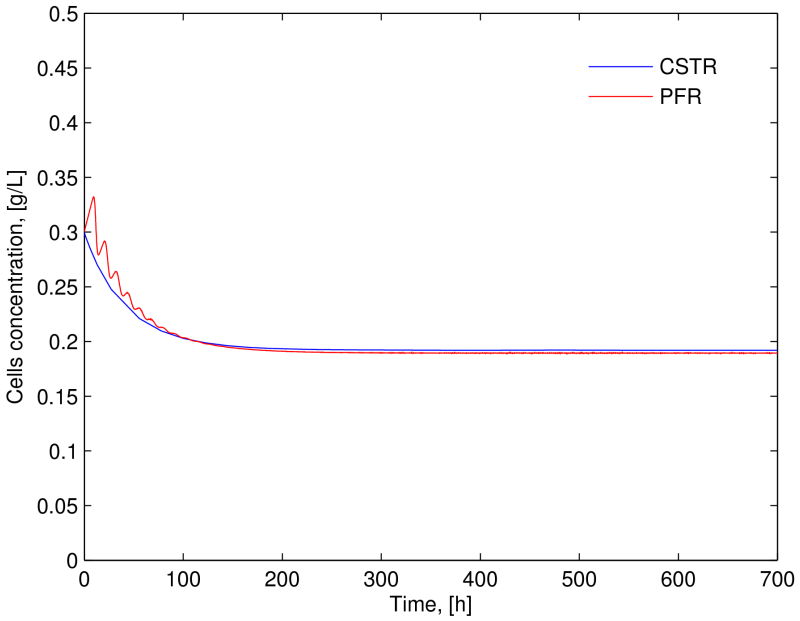

Figure 5.9: Cells concentration trend using the CSTR and the PFR for the simulation, respectively.

5.3.2 *Photosynthetic efficiency*

In order to understand the percentage of inlet radiation which is used for the formation of new cells, the photosynthetic efficiency is calculated for the PFR with $R = 3$. The biomass production rate at the steady state condition for the 2000 L volume reactor is:

$$P = V_r r_x = 192\,g/d. \tag{5.18}$$

Using Equation 3.26, the energy stored as biomass can be determined and the result is $\dot{E}_{stored} = 39.7$ W.
The power of radiation hitting the microalgae culture is:

$$\dot{E}_{in} = I_0 E_{pho} A = 918\,W \tag{5.19}$$

So, the photosynthetic efficiency for the pilot-scale photobioreactor is 4.32% of PAR, which corresponds to 1.86% of total solar energy.

5.3.3 *Energy balance*

The photosynthetic activity of microalgae strongly depends on the environment temperature; in particular, when a continuous artificial radiation is adopted, the temperature inside the reactor can exceed the optimum growth temperature, resulting in a decrease of the system performance. In fact, the portion of visible radiation which is not used for photosynthesis leads to an heating effect of the microalgae

culture.
For this reason, the energy balance is useful to evaluate if a temperature control system is necessary.
At the steady state condition, the energy balance for the PFR is expressed by the following equation:

$$\dot{m} c_p \frac{dT}{dx} = \dot{E}_{in} - \dot{E}_{stored} - \dot{E}_{main} - \dot{E}_k \tag{5.20}$$

where:

- $\dot{m}$ mass flow of medium, [kg/s]
- c_p specific heat capacity of medium, approximated to c_p of water, [J/(kg°C)]
- T temperature of medium, [°C]
- x longitudinal coordinate of the reactor, [m]

- $\dot{E}_{in}$ power of inlet radiation, [W/m]
- $\dot{E}_{stored}$ energy converted into biomass, [W/m]
- $\dot{E}_{main}$ energy required for maintenance process, [W/m]
- $\dot{E}_k$ conductive heat transfer between medium and the reactor walls, [W/m]

In particular, it is considered a variation in temperature only along the longitudinal coordinate, as the gas delivery system provides a good mixing along the vertical coordinate. The balance boundaries are set outside the photobioreactor, so the power of inlet radiation is calculated over the top polycarbonate sheets:

$$\dot{E}_{in} = I_{sheets} E_{pho} A \cdot L_r = 57.45\,W/m \tag{5.21}$$

where:

- I_{sheets} PAR reaching the reactor, that is before the first sheet of polycarbonate, = $\frac{I_0}{(1 - y_{PC})}$, [μE/(m²s)]. Value of y_{PC} is 0.2 for a 1 cm thick polycarbonate sheet;
- L_r reactor length, [m]

The energy converted into biomass for the entire system is provided by the previous section, $\dot{E}_{stored} = 39.7$ W; in order to use this value into the energy balance, $\dot{E}_{stored}$ has to be divided by the reactor volume, V_r, and multiplied by reactor depth, h, and width, L_r; the result is $\dot{E}_{stored} = 1.98$ W/m.
The same procedure is used for the energy required for the maintenance process: for the entire system it is calculated as in Section 4.4.2; this value is then divided by V_r and multiplied by $h \cdot L_r$; $\dot{E}_{main} = 0.61$ W/m is obtained.

The conductive heat transfer $\dot{E}_k$ can be divided into two contributions:

$$\dot{E}_k = \dot{E}_{k,1} + \dot{E}_{k,2} \tag{5.22}$$

The culture depth is 13.3 cm and the medium transfers heat directly to the side reactor walls and then to the external environment: this contribution is taken into account by $\dot{E}_{k,1}$. In addition, the reactor depth is 50 cm, and a space corresponding to (50 cm - 13.3 cm) = 36.7 cm is filled by air: the medium also transfers heat to this air, which transfers energy through the side and top polycarbonate sheets to the external environment; this contribution is represented by $\dot{E}_{k,2}$.
Therefore:

$$\dot{E}_{k,1} = U_{t,1} L_r (T - T_{amb}) \tag{5.23}$$

$$\frac{1}{U_{t,1}} = \frac{1}{U_{med}} + \frac{1}{U_{PC}} + \frac{1}{U_{air}} \tag{5.24}$$

$$\dot{E}_{k,2} = U_{t,2}((h_r - h) + L_r)(T - T_{amb}) \tag{5.25}$$

$$\frac{1}{U_{t,2}} = \frac{1}{U_{med}} + \frac{1}{U_{air}} + \frac{1}{U_{PC}} + \frac{1}{U_{air}} \tag{5.26}$$

where:

T_{amb} temperature of the external environment, [°C]
h_r reactor depth, [m]

Values of U_{med}, U_{PC}, and U_{air} are set to ∞, 4.6 W/(m^2°C) and 15 W/(m^2°C), respectively. So, $U_{t,1}$ = 3.5 W/(m^2°C) and $U_{t,2}$ = 2.9 W/(m^2°C) can be calculated.
The external temperature T_{amb} depends on the month of the year; for July and January, average temperatures for the location of Padua are 25 °C and 5 °C, respectively.
The system is represented by the photobioreactor which behaves as a PFR with a recycle ratio $R = 3$; so, the mass flow entering the reactor is calculated as follows:

$$\dot{m} = \dot{V}_0 (1 + R) \rho_{H_2O} \tag{5.27}$$

where:

ρ_{H_2O} density of water at 25 °C and 1 atm, [kg/m^3]

The result is $\dot{m} = 4.68 \cdot 10^{-2}$ kg/s.
In order to solve Equation 5.20, a Matlab® code, called *energybalance.m*, was developed; in particular the inputs for this code are the terms described in Table 5.4, where the final results are also reported. Figure 5.10 and Figure 5.11 show the temperature of the medium along the reactor length for the month of July and January, respectively.

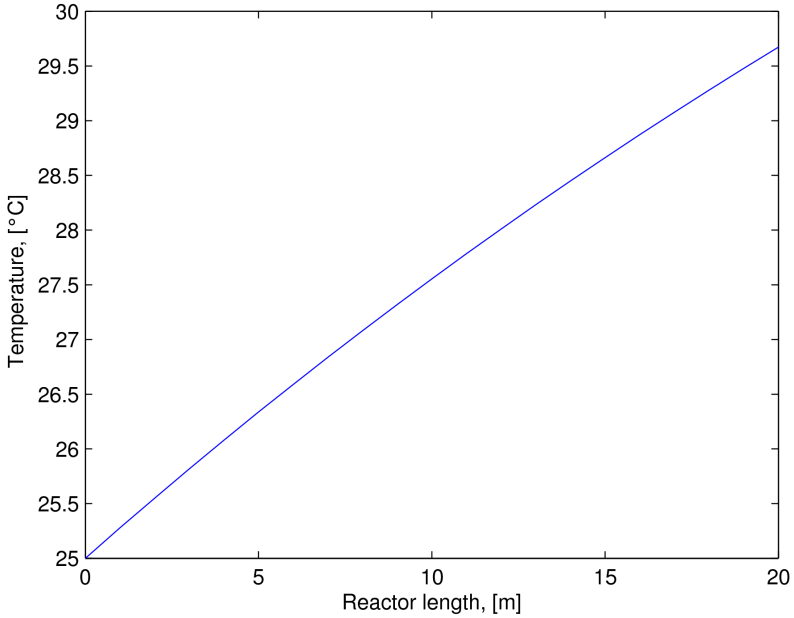

Figure 5.10: Temperature of the medium along the reactor length in July, when $T_{amb} = 25$ °C.

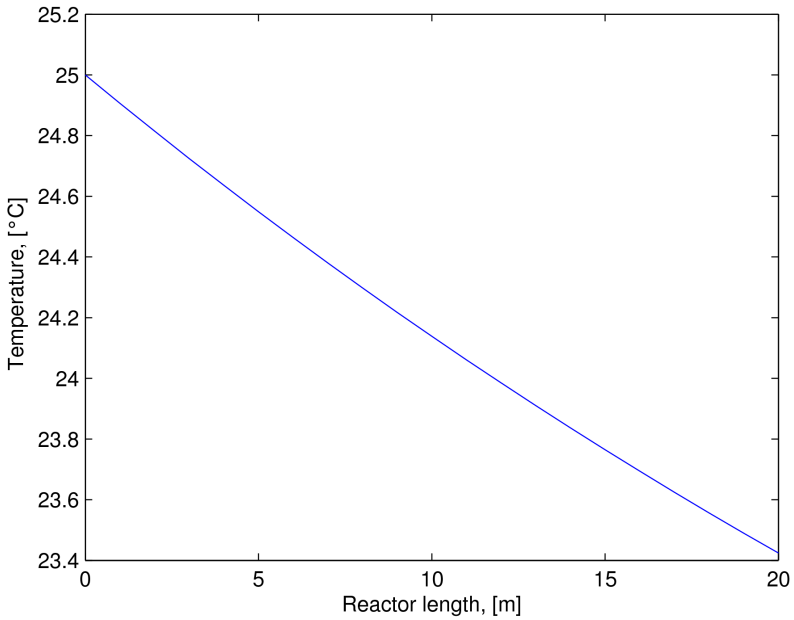

Figure 5.11: Temperature of the medium along the reactor length in January, when $T_{amb} = 5$ °C.

Table 5.4: Data referring to the energy balance.

Data	Symbol	U.m.	Value
Reactor depth	h_r	m	0.5
Reactor width	L_r	m	0.75
Reactor length	L	m	20
Reactor volume	V_r	m^3	2
Irradiated area	A	m^2	15
Culture depth	h	m	0.133
Medium specific heat capacity	c_p	J/(kg°C)	4186
Mass flow of medium	$\dot{m}$	kg/s	$4.68 \cdot 10^{-2}$
Polycarbonate thickness	s	m	0.01
Polycarbonate light absorption	y_{PC}	%	20
Energy to biomass	$\dot{E}_{stored}$	W	39.7
Energy for maintenance	$\dot{E}_{main}$	W	12.3
External temperature[a]	T_{amb}	°C	25
External temperature[b]	T_{amb}	°C	5
Medium free convection	U_{med}	$W/(m^2°C)$	∞
Conductance of polycarbonate	U_{PC}	$W/(m^2°C)$	4.6
Air free convection	U_{air}	$W/(m^2°C)$	15
Irradiance	I_0	$\mu E/(m^2 s)$	272
Temperature of inlet medium	T_{in}	°C	25
Temperature of outlet medium[a]	T_{out}	°C	29.7
Temperature of outlet medium[b]	T_{out}	°C	23.4

[a] in July

[b] in January

The trend of temperature inside the microalgae culture really changes depending on the season of the year. During the summer period, temperature of almost 30 °C can be reached, whereas in winter period, temperature slightly lower than 25 °C are calculated. As reported in literature (Xin, Hong-ying, and Yu-ping 2011), the species *Scenedesmus* maintains an high growth rate in the temperature range 20-30 °C; so, the irradiance $I_0 = 272$ $\mu E/(m^2 s)$ hitting the microalgae culture would not raise overmuch the internal temperature, and at low T_{amb} it would ensure proper growth conditions.

5.4 PLANT SIMULATIONS WITH SOLAR RADIATION

This section will investigate how the system behaves when the only radiation entering the photobioreactor is provided by the sun. During a typical day, the sun rises, reaches the highest point above the horizon at 12:00, and then it sets down. In summer, the day is longer than night and the irradiance reaching the terrestrial surface is the maximum, whereas, in winter, the light energy is low and available for a shorter period of time. For these reasons, a change in the photobioreactor performance during the year is a crucial issue.

The system is simulated in the months of July and January, as representative of summer and winter period, respectively. The photobioreactor is firstly considered as a CSTR with the following operating conditions:

- volume of the reactor $V_r = 2000$ L;
- depth of the culture $h = 13.3$ cm;
- volumetric inflow of medium $V_0 = 42.11$ L/h;

All simulations are performed by the Matlab® code *massbalance.m*. In particular, the inputs are now represented by the operating conditions above, by the parameters summarized in Table 4.5 and by the irradiance, changing along with the day. The implemented solver calculates $I_{dir}(0)$, $I_{dif}(0)$ and θ using the regression equations reported in Section 5.2.2 during the day; so, the irradiance along the reactor depth can be determined using the Cornet model and, after the determination of the average growth rate with respect to the depth, the mass balances are carried out.
It is expected that the cells concentration inside the reactor has a periodical trend during the day, as the available irradiance is zero during the night and has a maximum at 12:00; furthermore, when no light reaches the culture, the growth rate r_x has a negative value, since only maintenance process are active, as Equation 3.11 demonstrates.
The same code has been modified to simulate the photobioreactor as a PFR with a recycle ratio $R = 3$, $V_{in} = V_0(1 + R) = 168.44$ L/h and the same operating conditions as above.
Figure 5.12 shows the cells concentration change with the month of July when the CSTR and the PFR assumptions are made, respectively. The stationary cells concentration is 0.12 g/L for a CSTR, 0.10 g/L for a PFR. In terms of productivity, $P_r = 29.51$ tons/(ha·y) and 24.59 tons/(ha·y) for the CSTR and the PFR, respectively.
Table 5.5 reports simulation results for the PFR at different recycle ratios for the month of July.

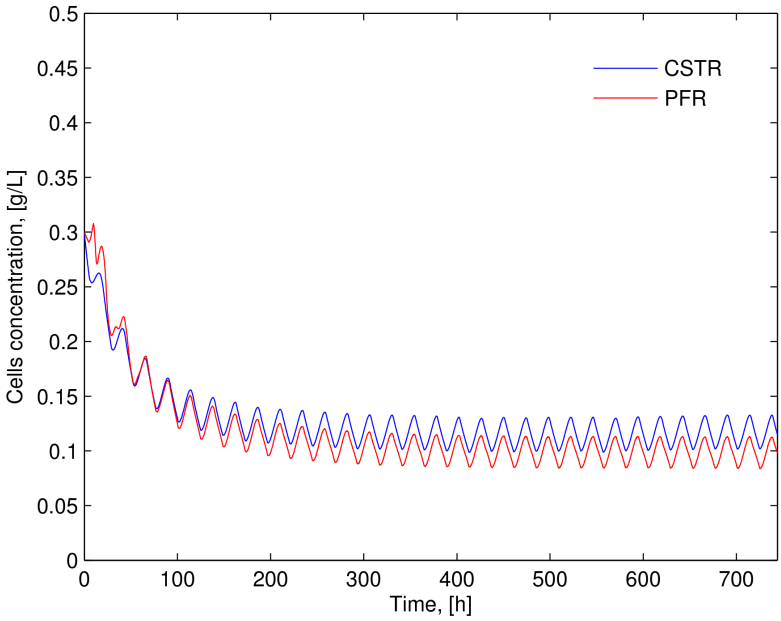

Figure 5.12: Cells concentration trend during the month of July using the CSTR and the PFR for the simulation, respectively.

Table 5.5: Results of the PFR simulation at different recycle ratios for the month of July.

Recycle ratio [adim]	$c_{x,out}$ [g/L]	τ_r [h]	P_r [tons/(ha · y)]	P_v [kg/(m^3y)]
0.1	0	43.18	0	0
0.2	0	39.58	0	0
0.5	0	31.66	0	0
0.7	0.03	27.94	7.38	5.5
1	0.06	23.75	14.76	11.1
2	0.09	15.83	22.13	16.6
3	0.10	11.87	24.59	18.4

It is noteworthy that the PFR has to maintain a high recycle ratio to avoid the wash-out problems. Nevertheless, the productivity achieved at high recycle ratios, that is in a condition similar to a CSTR behaviour, is about half of the productivity when the artificial continuous radiation $I_0 = 272$ μE/(m^2s) is used.
The simulations are performed considering the month of July, when the amount of solar energy is the highest. It is clear that the performance of the reactor lowers during the other months and the wash-out problems can not be avoided either if the reactor behaves as a CSTR. Figure 5.13 shows this condition for the month of January.

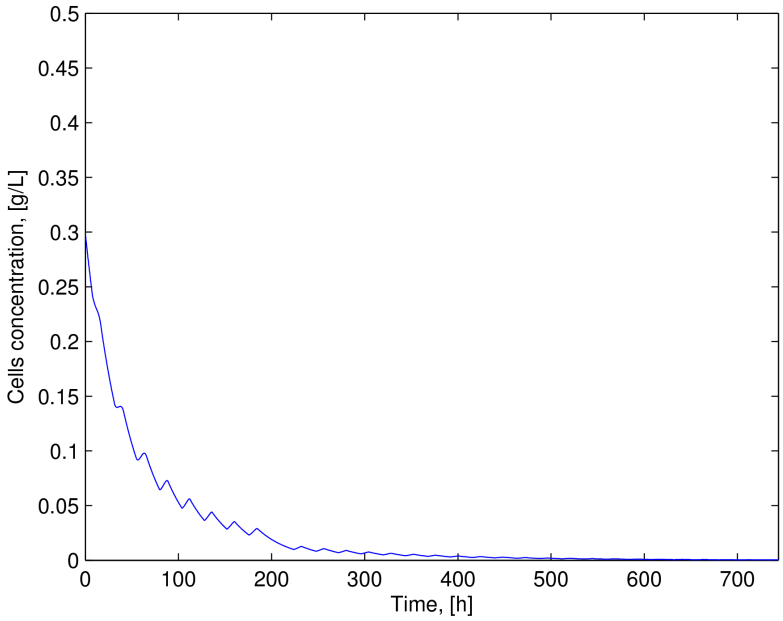

Figure 5.13: Cells concentration trend during the month of January using the CSTR simulation.

The solar radiation reaching the terrestrial surface and the day/night cycles are the limiting factors for the biomass productivity and they can not be changed. So, other operations or plant adjustments, which will be not further developed in the present work, are here described in order to improve the performance of the system using solar radiation:

- an investigation, similar the one performed for the artificial continuous radiation, can be carried out to determine the correct value of the system residence time τ which ensures the maximum biomass production rate; in this way, the make-up inflow V_0 has a different value depending on the month, i.e., on the availability of light;

- it can be useful to evaluate the convenience of stopping the make-up inflow, and so the biomass outflow, during the night; in fact, when no light is available, microalgae do not grow and a continuous extraction of biomass during this period, together with the effect of the maintenance process, decreases the cells concentration and, in the following morning, a lower number of microalgae can duplicate. On the other hand, the biomass productivity could be negatively affected by the fact that the biomass is not extracted from the system 24 hours a day;

- a mix between solar and artificial radiation contains the advantages of both configurations: during the day, the costless solar

radiation can be used for the microalgae cultivation; during the night, microalgae continue to grow and duplicate using the artificial radiation. In this way, the loss of biomass due to the only maintenance process is avoided;

- mixotrophic conditions could enhance several times the biomass production relative to the only phototrophy, as reported by Bhatnagar *et al.* 2011; this microalgae growth condition would be used especially during the winter, when the availability of light is limited.

5.4.1 *Photosynthetic efficiency*

In this section, a PFR with a recycle ratio $R = 3$ in the month of July is considered. At steady state condition, the daily amount of extracted biomass corresponds to:

$$P = \dot{V}_0 c_{x,out} = \dot{V}_p c_{x,p} = 101\,g/d \tag{5.28}$$

E_{stored} is determined using Equation 3.26 and the result is $E_{stored} = 20.9$ W.
The power of radiation entering the system is provided by Table 5.1: for a typical day of July, $\dot{E}_{in} = 21.82$ mJ/(m^{2}d) which corresponds to $\dot{E}_{in} = 3788$ W for the 15 m^2 exposed area.
The photosynthetic efficiency is so $\psi = 0.55\%$ of total solar energy, that is 1.28% of PAR.

5.4.2 *Energy balance*

As reported in Section 5.3.3, the portion of visible light which is not diverted to photosynthetic processes leads to an increase of the culture temperature; using sunlight, this effect is amplified by the infrared portion of the spectrum, which represents almost half of the solar radiation hitting the terrestrial surface. For this reason, the temperature along the reactor length is simulated at 12:00 of a typical day of the month of July, when the irradiance conditions are the strongest one.
The irradiance reaching the photobioreactor at 12:00 is $I(0) = 1228$ μE/(m^{2}s), which corresponds to a total solar irradiance $Q = 644$ W/m^2. $\dot{E}_{in}$ can be so determined:

$$\dot{E}_{in} = Q \cdot L_r = 483\,W/m \tag{5.29}$$

The values of $\dot{E}_{stored}$ and $\dot{E}_{main}$ for the energy balance are determined as in Section 5.3.3: the results are $\dot{E}_{stored} = 1.04$ W/m and $\dot{E}_{main} = 0.32$ W/m.
The external temperature for the month of July is the average $T_{amb} = 25$ °C and the medium is fed into the reactor at the same temperature.

Figure 5.14 shows the result obtained with the Matlab® code *energybalance.m*.
The temperature reaches 65 °C at the reactor outflow, a condition unsuitable for microalgae growth, leading to cells death. So, a cooling system has to be considered when the design of the reactor is performed.
In reality, the simulation is carried out at the steady state condition, that is when a continuous irradiance of 1228 $\mu E/(m^2 s)$ hits the microalgae culture, whereas the irradiance has a sine trend during the day and the highest values are reached only around 12:00, i.e., for few minutes. The assumption used in the simulation can be valid if the time required by the medium to cover the length of the channel is in the order of minutes; nevertheless, the residence time of the photobioreactor shows that this time is in the order of hours, being $\tau_r = 11.87$ h.

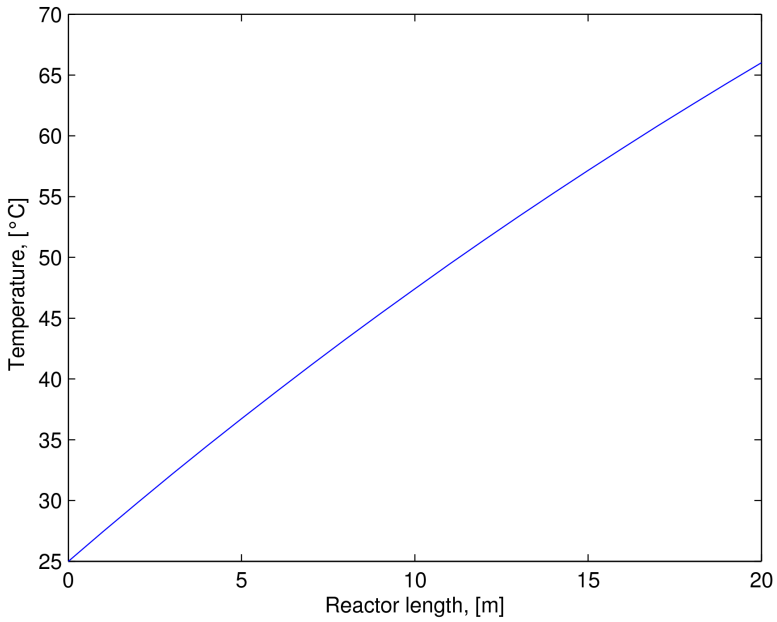

Figure 5.14: Temperature of the medium along the reactor length at 12:00 of a typical day of July, when $T_{amb} = 25$ °C.

However, the result in Figure 5.14 demonstrates that the culture has to be somehow protected from the irradiance peaks which can seriously worsen the performance of the system.
In parallel, it is clear that also an heating system has to be designed for the photobioreactor; in fact, especially during the winter period, the solar irradiance could not provide a sufficient heating because of its low value and, moreover, this effect is visible during the night, when no light is available. Figure 5.15 shows the simulation of the temperature along the reactor channel during a typical night for the month of January.

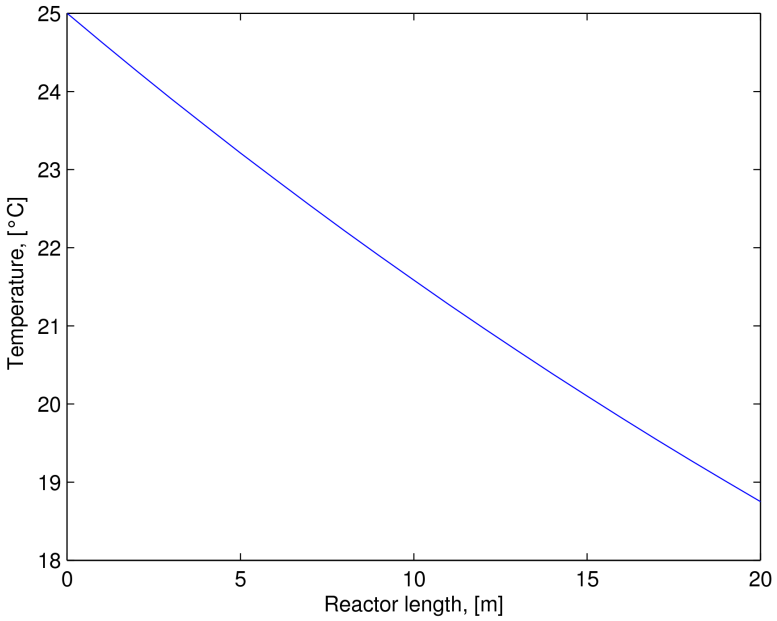

Figure 5.15: Temperature of the medium along the reactor length during a typical night of January, when $T_{amb} = 5$ °C.

5.4.3 *Conclusions*

When an artificial radiation of 272 $\mu E/(m^2 s)$ is used as energy source, the best system performance are provided by a PFR with an high recycle ratio ($R = 3$): in this way, the reactor acts as a CSTR and the wash-out problems are avoided. The culture depth h is set to 13.3 cm, so that $V_r = 2000$ L, because a lower value is impractical on a pilot-scale. A biomass productivity $P_r = 46.73$ tons/(ha·y) and a photosynthetic efficiency $\psi = 4.32\%$ of PAR are reached. The energy balance demonstrates that the irradiance entering the system is sufficient to maintain proper microalgae growth conditions during the winter and that it does not heat overmuch the culture during the summer period. The investigation of the system behaviour when the energy source is given by the solar radiation leads to different results. Good performances are reached only during the summer period, whereas wash-out problems are encountered during the winter time. Some considerations to avoid this conditions are proposed in Section 5.4. In the month of July, a biomass productivity $P_r = 24.59$ tons/(ha·y) and a photosynthetic efficiency $\psi = 1.28\%$ of PAR are reached. In addition, the optimum growth temperature can be maintained during the year only if the cooling/heating system, represented by the coils placed on the bottom of the reactor, is operated.

CONCLUSIONS

In this thesis, the microalgae production of *Scenedesmus obliquus* was firstly investigated at laboratory scale. Two continuous reactors were set up, and the steady state condition was reached in both systems. The second reactor was then equipped with a pump to partially recycle the biomass. The reactor residence time τ_r was kept at the same value as in the operation without recycle: the steady cells concentration increased but the biomass productivity slightly worsened.

In order to simulate the behaviour of the microalgal culture in the reactor with and without recycle, the Cornet model, generalized by Pruvost, was programmed in Matlab®. This model refers to systems in light-limited condition, that is when the light is the only limiting nutrient. The biomass production rate r_x is the sum of two contributions: a positive term, accounting for the duplication process, which depends on the irradiance along the culture depth, and a negative term to describe the maintenance process, which is a function of the cells concentration only. The light attenuation inside the reactor plays a fundamental role in the correct determination of r_x and it depends on the optical properties of the microalga, i.e., the absorption coefficient Ea and the backscattering coefficient bEs. The values of these parameters were obtained by fitting values of both back irradiance at different cells concentration and of the dynamic reactor with recycle, approximated to a CSTR. The maintenance term was then tuned in order to predict the correct value of stationary cells concentration in the continuous reactor with and without recycle.
The photosynthetic efficiency was calculated to be 4.78% of PAR, a small value compared to the maximum achievable (30.68%). The energy balance demonstrated that the incident energy converted into biomass is less than 5% of the total one; most of the irradiance is in fact used for the water heating.
A study on the maximum biomass production rate was performed to determine the value of τ which ensures the highest performance of the continuous reactor with recycle. In particular, the maximum r_x is characterized by the maximum duplication rate which is directly affected by the light availability at each reactor point: this condition forces the system to operate at a cells concentration such that the light can penetrate through all the culture depth. Once the optimum residence time was calculated, the reactor with recycle was approximated by a PFR. The system performances were found to worsen when the recycle ratio R decreased. So, a PFR with high recycle permitted an

high productivity and moreover it avoided wash-out problems.

The optimized model parameters were used to simulate an actual pilot-scale photobioreactor. The artificial irradiance was initially considered, and a study on the maximum biomass production rate was performed. Three values of culture depth were analyzed: it was shown by the simulation that the areal productivity does not change substantially; in fact, as the depth increases, the stationary cells concentration lowers so that light can penetrate through all the culture, but on the other hand the extraction rate increases, and the produced mass flow of biomass per unit area remains almost constant. As obtained for the laboratory reactor, a PFR with high recycle ratio has the highest performances and avoids wash-out problems.
The photosynthetic efficiency which can be achieved in this case was found to be 4.32% of PAR. The energy balance was discussed for the months of July and January, representative of the summer and the winter period, respectively: the artificial continuous irradiance reaching the culture was sufficient to preserve the proper microalgae growth conditions, so a cooling/heating system is not required.
Operating the system under the sunlight has a clear benefit, as the energy used by the microalgae is costless. On the opposite, several disadvantages were found to limit the use of solar radiation only. In the summer period, the photobioreactor can reach good performances in terms of productivity, whereas in January the wash-out problems cannot be avoided: this is due to the low value of irradiance reaching the culture during winter time, and to the long night periods when the microalgae are continuously extracted and the maintenance process on the biomass production prevails on the duplication process. In order to limit these problems the system residence time which ensures the maximum biomass production rate should be determined for each month; furthermore, during the night, especially in winter periods, the extraction of biomass could be stopped or the system can be operated with artificial radiation.
The photosynthetic efficiency for the month of July is 1.28% of PAR, that is only 0.55% of total solar energy. The energy balance showed that the microalgal culture has to be protected from the irradiance peaks, typical of summer, and that the solar energy is not sufficient to maintain proper growth conditions in the winter period. For these reasons, the design of the pilot plant has to include a cooling/heating system.

LIST OF SYMBOLS

Acronyms

CSTR	continuous stirred tank reactor
DW	dry weight, [g/L]
LHV	lower heating value
OD	optical density, [adim]
PBR	photobioreactor
PFR	plug flow reactor

Greek letters

α_i	initial slope of the relation between μ_{eff} and I, [$m^2 s/(\mu E \cdot d)$]
α	linear scattering modulus, [adim]
δ_{dif}	diffuse two flux extinction coefficient, [m^2/L]
δ_{dir}	direct two flux extinction coefficient, [m^2/L]
ϵ	extinction coefficient, [m^2/cell]
η_{ba}	biomass accumulation efficiency, [adim]
η_{ft}	photons transmission efficiency, [moles of transmitted photons/moles of hitting photons]
η_{fu}	photons utilization efficiency, [moles of used photons/moles of transmitted photons]
λ	wavelength, [nm]
$\mu_a(\lambda)$	absorption coefficient, [m^{-1}]
μ_e	maintenance constant, [h^{-1}]
μ_{eff}	specific growth rate measured experimentally, [h^{-1}] or [d^{-1}]
ϕ	mass quantum yield for Z-scheme of photosynthesis, [kg/μE]
ψ	photosynthetic efficiency, [adim]
ψ_{max}	maximum photosynthetic efficiency, [adim]
ρ_m	maximum energetic yield for photon conversion, [adim]
ρ_{H_2O}	density of water at 25 °C and 1 atm, [kg/m^3]

ρ_{dm} density of biomass dry material, [kg/(m^3)]

τ residence time, [h] or [d]

τ_r reactor residence time, [h] or [d]

θ incident radiation angle with respect to normal direction of reactor surface, [rad]

θ_t incident radiation angle with respect to normal direction of terrestrial surface at the maximum insolation time, that is at 12:00, [rad]

ε_c relative error between calculated and experimental cells concentration, [adim]

ε_I relative error between calculated and experimental back irradiance, [adim]

ε_{fin} absolute difference between estimated and calculated backscattering coefficient, [adim]

Roman letters

A irradiated area, [m^2]

A_r cross-section area, [m^2]

A_t reactor surface in contact with the external environment, [m^2]

A_{750} absorbance at $\lambda = 750$ nm, [adim]

b backscattering fraction, [adim]

bEs backscattering mass coefficient, [m^2/kg]

bEs_{calc} calculated backscattering coefficient, [m^2/kg]

bEs_{hypo} estimated backscattering coefficient, [m^2/kg]

c cells concentration, [cell/mL] or [g/L]

c_I calculated stationary cells concentration for the reactor with recycle, [g/L]

c_l speed of light, [m/s]

c_p specific heat, [J/(kg·K)]

c_x cells concentration, [g/L]

C_{ABS} absorption cross-section, [m^2]

c_{in} cells concentration entering the reactor, [g/L]

c_{out} cells concentration exiting the CSTR, [g/L]

C_{SCA} scattering cross-section, $[m^2]$

$c_{x,calc}$ calculated cells concentration, $[g/L]$

$c_{x,exp}$ experimental cells concentration, $[g/L]$

c_{II} calculated stationary cells concentration for the reactor without recycle, $[g/L]$

$c_{x,0}$ cells concentration in the make-up flow, $[g/L]$

$c_{x,in}$ cells concentration entering the reactor, $[g/L]$

$c_{x,out}$ cells concentration exiting the reactor, $[g/L]$

$c_{x,b}$ cells concentration in the collecting bottle, $[g/L]$

$c_{x,p}$ cells concentration exiting the system, $[g/L]$

$c_{x,R}$ cells concentration in the recycle stream, $[g/L]$

$c_{x,r}$ cells concentration in the reactor, $[g/L]$

E_{bio} biomass heat of combustion, $[J/g]$

E_{carb} carbohydrate heat of combustion, $[J/mol]$

E_{pho} average energy per mole of photons, $[J/mol]$

E_{sun} yearly total solar energy reaching the system per unit area, $[J/(m^2y)]$

Ea absorption mass coefficient, $[m^2/kg]$

$Ea_{pig.i}$ in vivo spectral mass absorption coefficient of pigment i, $[m^2/kg]$

Es scattering mass coefficient, $[m^2/kg]$

h depth of the culture, $[m]$

h_p Planck constant, $[Js]$

h_r reactor depth, $[m]$

H_{algae} recycle inlet enthalpy, $[W]$

H_{in} specific enthalpy of each reactant, $[J/kg]$

H_{nut} micronutrients inlet enthalpy, $[W]$

H_{out} specific enthalpy of each product, $[J/kg]$

I irradiance, $[\mu E/(m^2s)]$

$I(z)$ photosynthetic active radiation, $[\mu E/(m^2s)]$

$I_{back,calc}$ calculated back irradiance, $[\mu E/(m^2s)]$

$I_{back,exp}$ experimental back irradiance, [$\mu E/(m^2 s)$]

I_{back} back irradiance, [$\mu E/(m^2 s)$]

$I_{dif}(0)$ diffuse PAR at depth 0, [$\mu E/(m^2 s)$]

$I_{dif}(z)$ diffuse PAR at depth z, [$\mu E/(m^2 s)$]

$I_{dir}(0)$ direct PAR at depth 0, [$\mu E/(m^2 s)$]

$I_{dir}(z)$ direct PAR at depth z, [$\mu E/(m^2 s)$]

I_{layer} PAR reaching the first layer of microalgae, [$\mu E/(m^2 s)$]

I_{sheets} PAR reaching the reactor, [$\mu E/(m^2 s)$]

K half saturation constant for photosynthesis, [$\mu E/(m^2 s)$]

K specific growth rate, [d^{-1}]

k_λ imaginary part responsible for absorption, [adim]

l cuvette path length, [m]

L_m luminous flux, [lm]

L_r reactor length, [m]

m complex refractive index of the particle, [adim]

n real part responsible for scattering, [adim]

n_C moles of carbon, [mol]

N_p cell number density, [$1/m^3$]

$N_{CO_2,red}$ yearly CO_2 moles reduced to carbohydrate per unit area, [$mol/(m^2 y)$]

n_{pho} moles of photons, [mol]

P biomass production, [kg/s]

P_a areal biomass productivity, [$g/(m^2 d)$] or [tons/(ha·y)]

P_r real biomass productivity, [tons/(ha·y)]

P_v volumetric biomass productivity, [$kg/(m^3 d)$] or [$tons/(m^3 y)$]

P_{max} maximum biomass production, [tons/(ha·y)]

Q total solar irradiance, [W/m^2]

QR quantum requirement, [moles of photons/moles of reduced CO_2]

R recycle ratio, [adim]

r_x biomass production rate, [g/(L·d)]

$r_{x,max}$ maximum biomass production rate, [g/(L·h)]

$r_{x,out}$ biomass production rate, [g/(L·d)]

$r_{x,m}$ maintenance process rate, [g/(L·d)]

$r_{x,p}$ duplication rate, [g/(L·d)]

$r_{x,p}(z)$ duplication rate at depth z, [g/(L·d)]

$r_{x,t}$ global reaction rate, [g/(L·d)]

s polycarbonate sheet thickness, [m]

T temperature of the medium, [°C]

t time, [h] or [d]

T_{amb} temperature of the external environment, [°C]

T_{in} temperature of the medium inlet, [°C]

t_{in} time of sunrise

T_{out} temperature of the external environment, [°C]

t_{out} time of sunset

T_{ref} reference temperature, [K]

U_t overall heat transfer coefficient of the system, [W/(m^2°C)]

U_{air} air free convection, [W/(m^2°C)]

U_{med} medium free convection, [W/(m^2°C)]

U_{PC} conductance of the polycarbonate, [W/(m^2°C)]

V_b collecting bottle volume, [L]

V_r reactor volume, [m^3]

V_{32} mean (Sauter) particle volume, [m^3], taking into account the given size distribution

W transmitted light, [W]

W_0 lamp power reaching the first layer of microalgae, [W]

w_C mass fraction of carbon in microalgae, [adim]

W_e lamp total power, [W]

w_{oil} mass fraction of oil in microalgae, [adim]

$w_{pig.i}$ mass fraction of pigment i, [kg/kg of biomass]

$w_{residue}$ mass fraction of residue (non-oil) in microalgae, [adim]

x longitudinal coordinate of the reactor, [m]

x_w in vivo volume fraction of water in the cell, [adim]

x_{CO_2} CO_2 fraction in inlet flow, [%]

x_{alga} biomass weight per mole of carbon, [g/mol_C]

y_{PC} polycarbonate light absorption, [%]

z reactor dimension along the reactor depth, [m]

$\dot{E}_{in,area}$ power of solar radiation per unit area, [W/m^2]

$\dot{E}_{in,tot}$ energy entering the reactor, [W]

$\dot{E}_{in}$ power of incident radiation, [W]

$\dot{E}_{main}$ energy required for maintenance process, [W]

$\dot{E}_{out,tot}$ energy exiting the reactor, [W]

$\dot{E}_{out}$ power of radiation lost to the environment, [W]

$\dot{E}_{stored,area}$ energy flux per unit area stored as biomass, [W/m^2]

$\dot{E}_c$ convective heat transfer between the system and the external environment, [W]

$\dot{E}_k$ conductive heat transfer between the system and the external environment, [W]

ΔH_f^0 standard enthalpy of formation, [J/kg]

$\Delta H_{comb,algae}$ lower heating value of microalgae, [J/kg]

$\Delta H_{comb,elem}$ lower heating value of biomass elemental compounds, [J/kg]

$\Delta H_{f,i}^0$ standard enthalpy of formation of species i, [J/kg]

$\Delta\dot{H}$ enthalpy rate of change due to a reaction, [J/s]

$\dot{H}_{bio,out}$ enthalpy of biomass exiting the reactor, [W]

$\dot{H}_{nut,in}$ enthalpy of micronutrients entering the reactor, [W]

$\dot{H}_{nut,out}$ enthalpy of micronutrients exiting the reactor, [W]

$\dot{H}_{nut,re}$ enthalpy of micronutrients entering the reactor through the recycle, [W]

$\dot{H}_{rec,in}$ enthalpy of biomass entering the reactor through the recycle, [W]

$\dot{m}$ mass flow of medium, [kg/s]

$\dot{m}_{bio,out}$ biomass outflow, [g/s]

$\dot{m}_{in}$ mass flow of reactant, [kg/s]

$\dot{m}_{nut,in}$ micronutrients mass inflow entering the reactor, [g/s]

$\dot{m}_{nut,out}$ micronutrients mass outflow exiting the reactor, [g/s]

$\dot{m}_{nut,re}$ micronutrients mass inflow entering thorough the recycle, [g/s]

$\dot{m}_{out}$ mass flow of product, [kg/s]

$\dot{m}_{rec,in}$ biomass inflow through the recycle, [g/s]

MM_{CO_2} molar mass of carbon dioxide, [g/mol]

MM_C molar mass of carbon, [g/mol]

MM_{H_2O} molar mass of water, [g/mol]

MM_O molar mass of oxygen, [g/mol]

%PAR PAR percentage of total solar energy, [%]

$\dot{V}$ volumetric flow, [L/d] or [L/h]

$\dot{V}_0$ inlet volumetric flow of make-up, [L/h]

$\dot{V}_R$ recycle volumetric flow, [L/h]

$\dot{V}_{bo}$ recycle volumetric flow, [L/d]

$\dot{V}_{gas}$ CO_2-enriched air flow, [L/h]

$\dot{V}_{in}$ inlet volumetric flow, [L/d] or [L/h]

$\dot{V}_{out}$ outlet volumetric flow, [L/d] or [L/h]

$\dot{V}_{re}$ reactor volumetric outflow, [L/d]

BIBLIOGRAPHY

Baker, N.R.

2008 "Chlorophyll Fluorescence: A Probe of Photosynthesis In Vivo", *Annual Review of Plant Biology*, 59, pp. 89–113.

Bhatnagar, A. *et al.*

2011 "Renewable biomass production by mixotrophic algae in the presence of various carbon sources and wastewaters", *Applied Energy*, 88, 10, pp. 3425–3431.

Bodegom, P. van

2007 "Microbial Maintenance: A Critical Review on Its Quantification", *Microbial Ecology*, 53, pp. 513–523.

Brennan, L. and P. Owende

2010 "Biofuels from microalgae - A review of technologies for production, processing, and extractions of biofuels and co-products", *Renewable and Sustainable Energy Reviews*, 14, pp. 557–577.

Chaplin, M

Water structure and science, http://www.lsbu.ac.uk/water/vibrat.html.

Chisti, Y.

2007 "Biodiesel from microalgae", *Biotechnology Advances*, 25, pp. 294–306.

Cornet, J.F., C.G. Dussap, and J.B. Gros

1995 "A simplified monodimensional approach for modeling coupling between radiant light transfer and growth kinetics in photobioreactors", *Chemical Engineering Science*, 50, 9, pp. 1489–1500.

Grobbelaar, J.U., L. Nedbal, and V. Tichy

1996 "Influence of high frequency light/dark fluctuations on photosynthetic characteristics of microalgae photo acclimated to different light intensities and implications for mass algal cultivations", *Journal of Applied Phycology*, 50, 8, pp. 335–343.

Hartmut, M.

2012 "The Nonsense of Biofuels", *Angewandte Chemie International Edition*, 51, pp. 2516–2518.

Herman, J.G. and R.M. Luuc

1980 "Energy Requirements for Growth and Maintenance of *Scenedesmus protuberans* Fritsch in Light-Limited Continuous Cultures", *Archives of Microbiology*, 125, pp. 9–17.

Huld, T and M. Suri

PVGIS Solar Irradiation Data, 2007, http://re.jrc.ec.europa.eu/pvgis/apps/radmonth.php?lang=en&map=europe/, [PVGIS© European Communities, 2001-2007].

Luo, H.P. and M.H. Al-Dahhan

2003 "Analyzing and Modeling of Photobioreactors by Combining First Principles of Physiology and Hydrodynamics", *Biotechnology and Bioengineering*, 85, pp. 382–393.

Mata, T., A. Martins, and N. Caetano

2010 "Microalgae for biodiesel production and other applications: A review", *Renewable and Sustainable Energy Reviews*, 14, pp. 217–232.

Palma, G.

2011 *Produzione di microalghe in fotobioreattori: influenza della luce e sfruttamento della biomassa esausta*, MA thesis, Facoltà di Ingegneria, Dipartimento di Princici e Impianti di Ingegneria Chimica "I. Sorgato".

Pope, R.M. and E.S. Fry

1997 "Absorption spectrum (380-700 nm) of pure water. II. Integrating cavity measurements", *Applied Optics*, 36, 33, pp. 8710–8723.

Posten, C.

2009 "Design principles of photo-bioreactors for cultivation of microalgae", *Engineering Life Science*, 9, 3, pp. 65–177.

Pottier, L. *et al.*

2005 "A fully predictive model for one-dimensional light attenuation by *Chlamydomonas reinhardtii* in a torus photobioreactor", *Biotechnology and Bioengineering*, 91, 5, pp. 569–582.

Pruvost, J. *et al.*

2010 "Modeling Dynamic Functioning of Rectangular Photobioreactors in Solar Conditions", *AIChE Journal*, 57, 7, pp. 1947–1960.

Pruvost, J. *et al.*

2011 "Systematic investigation of biomass and lipid productivity by microalgae in photobioreactors for biodiesel application", *Bioresource Technology*, 102, pp. 150–158.

Reference Solar Spectral Irradiance: Air Mass 1.5, http://rredc.nrel.gov/solar/spectra/am1.5/, [American Society for Testing and Materials (ASTM) Terrestrial Reference Spectra for Photovoltaic Performance Evaluation].

Richmond, Amos

2004 *Handbook of Microalgal Culture: Biotechnology and Applied Phycology*, Blackwell Science.

Sciortino, A.

2010 *Modellazione ed analisi di fotobioreattori per la produzione di microalghe su scala industriale*, MA thesis, Facoltà di Ingegneria, Dipartimento di Princici e Impianti di Ingegneria Chimica "I. Sorgato".

Tang, D. *et al.*

2011 "CO_2 biofixation and fatty acid composition of *Scenedesmus obliquus* and *Chlorella pyrenoidosa* in response to different CO_2 levels", *Bioresource Technology*, 102, pp. 3071–3076.

Tichy, V. *et al.*

1995 "Photosynthesis, growth and photoinibition of microalgae exposed to intermittent light", *Photosynthesis: From Light to Biosphere*, 50, 5, pp. 1029–1032.

Verma, N.M. *et al.*

2010 "Prospective of biodiesel production utilizing microalgae as the cell factories: A comprehensive discussion", *African Journal of Biotechnology*, 9, 10, pp. 1402–1411.

Weyer, K.M. *et al.*

2010 "Theoretical Maximum Algal Oil Production", *Bioenergy Resources*, 3, pp. 204–213.

Xin, L., H. Hong-ying, and Z. Yu-ping

2011 "Growth and lipid accumulation properties of a freshwater microalga *Scenedesmus* sp. under different cultivation temperature", *Bioresource Technology*, 102, pp. 3098–3102.